NOTICE

The quality of this microform is heavily dependent upon the quality of the original thesis submitted for microfilming. Every effort has been made to ensure the highest quality of reproduction possible.

If pages are missing, contact the university which granted the degree.

Some pages may have indistinct print especially if the original pages were typed with a poor typewriter ribbon or if the university sent us an inferior photocopy.

Previously copyrighted materials (journal articles, published tests, etc.) are not filmed.

Reproduction in full or in part of this microform is governed by the Canadian Copyright Act, R.S.C. 1970, c. C-30.

AVIS

La qualité de cette microforme dépend grandement de la qualité de la thèse soumise au microfilmage. Nous avons tout fait pour assurer une qualité supérieure de reproduction.

S'il manque des pages, veuillez communiquer avec l'université qui a conféré le grade

La qualité d'impression de certaines pages peut laisser à désirer, surtout si les pages originales ont été dactylographiées à l'aide d'un ruban usé ou si l'université nous a fait parvenir une photocopie de qualité inférieure.

Les documents qui font déjà l'objet d'un droit d'auteur (articles de revue, tests publiés, etc.) ne sont pas microfilmés.

La reproduction, même partielle, de cette microforme est soumise à la Loi canadienne sur le droit d'auteur, SRC 1970, c. C-30.

Conversion of Aqueous Ethanol to Ethylene Over Zeolite ZSM-5 and Chryso-zeolite ZSM-5 Catalysts

Thanh My Nguyen

A Thesis

in

The Department

of

Chemistry

Presented in Partial Fulfillment of the Requirements
for the Degree of Master of Science at
Concordia University
Montréal, Québec, Canada

July 1988

ISBN 0-315-44849-0

ABSTRACT

Conversion of Aqueous Ethanol to Ethylene Over Zeolite ZSM-5 and Chryso-zeolite ZSM-5 Catalysts.

Thanh My Nguyen

In this study, ethanol in very aqueous solutions such as in an ethanol fermentation broth, was converted to ethylene over zeolite ZSM-5 and chryso-zeolite ZSM-5 catalysts. The conversion and selectivity to ethylene were observed to be strongly dependant on the temperature and contact time of the reaction as well as the chemical composition of catalysts. The complete conversion was achieved at temperatures between 250°C and 400°C with weight hourly space velocity (WHSV) between $0.5h^{-1}$ and $100h^{-1}$.

Several characterization techniques were employed to investigate the physical and chemical properties of both types of zeolite, particularly, the effect of steam on the variation of the structure and acidity of zeolite ZSM-5. The results show that steam caused de-alumination and altered the surface properties and acidity of zeolite ZSM-5 which did not favor the formation of hydrocarbons other than ethylene. This observation led to the use of steam treated zeolite ZSM-5 for the conversion of aqueous ethanol

to ethylene rather than untreated zeolite ZSM-5.

The conversion of aqueous ethanol over steam treated zeolite ZSM-5 and chryso-zeolite ZSM-5 was suspected to occur through a diethyl hydroxonium intermediate. The nature of the products formed was found to be dependant on the reaction temperatures with either diethyl ether or ethylene being produced. However, the presence of dual basic and acidic sites in chryso-zeolite ZSM-5 could convert ethanol directly to ethylene by an E2 mechanism at high temperatures.

ACKNOWLEDGEMENT

I wish to express my sincere appreciation to my thesis supervisor, Dr. R. Le Van Mao, for his guidance and direction throughout my work.

I would like to thank the members of my Committee, Drs. A. English and R. Pallen, for their time and valuable suggestions.

Also, I thank my colleagues in the Catalysis Laboratory: Mr. G. McLaughlin, who gave technical as well as moral support throughout my work as a graduate student, Mrs. J. Yao for carrying out the TPD-NH_3 experiments, and Dr. P. Levesque, for the patience and interest he took in integrating me into the chemistry of heterogeneous catalysis.

I am indebted to Dr. J.A. Ripmeester of the National Research Council for the invaluable Solid State NMR results.

Finally, I would like to thank J. Parris for the interest and time she took in the typing and editing of this thesis.

Dedicated to my wife,

Thi Nhan Bui

and children,

Brian and Christina

TABLE OF CONTENTS

LIST OF FIGURES

LIST OF TABLES

LIST OF APPENDICES

INTRODUCTION

Ethylene or ethene is an organic "commodity" chemical which is consumed worldwide (80 billion pounds/year) (1). It is a basic feedstock for a large variety of industrial products, either directly as polyethylene, or after reaction with other chemicals as in the production of polyvinyl chloride, polystyrene, polyester, ethylene glycol, ethene oxide etc. The majority of ethylene is currently produced by the steam cracking of the available and low cost natural gas, paraffins and naphtha. As a consequence of the international oil crisis in 1973, gas and oil are no longer inexpensive and are becoming more costly each year. Furthermore, there is an increasing awareness of the finite nature of the fossil liquids and gaseous hydrocarbons and their ultimate depletion, while the demand for ethylene by the chemical industry is continuously increasing. Therefore, with other non-petroleum materials, the renewable biomass is expected to become an important alternative source for the production of ethylene during the next several decades when petroleum is no longer readily available.

The first step toward the utilization of biomass as an ethylene source involves the production of ethanol from biomass (figure A). This process can be carried out in three steps;

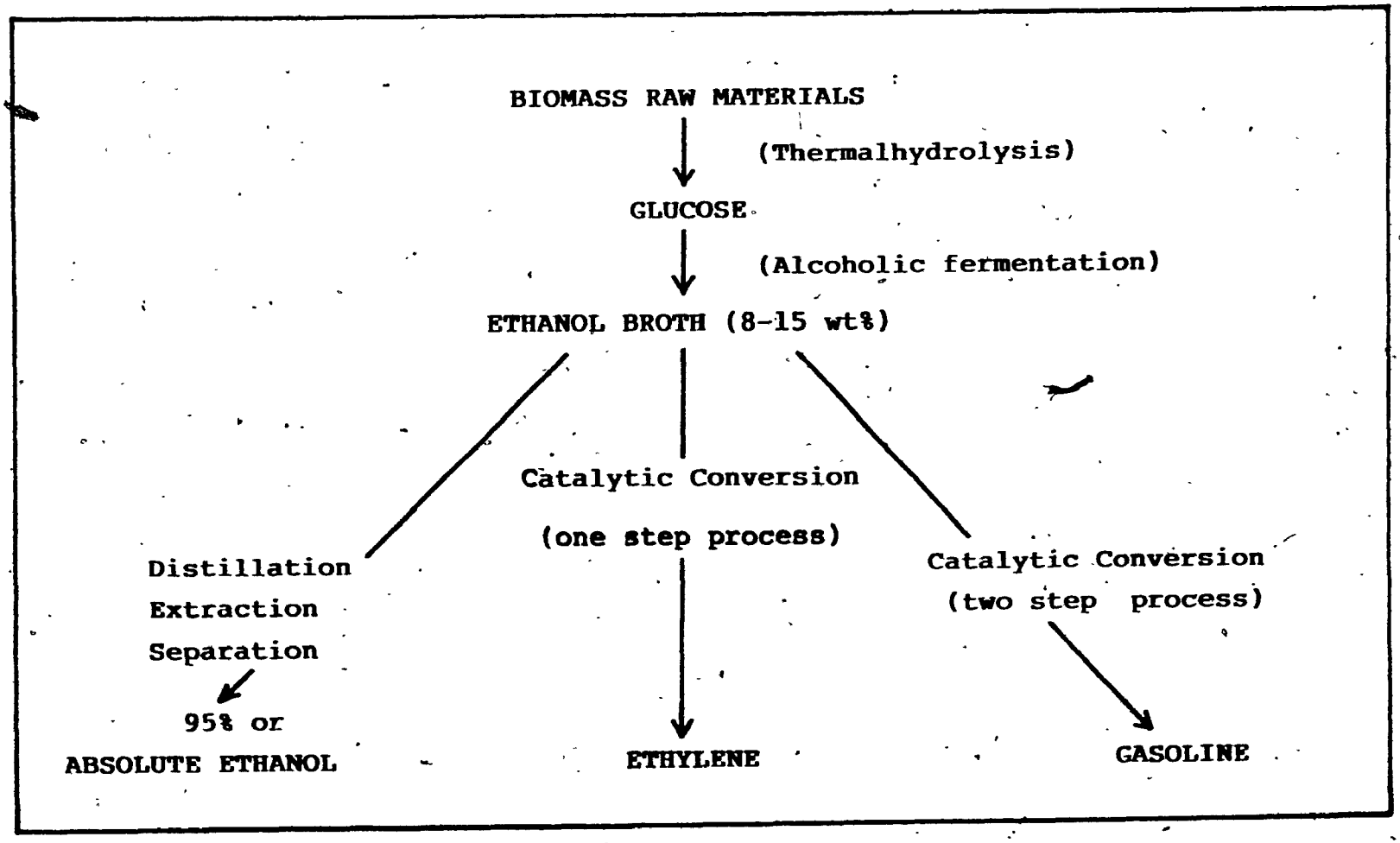

Figure A. Ethylene from biomass materials.

(1) Thermal hydrolysis of cellulose to fermentable sugars, mainly pentosan and hexosan (glucose).

(2) Fermentation of glucose to ethanol.

(3) Recovery of ethanol from the fermentation broth.

The last step is the most energy intensive one, primarily because ethanol is produced in small concentrations (typically 5 - 15wt%) in the fermentation broth and because of the existence of an azeotrope in the ethanol-water system at an ethanol concentration of about 95 wt% (2).

The next step is the catalytic conversion of ethanol to ethylene. So far an ethanol concentration of at least 90 wt% is necessary to provide a significant yield in ethylene, since all the catalysts, such as alumina, silica-alumina and mixed oxide, being used in the current ethanol dehydration processes are inhibited or destabilized by the presence of water (3,4). Thus, from a purely economic point of view, the use of biomass-based ethanol as an ethylene source is not an attractive route.

The great interest on the dehydration process with zeolites as catalysts began with the development of the methanol to gasoline process pioneered by Mobil Oil using zeolite ZSM-5. This was followed by some promising results on the conversions of aqueous ethanol to gasoline from the fermentation broths in the last few years (3-8). However, not much information about the conversion of aqueous ethanol

to ethylene over ZSM-5 zeolites have been published in the literature to date.

Therefore, the objective of this study is to investigate the feasibility of directly converting aqueous ethanol from the fermentation broth to ethylene over zeolite ZSM-5 and chryso-zeolite ZSM-5. The effects of chemical compositions of the catalysts and process variables on the conversion are established. The mechanisms and kinetics of the dehydration of aqueous ethanol to ethylene are finally examined.

CHAPTER 1 - INTEREST IN BIOMASS

1.1 Conversion of Biomass to Ethanol

Biomass refers to material produced by plants. It is comprised of the three following basic components:

(1) Cellulose (40-50%) is a linear polymer of D-glucose (a six carbon sugar) molecules held together by beta-glycosidic bonds. Cellulose fibers are arranged in bundles of parallel chains in which adjacent chains are bound together by hydrogen bonding between hydroxyl groups and hydrogen atom, forming a crystalline material with great mechanical strength and high chemical stability. Since the bond between the glucose units is the weak link in the chain, the polymer can be broken (hydrolyzed) into its component sugars.

(2) Hemicellulose (20-25%) is a polymer consisting primarily of five carbon sugars (pentosans and xylans), six carbon sugars and organic acids. These six carbon sugars are readily fermentable to ethanol, but standard industrial yeasts cannot ferment the five carbon sugars. Unlike cellulose, the structure and composition of

hemicellulose may vary widely between species. Hemicellulose is not crystalline and is readily hydrolyzed.

(3) Lignin (20-25%), the non-carbohydrate portion of the cell wall, is chemically bonded to and mixed with the hemicellulose. Lignin is a phenolic polymer, and cannot be converted to fermentable sugar (9).

The biomass conversion to ethanol process, in general, is comprised of three main steps:

(1) The biomass pre-treatment step: Due to the protection of the lignin sheath and the crystalline structure, the cellulose in wood or other plant tissues is normally not degradable to any appreciable extent by extracellular enzymes or acids. Pre-treatment methods can be chemical or physical processes, which are designed to modify the complex chemical and physical structure of biomass, to enhance the subsequent conversion rate and improve the sugar yields. Among the physical treatments, grinding, ball milling and ultimately steam explosion have been tried. While steam explosion appears to be the relatively cheap method, it is only effective for select hardwoods and annual plants and produces copious amount of furfurals from the extracted hemicellulose. Chemical treatments, on the other

hand, are designed to swell the cellulose and remove part of lignin, while physical treatments reduce the particle size and increase the surface area for attack (10).

(2) Hydrolysis step: Two general methods are available for hydrolysis of cellulose from biomass to glucose, viz, enzymatic and chemical (acid) processes. Enzymatic hydrolysis of cellulose requires prior disruption of lignin from biomass and is relatively slow due to the recalcitrant nature of the crystalline substrate. Additionally, the cost of producing the enzyme is extremely high, however, enzymatic hydrolysis is extremely efficient with conversion efficiencies greater than 95% achieved. In contrast, hydrolysis by strong acids is rapid and efficient (80-90% conversion) but utilizes considerable amounts of acid and necessitates extremely high capital investment for the corrosion resistant equipment. The use of dilute acid requires less capital but needs high temperature and pressure and yields relatively low conversion efficiencies (50-60%) and high by-products. A choice between those three options is thus not clear cut (11).

(3) Fermentation step: Both batch and continuous fermentation processes are currently available. Yeasts are the most commonly used microorganisms for ethanol production from a glucose solution. A schematic representation of the

anaerobic and aerobic yeast metabolic pathways is presented in figure 1.1. Under anaerobic conditions, glucose is converted to ethanol and carbon dioxide by glycolysis. The overall reaction to liberate energy for biosynthesis produces two moles of ethanol and two of carbon dioxide for every mole of glucose consumed.

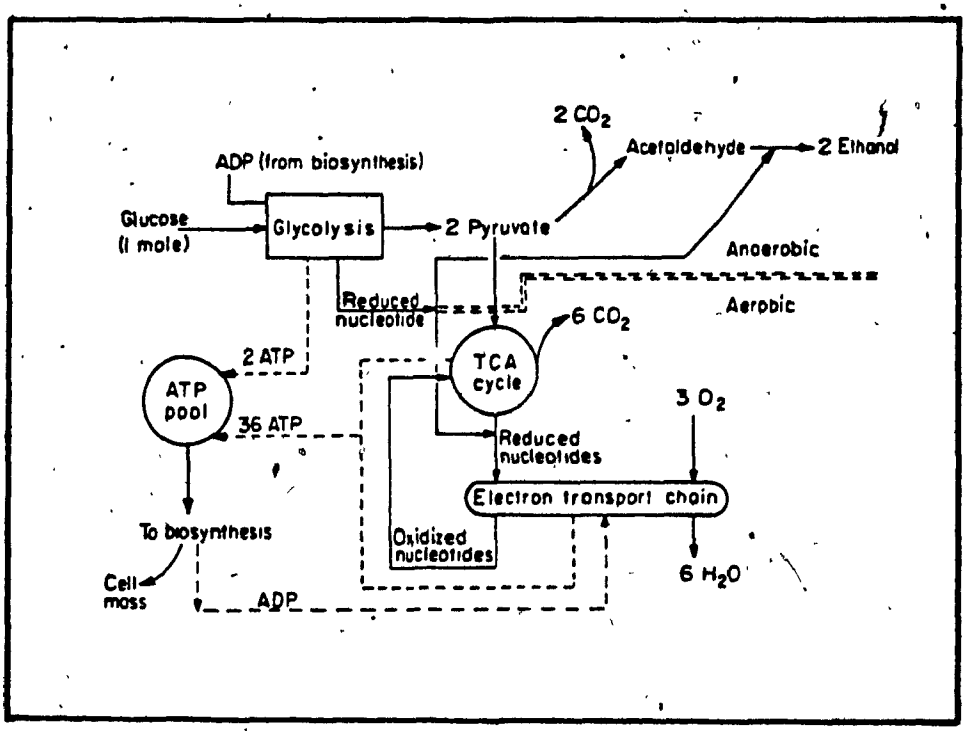

Figure 1.1 Simplified chart of anaerobic and aerobic catabolism of Saccharomyces cerevisiae.

Theoretically;

$$C_6H_{12}O_6 \longrightarrow 2C_2H_5OH + 2CO_2 + \text{Energy(stored as ATP)} \quad (1.1)$$

On a weight basis, every gram of glucose can theoretically yield 0.51g of ethanol. In practice though, actual ethanol yields are about 90% of the theoretical (i.e. 5-15wt%) of ethanol obtained from 25 - 35 wt% glucose media. A portion of the glucose carbon source is used for synthesis of new cell mass.

$$\underset{1.0g}{C_6H_{12}O_6} \longrightarrow \underset{0.46g}{C_2H_5OH} + \underset{0.44g}{CO_2} + \underset{0.10g}{\text{New Cells}} \quad (1.2)$$

Under aerobic conditions, glucose is converted to carbon dioxide and new cell mass, with no ethanol being formed (12).

1.2 Ethanol Dehydration

The chemistry of ethanol dehydration dates back to the eighteenth century when it was first reported that ethylene was released by passing ethanol or ether over heated alumina or silica. Since then, much research has been devoted to the investigation of various metal oxide catalysts, although only activated alumina and phosphoric acid on a suitable

support have become of industrial importance (13).

To date, the actual reaction mechanism of ethanol dehydration is not fully understood. It has been postulated by Knozinger, et al. (14) that the dehydration of ethanol to ethylene over alumina catalysts can be represented by the following scheme:

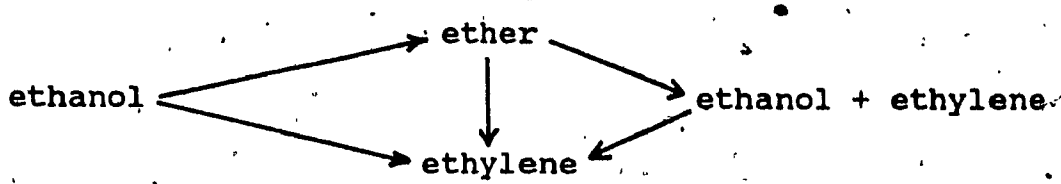

The formation of ether is favored at temperatures of approximately 230°C while at temperatures between 300°C to 400°C, ethylene, with a minimum content of ether is obtained. The practical ethylene yield is approximately 94% of the theoretical value of ethanol (95 wt%) in the feed. However, a lower yield is expected if aqueous ethanol (8-15 wt%) is used (3,4).

Figure 1.2 presents a simplified processing scheme for the conversion of commercial ethanol to ethylene using a fixed bed process. The ethanol feed is pumped into a steam heated vaporizer. The ethanol vapors, preheated with high pressure steam, are passed over catalysts of specially treated activated alumina for dehydration. A high yield (94%) of ethylene is produced in one pass, 1% remains unconverted and the remainder is

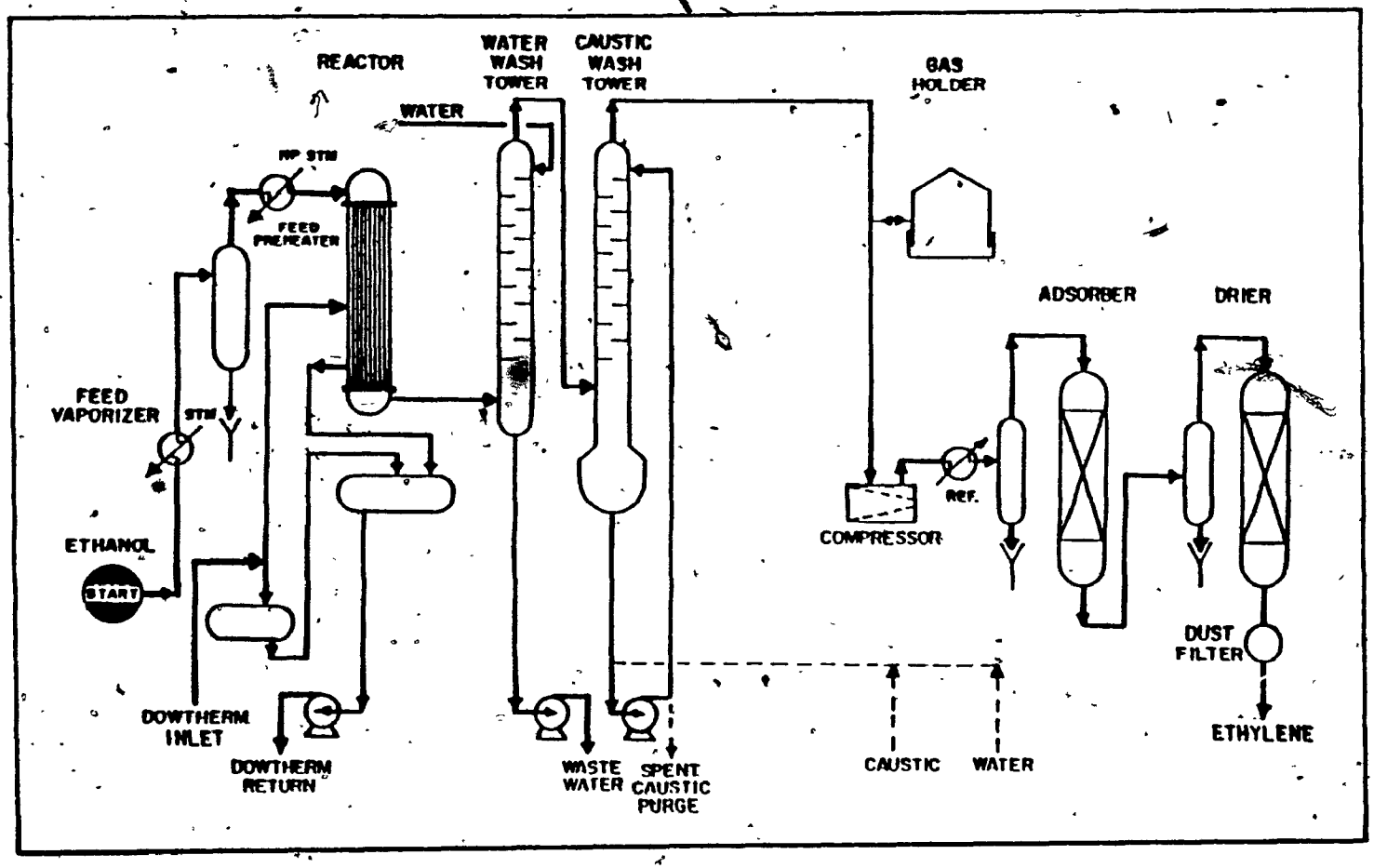

Figure 1.2. Ethanol to ethylene process.

converted to undesirable by-products such as aldehydes, acids, higher hydrocarbons and carbon dioxide.

The heat required for the reaction is supplied by condensing dowtherm vapor in the reactor shell. Temperature control is important, if it is too high, aldehydes are formed; if it drops too low, ethers are obtained. The reactor is designed to distribute heat evenly and to avoid hot spots. The catalyst is regenerated with air and steam every few weeks to remove carbon deposits.

The ethylene rich gaseous reactor effluent is quenched and water washed to cool the vapors while at the same time removing the unreacted alcohol and traces of aldehydes and acids. This is followed by washing with dilute caustic soda to remove carbon dioxide. The gas is then sent to a gas holder.

The gas from the gas holder is compressed, cooled by a refrigeration system, and sent first through an adsorber containing a bed of activated carbon, which selectively adsorbs "heavy" impurities such as butane and butylene, and then through a second vessel containing a desiccant, which removes water vapor from the ethylene. Dual systems are provided to permit continuous operation during reactivation of the adsorbents.

The purified ethylene is dried and has a purity in excess of 99 mole%. It meets the customary specification for polymerization grade ethylene.

Fluid bed processes, in place of the fixed bed externally heated reactor system, have been investigated extensively but have so far not found industrial applications.

Fluidized bed systems have a number of highly useful characteristics, namely ease of temperature control, improved heat and mass transfer, continuity of operation, and the ability to process large tonnages of reactants. Instead of multiple fixed bed reactors together with their auxiliary equipment, only a single fluidized bed reactor and regeneration system are required. The required heat for the reaction is supplied by circulating the fluidized catalyst through the regenerator. Just as in the fixed bed process, close temperature control is important for the ethanol dehydration reaction and is easily achieved in a fluidized bed. In a fluidized system, a uniform temperature is quickly established throughout the fluidized bed without formation of hot or cold spots.

Ethylene yields of 99% are obtained as compared to 94 to 96% with fixed bed systems. In addition to close temperature control, higher yields are also obtained by maintaining the catalyst at high activity at all times. This is accomplished by circulating the catalysts through a regenerator and by replacing catalyst which is lost due to attrition. Preliminary estimates indicate that an ethanol dehydration plant employing a fluidized bed process will

require a substantially lower capital investment than does a plant using fixed bed reactor.

CHAPTER 2 - ZEOLITES

2.1 Zeolite Materials

Zeolites are crystalline inorganic polymers based on a framework of XO_4 tetrahedra linked to each other by the sharing of oxygen ions, where X may be trivalent (e.g. Al, B or Ga), tetravalent (e.g. Ge or Si), or pentavalent (e.g. P) (15). The crystal structure of a zeolite is defined by the specific order in which a network of tetrahedral units are linked together. Their acidity is derived from the protons that are required to maintain electrical neutrality in the structure. The size of the zeolite pore openings are determined by: the number of tetrahedral units or alternately, oxygen atoms required to form the pore; and the nature of the cations that are present in the pore or at the apertures of the pore.

Zeolites are commonly grouped into three classes:(16)

PORE SIZE	NO. OF TETRAHEDRA	MAX. FREE DIAMETER
small	6,8	4.3Å
medium	10	6.3Å
large	12	7.5Å

Zeolites with more than one pore system are classified by

their largest accessible pore. The structures and pore sizes of characteristic large, medium and small pore zeolites are shown in figure 2.1.

The number and strength of the acid sites are complex functions of the nature and concentration of tetrahedral trivalent X groups, their location and the nature and concentration of exchangeable cations that are present. For convenience, zeolites are often classified according to their silicon to aluminum ratios. Generally, with the alumino silicate, the higher the silicon to aluminum ratio, the more thermally stable is the zeolite. Zeolites with silicon to aluminum (Si/Al) ratios greater than 10 are typically classified as high silica materials.

Zeolites can exist as natural or synthetic solids. However, only the latter, which can be produced with higher purity and less structural defects, have found their way into commercial catalytic processes. Their applications have expanded well beyond the boundaries of traditional petroleum refining. Presently, a substantial amount of effort by petroleum and chemical companies is directed toward the discovery and use of unique zeolites for the following areas:

Petroleum refining

Synfuels production

Petrochemical manufacturing

NO_x abatement

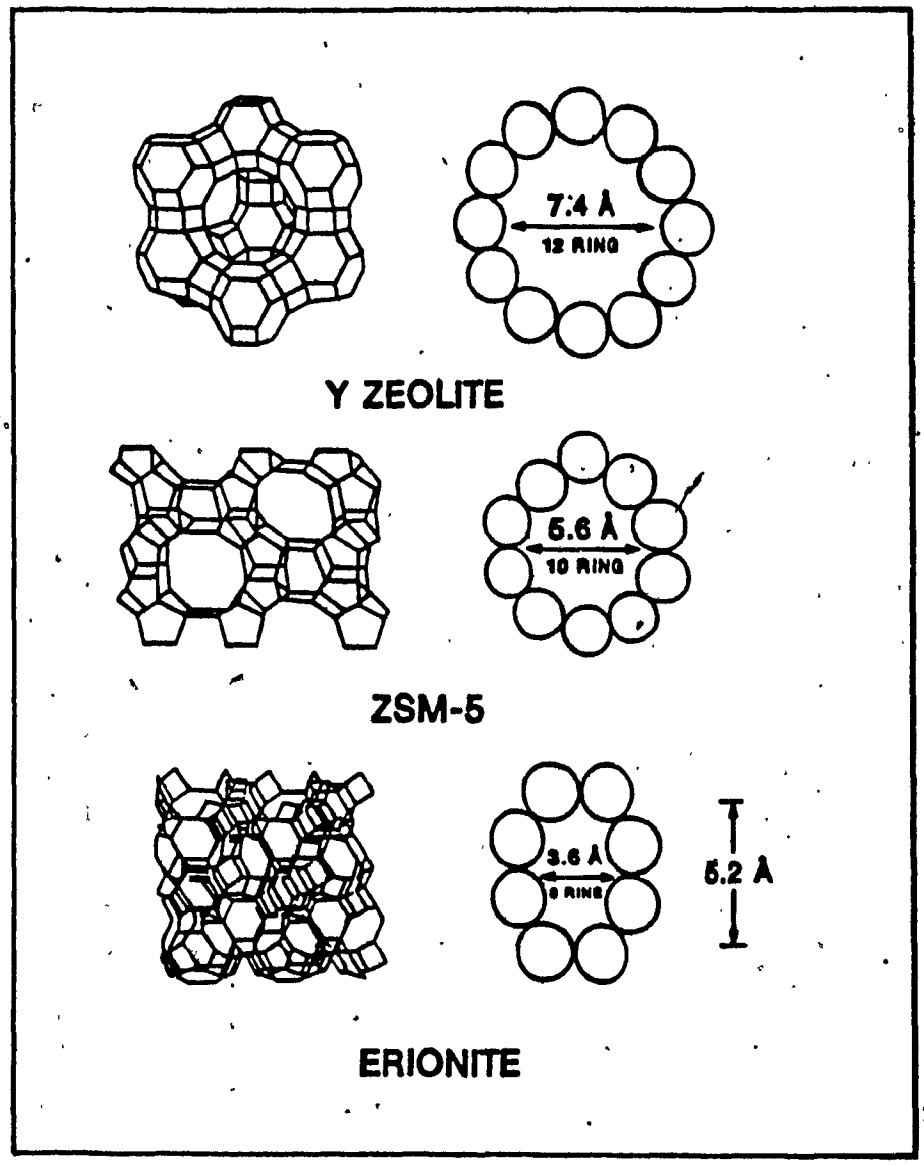

Figure 2.1. Framework structure and projection of zeolites.

Zeolite are crystalline materials that share the following six properties that make them attractive as heterogeneous catalysts:(15)

1. Well defined crystalline structure.
2. High internal surface areas (>400m^2/g).
3. Uniform pore with one or more discrete sizes.
4. Good thermal stability.
5. Ability to adsorb and concentrate hydrocarbon.
6. Highly acidic sites when ion exchanged with protons.

Almost all zeolite-catalyzed processes have exploited the high acid site density and the acid site strength as well as the specific control over ingress and egress of products and reactants afforded by unique zeolite pore systems. Presently, there are at least seven out of several hundred synthetic zeolites that are of industrial catalytic importance, see Table 2.1 (17).

2.2 Zeolite ZSM-5 (Zeolite Socony Mobil)

Zeolite ZSM-5 belongs to the crystalline alumino-silicate pentasil family. It is a shape selective synthetic zeolite with the channel system as shown in figure 2.2a (16).

Zeolite	Channel System*	Cavity**
Large Pore		
Faujasite	(12) 7.4, 3-Dimensional	6.6, 11.4
Mordenite	(8) 2.9 x 5.7, 1-D	Interconnected
	(12) 6.7 x 7.0, 1-D	Channels
L	(12) 7.1, 1-D	Unidimensional
Medium Pore		
ZSM-5	(10) 5.4 x 5.6, 1-D	Interconnected
	(10) 5.1 x 5.6, 1-D	Channels
Synthetic	(8) 3.4 x 4.8, 1-D	Interconnected
Ferrierite	(10) 4.3 x 5.5, 1-D	Channels
Small Pore		
Erionite	(8) 3.6 x 5.2, 2-D	6.3 x 13

* Number of oxygen atoms constituting the smallest ring determining pore size (in parentheses), pore diameter(s) in Å, and number of directions in which the channel runs.

** Cavity free dimension(s) in Å.

Table 2.1. Commercially important zeolites used in catalytic applications.

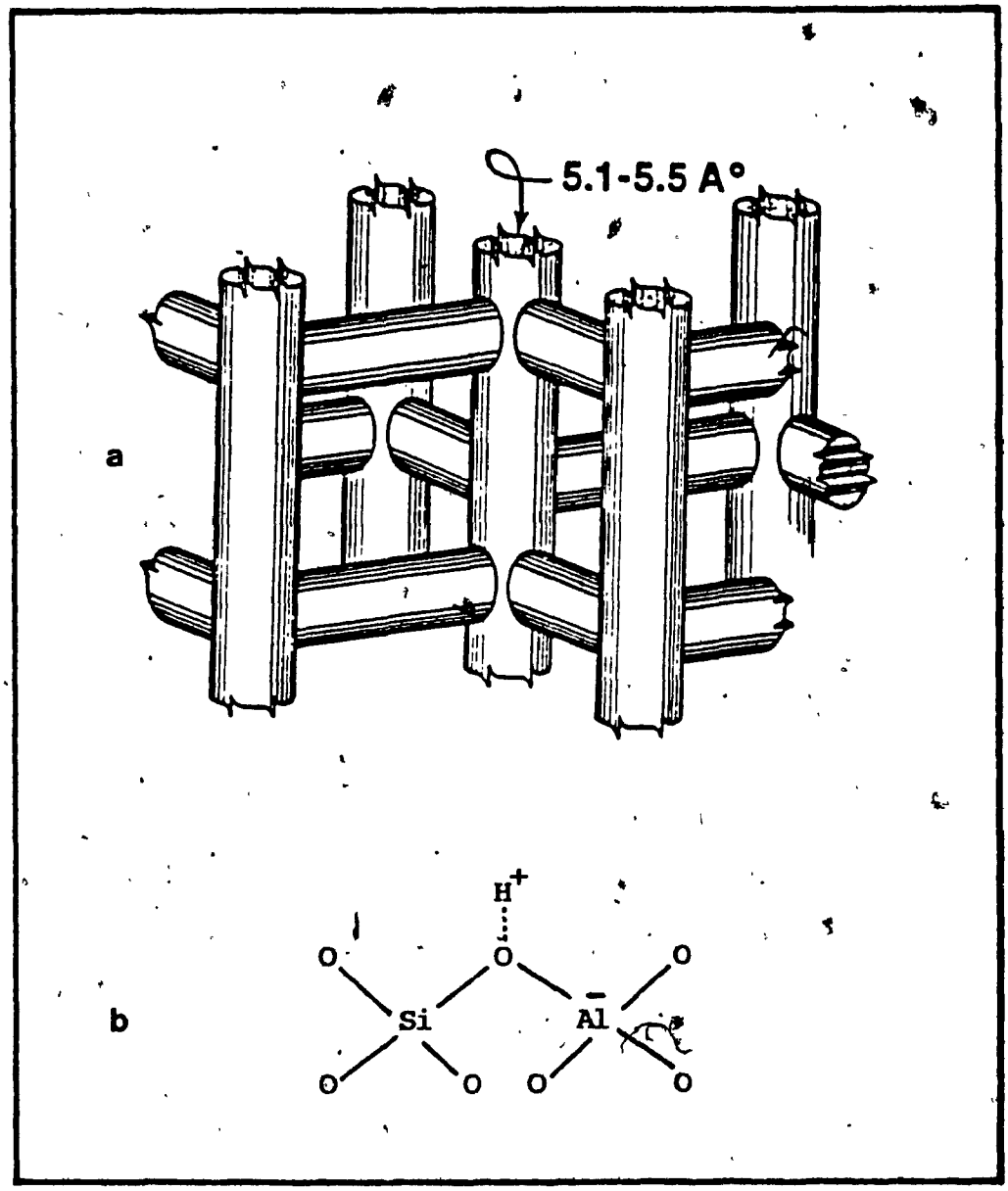

Figure 2.2. (a) Channel system and (b) Bronsted acid center of zeolite ZSM-5.

The general chemical formulation of zeolite ZSM-5 is:

$$M_{x/n}[(AlO_2)_x(SiO_2)_y]\cdot zH_2O$$

where n is the charge on the cation, z is the water of hydration, y/x or Si/Al is ranged from 5 to infinity, and M is the cation (Li^+, Na^+, K^+ ...) which neutralizes the negative charge located on the aluminum. When M is exchanged with a proton, the zeolite becomes a strong Bronsted acid, and the presence of the acid center within the zeolite ZSM-5 framework can be visualized in figure 2.2b.

Presently, zeolite ZSM-5 is used in several important industrial processes such as:

Methanol to gasoline (MTG)
Distillate dewaxing
Xylene isomerization
Toluene disproportionation
Ethylbenzene synthesis
Lubrification oil-dewaxing

all using fixed bed reactors.

2.3 Chryso-Zeolite ZSM-5

Chryso-zeolite ZSM-5 was successfully synthesized by Le Van Mao et al. (18) at Concordia University, in which chrysotile asbestos fibers were used as starting materials.

Chrysotile asbestos is available in Quebec with the long fibers being used in many industrial materials. The short fibers (grade 7) are usually rejected and it is possible to modify those low cost fibers for a specific purpose.

The chrysotile asbestos fibers contain silica, magnesium oxide, iron oxide and some impurities (figure 2.3 and Table 2.2). By partially leaching out the magnesium with organic or mineral acids, the remaining silica is available for synthesis of zeolite. To the thus leached asbestos materials, a source of aluminum is added and the chryso-zeolite is synthesized under appropriate hydrothermal conditions.

Asbestos is a toxic material, therefore tests were performed, by J. Dunnigan at the University of Sherbrooke, on chrysotile asbestos and chryso-zeolite type A to evaluate their toxicity. It was observed that chryso-zeolite was safe. It did not damage the cell membrane of the red blood cells. In addition, the viability and the leakage of two marker enzymes were tested on cultured pulmonary macrophages. The results show that chrysotile asbestos fibers induced cytotoxic responses, whereas equivalent

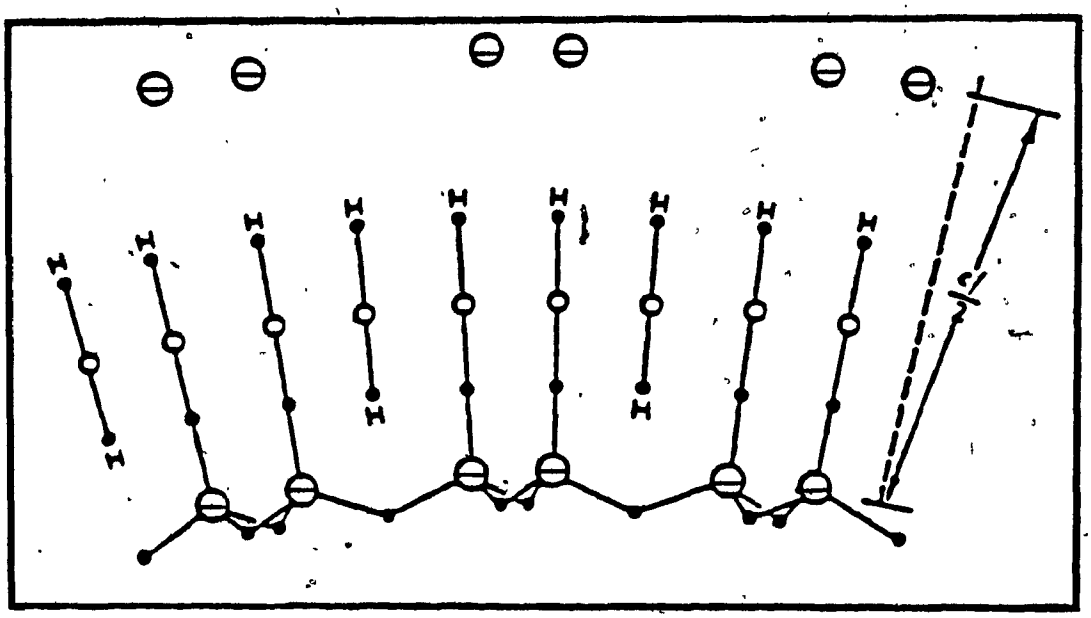

● Oxygen O Magnesium ⊖ Silicon

Figure 2.3. Structure of chrysotile asbestos fiber, $Mg_3Si_2O_5(OH)_4$.

Chemical composition	Weight percent
SiO_2	42.8
MgO	50.2
FeO, Fe_2O_3	6.6
Al_2O_3	0.1
Na_2O	0.1
Others	0.2

Table 2.2. Chemical composition of chrysotile asbestos fiber (7 TF 12) in dried oxide basic.

Samples	Percentage of hemolysis in 60 min.
Control	0.0
Chrysotile	95.0
Chryso-zeolite	0.0

* 1.0 ug of each solid

Table 2.3. Hemolytic response to chrysotile versus chryso-zeolite.

Samples	Viability (% control)	Enzyme leakage (% liberation)	
	ATP(1)	LDH(2)	GAL(3)
Control	100.0	2.1	1.2
Chrysotile	28.4	62.6	59.6
Chryso-zeolite	98.9	7.6	5.2

* 250 ug of each solid

(1) ATP : Adenosine triphosphate

(2) LDH : Lactic dehydrogenase

(3) GAL : Beta-Galactosidase

Table 2.4. Pulmonary macrophase response to chrysotile versus chryso-zeolite.

amounts of chryso-zeolite A gave essentially no significant response (Tables 2.3 and 2.4). The same results should be valid for chryso-Zeolite ZSM-5.

Chryso-Zeolite ZSM-5 was observed to be very effective in the conversion of methanol to gasoline. When metals, such as Zn and Mn, were incorporated into its structure there resulted a dramatic enhancement of the selectivity of the reaction towards olefins and aromatics in the gasoline products (19,20).

CHAPTER 3 - EXPERIMENTAL

3.1 Synthesis

3.1.1 Source of Chemicals

Chemicals used in the synthesis, preparation and characterization of zeolite ZSM-5 and chryso-zeolite ZSM-5 catalysts in this work were purchased from several suppliers as given in the following list,

CHEMICALS	SUPPLIER
Alumina (70-230 mesh)	Merck
Ammonium Chloride (99%)	Fischer Scientific Co.
Asbestos (7TF12)	Asbestos Institute
Bentonite, U.S.P.	Fischer Scientific Co.
Ethanol (99%)	Aldrich Chemicals
n-Hexane (99.99%)	Aldrich Chemicals
Silica gel (60-200 mesh)	J.T. Baker Chemical
Sodium aluminate	Anachemia
Sodium hydroxide (granular, 97%)	Aldrich Chemicals
Tetrapropylammonium Bromide (98%)	Aldrich Chemicals

3.1.2 Synthesis of Zeolite ZSM-5

Zeolite ZSM-5, used as catalysts in this work, were

prepared in our laboratory according to Argauer and Landolt's method (21) which can be described as follows:

(A) Hydrothermal Synthesis of Zeolite ZSM-5

The sodium form of zeolite ZSM-5 was prepared by adding silica gel to an aqueous solution of sodium hydroxide and tetrapropylammonium bromide. The gel mixture was then heated at 70°C to 80°C for one hour with vigorous stirring. To this, an aqueous solution of sodium aluminate (Fisher), was added. The mixture was heated at 70°C to 80°C for another fifteen minutes with rapid stirring. The gel mixture was then poured into a Hastelloy container and loaded into an autoclave. The autoclave was heated at 170°C for ten days under an autogeneous pressure of circa eight atmospheres.

After unloading, the solid was filtered, washed with double deionized water, dried at 120 °C for 12 hours, and finally calcinated at 550°C for 12 hours in the air (Table 3.1)

(B) Preparation of the acidic form of ZSM-5 Zeolite

The acidic form of zeolite ZSM-5 was obtained either by direct ion exchange with protons (from a dilute acid medium) or by ion exchange with ammonium ions and subsequent calcination. The second technique is used in the present work. The sodium form of zeolite ZSM-5 was brought in

Catalyst Precursors	SiO_2 source		Na aluminate (g)	TPA.Br (g)	NaOH (g)	Water (ml)	Synthesis		Products (g)
	source	weight (g)					temp (^oC)	time (days)	
P-(21)	Silica	110	11.50	110	7.0	390	170	10	114.2
P-(45)	Silica	52	4.00	80	5.0	320	170	10	48.8
P-(75)	Silica	55	1.55	55	3.5	195	170	10	53.7
P-(124)	Silica	55	1.10	55	3.5	195	170	10	54.8
A-(21/83)	Alix(83)	52	3.00	80	5.0	360	170	10	49.8
A-(22/92)	Alix(92)	52	3.00	80	5.0	360	170	10	44.2
A-(26/99)	Alix(99)	135	10.50	110	7.0	390	170	10	115.0

Table 3.1. Preparation of zeolite ZSM-5 and chryso-zeolite ZSM-5.

contact with a solution of NH_4Cl at 5% by weight, using 10mL of solution per gram of solid. The suspension was heated between 70°C and 80°C under reflux conditions and with moderate stirring. After one hour of heating, the suspension was allowed to settle and the liquid then rapidly removed. A fresh volume of NH_4Cl solution was added and the suspension was heated again for another hour. The exchange lasted five hours.

The suspension was filtered and the solid washed with double deionized water until Cl^- ions were no longer present in the washing. The compound was then dried at 120°C and calcinated in air at 550°C for 12 hours. The NH_4^+ was exchanged with Na^+ inside the zeolite particle, and during activation, NH_3 was released and the acid form of zeolite ZSM-5 was obtained.

At this stage, the zeolite ZSM-5 was characterized using several techniques as described in section 3.4.

3.1.3 Synthesis of Chryso-Zeolite ZSM-5

Chryso-zeolite ZSM-5 was prepared according to a technique described by Le Van Mao et al. (18) in which the chrysotile asbestos fibers (7TF12 short fiber grade) were digested with mineral acid solution (usually HCl) at 80°C for several hours. After dilutions with cold water, the suspension was allowed to settle for 12 hours, filtered,

washed with water and finally dried at 120°C for 12 hours. The obtained solid was named Alix, which was used to replace silica gel for synthesis of chryso-zeolite ZSM-5. The experimental parameters for the preparation of the leached asbestos fiber (Alix) are reported in Table 3.2.

The hydrothermal synthesis and the preparation of chryso-zeolite ZSM-5 are similar to the synthesis and ion exchange for zeolite ZSM-5 as described in section 3.1A and B.

3.1.4 Preparation of Catalyst Pellets

The zeolite ZSM-5 obtained after ion exchange was in the form of a powder, which gave rise to excessive pressure drops and was very difficult to handle when it was used in a fixed bed reactor. Therefore, the catalysts used in this work were in the form of pellets which were prepared by intimately mixing the zeolite with bentonite (binding agent) in the weighted ratio of 4:1. Bentonite is a mineral clay which does not react with the zeolite nor does it promote the conversion of alcohols to hydrocarbons. Distilled water was then added, 1.0mL/gram solid. The wet paste was then extruded into small catalyst pellets (1.0mm) and finally dried at 120°C for 12 hours and activated at 550°C for another 12 hours.

Alix	Amount of 7 TF-12 (g)	HCl N	Sol. ml	Heating time (80 °C)	Products (Dehyd) (g)	SiO_2 (%)	Al_2O_3 (%)	Na_2O (%)	MgO (%)	Fe_2O_3 (%)	MLD (%)
83	150	2.4	1500	2.0 h	65	88.0	0.35	0.10	7.70	3.86	85
92	150	2.4	1500	5.0 h	65	89.0	0.35	0.13	4.10	6.43	92
99	600	2.4	6000	3.5 h	257	92.5	0.36	0.11	2.46	4.52	95

Table 3.2. Preparation of ALIX from asbestos fibers 7 TF 12.

3.1.5 Hydrothermal Treatment of Zeolite ZSM-5

Many types of zeolites are well known to undergo structural degradation when subjected to water vapour at elevated temperatures (22). Therefore, if zeolite ZSM-5 is used in the moisture-rich atmospheres, as encountered in the conversion of aqueous ethanol to ethylene, the effects of steam on the physical and catalytic properties of zeolite must be understood. In order to investigate the effects of steam in advance, some previously prepared zeolite ZSM-5 samples were hydrothermally treated and then characterized by several techniques. The hydrothermal treatment procedure is described as follows:

The zeolite ZSM-5 sample (5.0g) was loaded in a fixed bed reactor and heated to 500 °C. A gaseous mixture of nitrogen and steam was obtained by vaporizing water which was delivered by an infusion pump (13g/h .). The nitrogen flow rate was maintained at 20mL/min. The resulting zeolite sample was called Steamed Catalysts.

3.2 Physical and Chemical Characterization

In order to obtain the physical and chemical properties of zeolite ZSM-5 and chryso-zeolite ZSM-5 the following techniques were used:

Atomic Absorption Spectroscopy

Powder X-ray Diffraction

Surface Measurement (BET)

Magic Angle Spinning NMR

Ammonium Temperature Programmed Desorption

Measurement of Hydrophobicity

3.2.1 Atomic Absorption Spectroscopy

Atomic absorption spectroscopy was used to determine the concentrations of Si, Al, Na, Mg and Fe contained in the Alix and zeolite. A sample of 0.1g was weighed in a platinum crucible, calcinated at 750°C for one hour, then reweighed to obtained the dry weight. A fusion mixture was added to the zeolite material (0.9g of potassium carbonate and lithium tetraborate in ratio 2:1), mixed and placed at 750°C for one hour. The resulting solid was dissolved in acid (5mL concentrated HCl and 10mL 10% H_2SO_4), and oxygenated by addition of 5.0mL hydrogen peroxide (30%). The mixture was then diluted to 100mL and atomic absorption run on a Perkin Elmer Model 503. Further dilutions were occasionally required. The content in metal oxides were calculated from external standards.

From the atomic absorption results, two significant quantities were derived:

(1) The Magnesium Leaching Degree (MLD) of the chryso-zeolite ZSM-5 was defined as:

$$MLD\% = \frac{(MgO)_i - (MgO)_f}{(MgO)_i} \times 100 \qquad (3.1)$$

where $(MgO)_i$ is the initial magnesium oxide content in the chrysotile asbestos fiber and $(MgO)_f$ is the magnesium oxide content in the Alix or in the chryso-zeolite ZSM-5 samples (based on the dried oxide basis).

(2) The silicon to aluminum ratio was defined as:

$$\frac{Si}{Al} = \frac{moles(SiO_2)}{moles(Al_2O_3)} \times \frac{MW(Si)}{MW(Al)} \qquad (3.2)$$

where W refers to the weights percents and MW the molecular weights.

3.2.2 Powder X-ray Diffraction

The structures of zeolite ZSM-5 and chryso-zeolite ZSM-5 were identified by means of their characteristic powder diffraction pattern (21). The catalyst sample was ground mechanically with NaCl (internal standard) in a ratio of 2:1 by weight. The solid mixture was then pressed in a plexi-glass sample holder and the powder X-ray diffraction

recorded. A powder X-ray diffractometer, CuK_α radiation, (λ = 1.54178Å, Ni filter) with an integration system was used. The counts recorded during scanning of the peaks were used to evaluate the degree of crystallinity.

The degree of crystallinity (DC) in the zeolite ZSM-5 structure of the samples was determined by a procedure similar to that of Kulkarmi et al. (23). However, to ensure that the measurement did not depend on the sample preparation, NaCl was used as an internal standard (24). This compound exhibits strong diffraction peaks between 31.0-32.5°(2θ). The zeolite ZSM-5 sample, which had the highest crystallinity, was assigned a DC value of 100%.

3.2.3 Surface Measurement (BET)

The surface area of a solid catalyst is an important parameter in heterogeneous catalysis. It was measured by physical adsorption of nitrogen in a static system at liquid nitrogen temperatures, and is known as BET (Brunauer, Emmett and Teller) method (25).

The BET theory is mainly based on the following assumptions:

(1) Homogeneous surfaces which could only accommodate one adsorbate molecule per site (nitrogen-zeolite interactions).

(2) Multi-layer adsorption due to nitrogen-nitrogen

interaction. No lateral interaction between adsorbed molecules are present.

(3) An adsorption - desorption equilibrium between molecules reaching and leaving the solid surface.

The physical and mathematical treatment of these hypothesis lead to the BET equations:

$$\frac{P}{V(P_o-P)} = \frac{1}{V_mC} + \frac{C-1}{V_mC}\cdot\frac{P}{P_o} \qquad (3.3)$$

where: P = Pressure of the N_2 gas in equilibrium with the surface.

P_o = Saturated vapor pressure of N_2 at liquid N_2 temperature (77.3k) with P_o = 760mm Hg.

V = Volume of N_2 (STP) adsorbed by the sample.

V_m = Volume of N_2 (STP) corresponding to the formation of a monolayer.

C = Constant varying with the adsorbent - adsorbate interaction. It is related to the differential heat of adsorption E_A and the heat of liquefaction E_L by the following equation:

$C = \mathrm{Exp}(E_A - E_L/RT)$

where: R = ideal gas constant

T = absolute temperature

From the plot of $P/V(P_o - P)$ versus P/P_o at low partial

pressures ($0.05 < P/P_o < 0.35$), V_m was obtained, which is:

$$V_m = 1/(\text{slope} + \text{intercept})$$

The value of V_m (cm^3/g) was then used to obtain the specific area of the solid.

$$\text{Area} = [V_m/22414] \times N \times A_m \times 10^{-20} \quad (m^2/g) \qquad (3.4)$$

where: N = Avogadro's number.

A_m = Area occupied by a nitrogen molecule (taken to be $16.2m^2$).

The surface area of the catalysts used in this work were measured on the conventional BET apparatus as shown in figure 3.1. The measurement procedure was performed as follows:

(1) Sample Degassing

The sample was degassed at 300°C for three hours under vacuum ($P < 10^{-4}$mm Hg).

(2) Calibration of the Dead Volume

Helium was introduced into the BET apparatus, sample chamber closed and the mercury level on the volumetric column adjusted to obtain the corresponding pressure. The

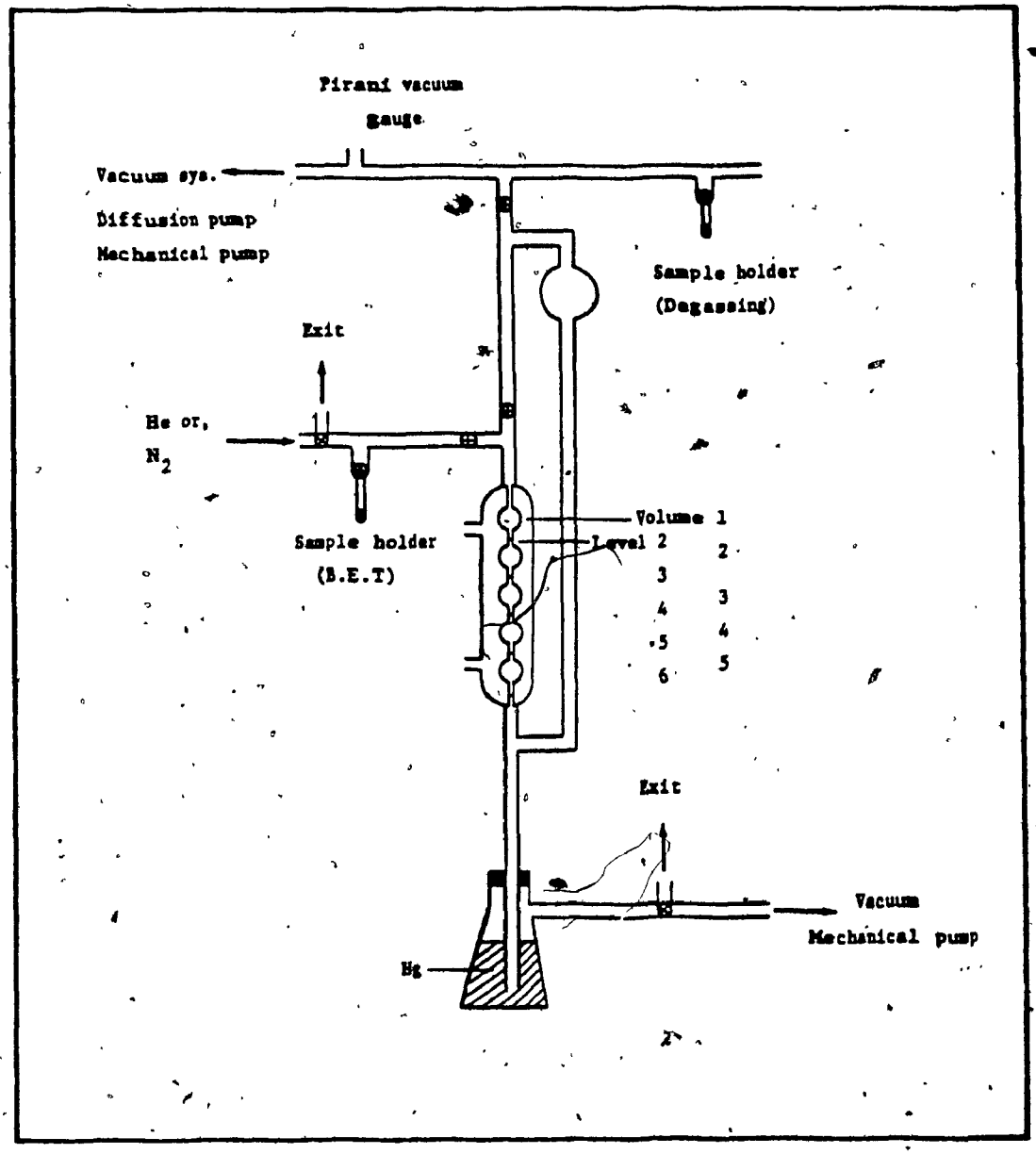

Figure 3.1. B.E.T. apparatus.

dead volume, X, was calculated by:

$$P_5(V_5 + X) = P_6(V_6 + X) \qquad (3.5)$$

and gave:

$$X = \frac{P_5V_5 - P_6V_6}{P_6 - P_5} \qquad (3.6)$$

where P_5 and P_6 are the pressures recorded (mm Hg) when the mercury was above the level 5 or 6. V_5 and V_6 are the volumes above the level 5 or 6.

All the volumes measured are converted to STP by using:

$$\frac{P_1V_1}{T_1} = \frac{P_2V_2}{T_2} \qquad (3.7)$$

where 1 is the experimentally obtained data and 2 are under STP.

The sample chamber was opened and the mercury levels adjusted. The pressures were recorded at each level. From the measurements, the free space was obtained (space available in the sample holder between the zeolite particles at various pressures).

(3) Nitrogen Adsorption Isotherm

The helium was evacuated from the system and was replaced by nitrogen. By keeping the sample holder closed,

the total nitrogen introduced was evaluated by measuring the pressure at various volumes. After the opening of the sample chamber, nitrogen was adsorbed in the sample which was in liquid nitrogen (-195°C). The pressure was measured at various volumes and the partial pressure (P/P_o) were evaluated as well as adsorbed volumes of nitrogen. From the results, the slope and the intercept of a $P/(P_o - P)V$ versus P/P_o plot gave V_m, the volume of a monomolecular layer. The specific surface area of the different zeolite and chryso-zeolite was calculated from V_m.

The experimental readings were computed using a computer program (Basic language) on an Olivetti M24 Computer (Appendix I).

3.2.4 Magic Angle Spinning NMR

The magic angle spinning NMR technique was used to investigate the local structure of silicon and aluminum present in zeolite ZSM-5. All the ^{29}Si-MAS-NMR and ^{27}Al-MAS-NMR spectra were obtained on a VARIAN VXR 300 Ft-NMR spectrometer (Université de Montréal), equipped with a superconducting solenoid magnet. A VXR 300 model computer was used for data acquisition in conjunction with KEL-F Doty probes (Doty Sc.). The NMR parameters used to scan the spectra of the ^{29}Si and ^{27}Al nucleus are summarized in Table 3.3.

Parameters	Nucleus ^{27}Al	Nucleus ^{29}Si
Resonance frequency / MHz	78.159	59.592
Spin rate / Hz	3820	4060
Spectra width / Hz	30,030	20,000
Pulse width / degree	36	36
Reference	$Al(H_2O)_6^{3+}$	$Si(CH_3)_4$

Table 3.3. NMR Parameters for ^{27}Al and ^{29}Si Nuclei.

3.2.5 Temperature Programmed Desorption of Ammonia (TPD-NH_3)

The temperature programmed desorption of ammonia was used to study the total acidity and the acid strength distribution of both zeolite ZSM-5 and chryso-zeolite ZSM-5 catalysts.

The theory behind the TPD-NH_3 experiment was adapted from that of the flash-filament experiment used in surface science. There were two assumptions made: First, no re-adsorption of ammonia took place during desorption and second, the ammonia molecules were adsorbed on a homogeneous

surface without interaction among adsorbed molecules (26). These assumptions presumed that all molecules adsorbed with the same activation energy. It was assumed that the intracrystalline zeolite surface was homogeneous and the amount of ammonia adsorbed in the experiment was less than that required for monolayer coverage.

The TPD-NH_3 experiments were performed according to the technique described by Le Van Mao et al. (27) on the apparatus, which is shown schematically in figure 3.2.

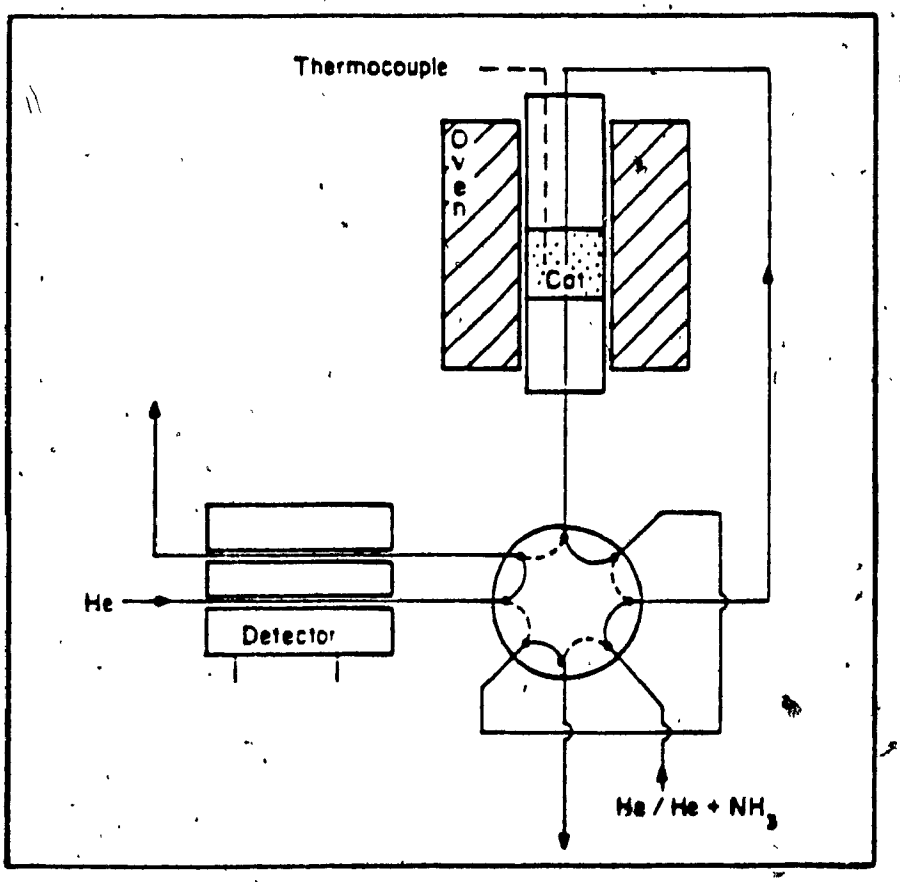

Figure 3.2. TPD-NH_3 apparatus.

Before adsorption, the pellet zeolite catalyst (0.9 - 1.0g) was dried at 120°C for 6 hours and activated at 540°C for 10 hours under flowing of pre-dried helium with a flow rate of 20mL/min. The adsorption took place at 100°C with pre-dried ammonia flowing at 20mL/min. for 40 min. The catalyst was then flushed with He at 100°C for 40 min. The desorption was done by heating the catalyst from 100 to 220°C with a heating rate of 15°C/min. under flowing He. The catalyst was maintained at 220°C for 30 min., then heating continued to 355°C at the same heating rate, and then kept at this temperature for another 30 min. Finally, the catalyst was heated up to 540°C at the heating rate indicated above. During desorption, the desorbed ammonia was recorded by an integrator (Hewlett Packard, Model 3392A) which was interfaced to a gas chromatographer equipped with a thermal conductivity detector (TCD). Quantitatively, the amount of the desorbed ammonia was obtained by using a calibration curve. This calibration curve was set up by injecting known amounts of ammonia and then recording the corresponding TCD responses.

3.2.6 Measurement of Hydrophobicity of Zeolites

The hydrophobicity of zeolite ZSM-5 and chryso-zeolite ZSM-5 were evaluated by the adsorption of water and n-hexane technique as described by Le Van Mao et al. (28,29). The

adsorption was done by degassing about 0.2g of zeolite at 300°C for 3 hours under vacuum. The samples were cooled down to room temperature, reweighed and then brought in contact with the vapors of water or n-hexane until equilibrium was reached. The sampling tubes were weighed and the equilibrium adsorption capacity (weight of adsorbed vapor per weight of zeolite) was calculated. The operating conditions are summarized in Table 3.4.

The relative affinity index (R.A.I.) is defined as:

$$RAI = \frac{\text{Volume of adsorbed n-hexane per gram zeolite}}{\text{Volume of adsorbed water per gram zeolite}} \quad (3.8)$$

which is greater than or equal to one. The higher the RAI value, the larger the hydrophobicity of zeolite is. The n-hexane adsorption into zeolite ZSM-5 can sometimes be used to measure the degree of crystallinity. It is better than the powder X-ray diffraction technique when the degree of crystallinity is low.

3.3 Catalysis

Catalytic tests were performed by injecting an aqueous solution of ethanol (concentration from 5wt% to 15wt%) using an injection syringe on an infusion pump into a vaporizer-gas mixer. Nitrogen gas was supplied to the vaporizer-gas

Adsorbate	Critical diameter (A)	Vaporization temperature (^{o}C)	Vapor pressure (mm Hg)	Adsorption temperature (^{o}C)	time required (hours)
n-hexane	4.9	0	45	25	4
water	2.8	22	22	25	12

Table 3.4 Operating condition for the n-hexane and water adsorption.

mixer from a cylinder connected in series with a flowmeter. The vaporized feed was then carried by the nitrogen gas through a catalyst bed set in a tubular reactor (fixed bed reactor) contained inside a furnace which was thermo-regulated. A chromel-alumel thermocouple was placed in the catalyst bed in conjunction with a digital thermometer unit, to monitor the temperature of the catalyst bed. The gaseous mixture flowing out of the reactor was run through a series of condensers, maintained at 5 - 10°C, to a liquid collector immersed in an ice bath followed by a cylinder from which gas sampling was carried out (figure 3.3).

Following a pre-run of 10 minutes, the liquid products were collected and the gaseous ones were analyzed periodically by gas chromatography (GC) using a 5m long column packed with chromosorb-P coated with 20% by weight of squalene, connected in series with a 2.5m long column packed with carbopack graphite coated with picric acid (0.10% by weight). The GC used was a dual FID Hewlett Packard Model 5790 equipped with a 3392 A Model integrator. It was also equipped with a capillary column (length 50m; PONA type fused silica coated with a cross linked polymer) which was used for accurate analyses of the liquid fraction after the completion of a run. The composition of the aqueous layer was also determined by GC using an ethanol in water calibration standard curve.

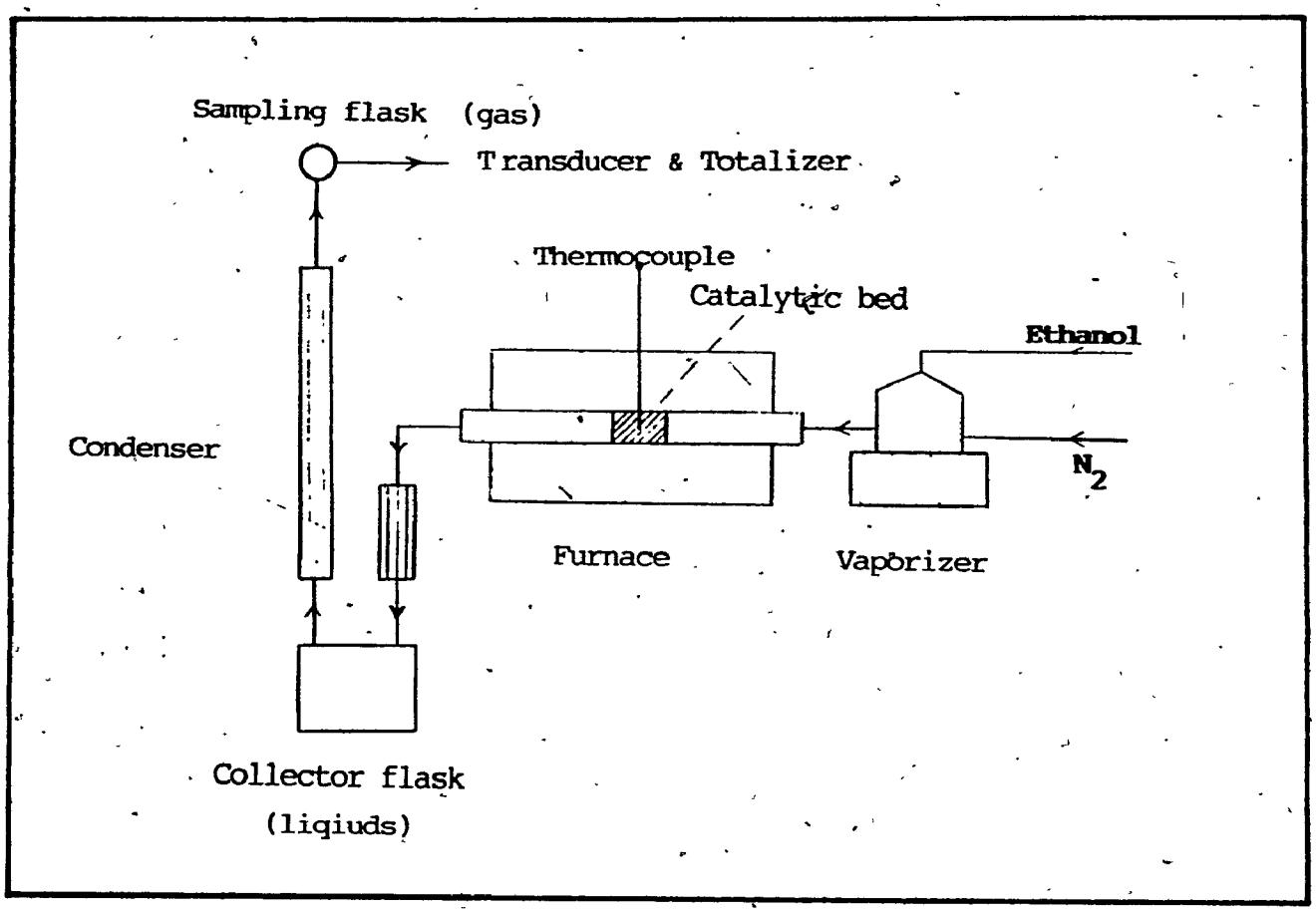

Figure 3.3. Experimental set-up for reaction at atmospheric pressure.

The reaction conditions used in this experiment were as follows:

Temperature	175 - 400°C
Catalyst weights	0.10 - 5.0g
Total pressure	1 atm
Inert gas (N_2)	20mL/min
Weight hourly space velocity	2.5 - 140 h^{-1}
Duration of run	3.5 hours

In the study of the effect of steaming on the catalyst, at the end of each run, the catalyst bed was regenerated by heating it at 550°C with air passing through it. The regeneration operation usually lasted 12 hours in order to completely remove the carbon eventually deposited on the catalyst surface.

In the kinetic and mechanistic studies, the reaction of aqueous diethyl ether was also investigated. Since diethyl ether was not soluble in water, the following procedure was applied: A flask containing 50g liquid diethyl ether was kept at 10°C by using a cooling device. The nitrogen gas, before going to the vaporizer gas mixer, was passed through the ether flask at a flow rate of 20mL/min. The ether vapour was carried by nitrogen to the vaporizer-gas mixture where water was injected by an injection pump at a rate of 13.3g/h . The vaporized water and ether vapour gaseous

mixture were then carried through the catalyst bed by nitrogen gas. The concentration of the gaseous diethyl ether obtained under these conditions was 6.5±0.1 weight %, which was suitable for investigations.

The total conversion of the reaction was calculated by:

$$\text{Total (\%)} = \frac{(\text{EtOH})_{in} - (\text{EtOH})_{out}}{(\text{EtOH})_{in}} \times 100 \qquad (3.9)$$

where $(\text{EtOH})_{in}$ was the number of carbon atoms (C-atoms) of ethanol in the feed, $(\text{EtOH})_{out}$ was the C-atoms of ethanol recovered in the product. The number of carbon atoms of an organic compound was determined by:

$$\text{C-atom} = \frac{\text{Weight} \times \text{N-carbon}}{\text{Molecular weight}} \qquad (3.10)$$

where N-carbon is the number of carbons in the structure.

The conversion to hydrocarbon, HC, was calculated by:

$$\text{HC\%} = \frac{(\text{EtOH})_{in} - (\text{EtOH})_{out} - (\text{Oxygenated})_{out}}{(\text{EtOH})_{in}} \times 100 \qquad (3.11)$$

where $(\text{Oxygenated})_{out}$ was the C-atoms of oxygenated compounds such as diethyl ether, which was found in the product.

Since the conversion to hydrocarbons was defined as the

yield in hydrocarbons recovered during the run divided by the maximum theoretical yield in hydrocarbons according to the equation:

$$C_2H_5OH \longrightarrow C_2H_4 + H_2O \qquad (3.12)$$

product selectivity towards the reaction product "i" was defined as follows:

$$\text{Selectivity}(\%)_i = (Y_i/HC) \times 100 \qquad (3.13)$$

where Y_i was the yield of the product "i". Similar definitions were also applied where diethyl ether was used as a reactant. The calculations were computed by using a computer program on an Olivetti M24 computer (Appendix II). Determination of the conversion of ethanol to ethylene incorporates two main sources of errors. The first occurs within each catalytic run and includes thermal gradients and fluctuations in the flow rate of the carrier gas. These are essentially instrumental errors and are fixed and can be assumed to be small (<1%). The second source of error occurs between catalytic runs and is due to human error introduced in sample preparation and handling. These are variable and can be expected to fluctuate and be relatively larger (about 3%).

CHAPTER 4 - RESULTS AND DISCUSSION

4.1 Characterization of Zeolites

The chemical and physical properties of zeolite ZSM-5 and chryso-zeolite ZSM-5 such as the silicon to aluminum ratio, crystallinity, acidity, surface area and local structure may influence the catalytic performance of these solids. Therefore, it is necessary to measure those parameters in order to get a better understanding of the catalysts.

4.1.1 Chemical Composition

Table 4.1 reports the chemical characteristics of the samples studied. The label HP represents the catalysts (under H^+ form) made from silica gel (pure zeolite ZSM-5). HA stands for catalysts (under H^+ form) prepared from leached 7TF12 asbestos fibers.

As described previously, the acidic form of zeolite ZSM-5 was obtained by ion exchange of protons with sodium. Therefore, in order to have an active catalyst, the concentration of sodium has to be low.

The main difference between the two types of zeolite catalysts was the presence of magnesium (and iron) in the chryso-zeolite which might affect the catalytic activity and

Catalysts	Al_2O_3 (%)	Na_2O (%)	MgO (%)	Fe_2O_3 (%)	SiO_2 (%)	Si / Al	MLD (%)
HP-(21)	3.96	0.09	----	----	95.95	21.4	----
HP-(45)	1.93	0.17	----	----	97.91	44.9	----
HP-(75)	1.16	0.09	----	----	98.75	75.1	----
HP-(124)	0.70	0.13	----	----	99.17	124.4	----
HA-(26/99)	2.94	0.16	0.62	4.92	91.36	26.4	98.8
HA-(22/92)	3.38	0.15	3.90	4.70	87.87	22.1	92.2
HA-(21/83)	3.41	0.10	8.59	3.60	84.84	21.1	82.9

Table 4.1. Chemical composition of Zeolite ZSM-5 (HP) and Chryso-Zeolite ZSM-5 (HA) obtained from the atomic absorption technique.

product selectivity in the conversion of aqueous ethanol to ethylene.

4.1.2 Surface Area and Degree of Crystallinity

Table 4.2 reports the surface area (Area) and the degree of crystallinity (DC) on the HP and HA catalysts. The surface area of the zeolite ZSM-5 synthesized in our laboratory was in the 430m^2/g range which was the expected value (30). Since zeolite is porous material, this surface area was mainly located inside the particles.

Catalysts	Surface area (m^2/g)	Degree crystallinity (%)
HP-(21)	440	100
Steamed HP-(21)	412	77
HP-(45)	437	98
HP-(75)	446	98
HP-(124)	430	99
HA-(26/99)	394	92
HA-(22/92)	368	75
HA-(21/83)	320	67

Table 4.2. Surface area and degree of crystallinity of zeolite ZSM-5 (HP) and chryso-zeolite ZSM-5 (HA).

The outside represented only 1 to 2% of the total surface area. The surface area of chryso-zeolite ZSM-5 (HA catalyst) was observed to be lower than zeolite ZSM-5 (HP catalyst) and when the MLD decreased, a smaller total surface area was measured. However, the external surface area increased due to the presence of the asbestos remnants, representing between 15 to 20% of the total surface (31).

The powder X-ray diffraction pattern of zeolite ZSM-5 and chryso-zeolite ZSM-5 are shown in figures 4.1 and 4.2. The DC of chryso-zeolite ZSM-5 was low compared to zeolite ZSM-5, and it was lower for the chryso-zeolite ZSM-5 which had low MLD. This might be due to the fact that less silicon was free and accessible for the synthesis. The DC of zeolite ZSM-5 which was steam treated at 500°C, under 0.9atm of water vapour for five hours (steamed zeolite ZSM-5) decreased by about 23% when compared with fresh zeolite ZSM-5. This might be due to the de-alumination which occurred upon hydrothermal treatment.

The degree of crystallinity might influence the catalytic activity. A low degree of crystallinity implies the presence of an amorphous phase in the sample which would create a pore blockage and thus limit the diffusion of reacting and product molecules.

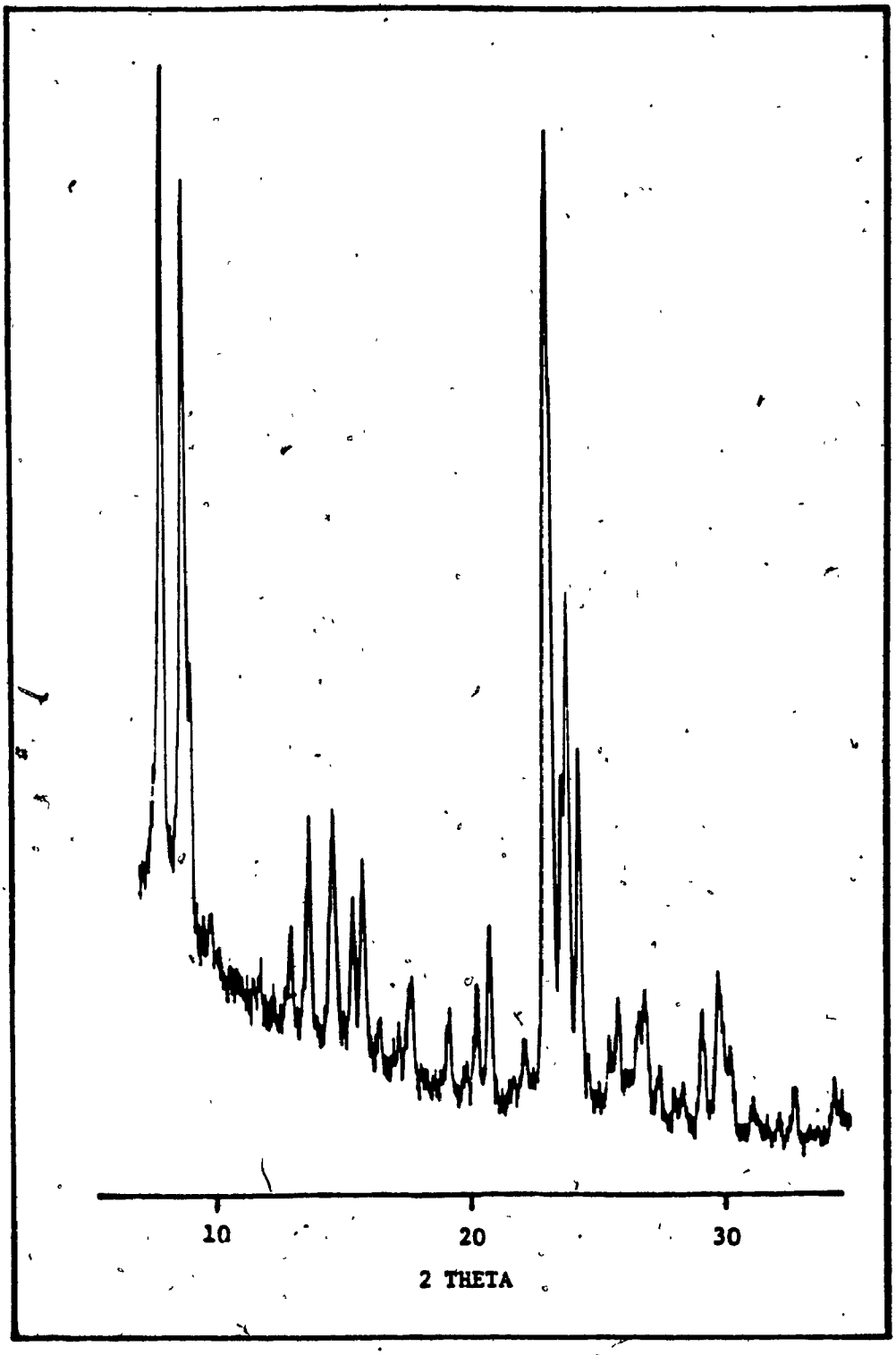

Figure 4.1 X-ray powder pattern of Zeolite ZSM-5 ,HP-(21).

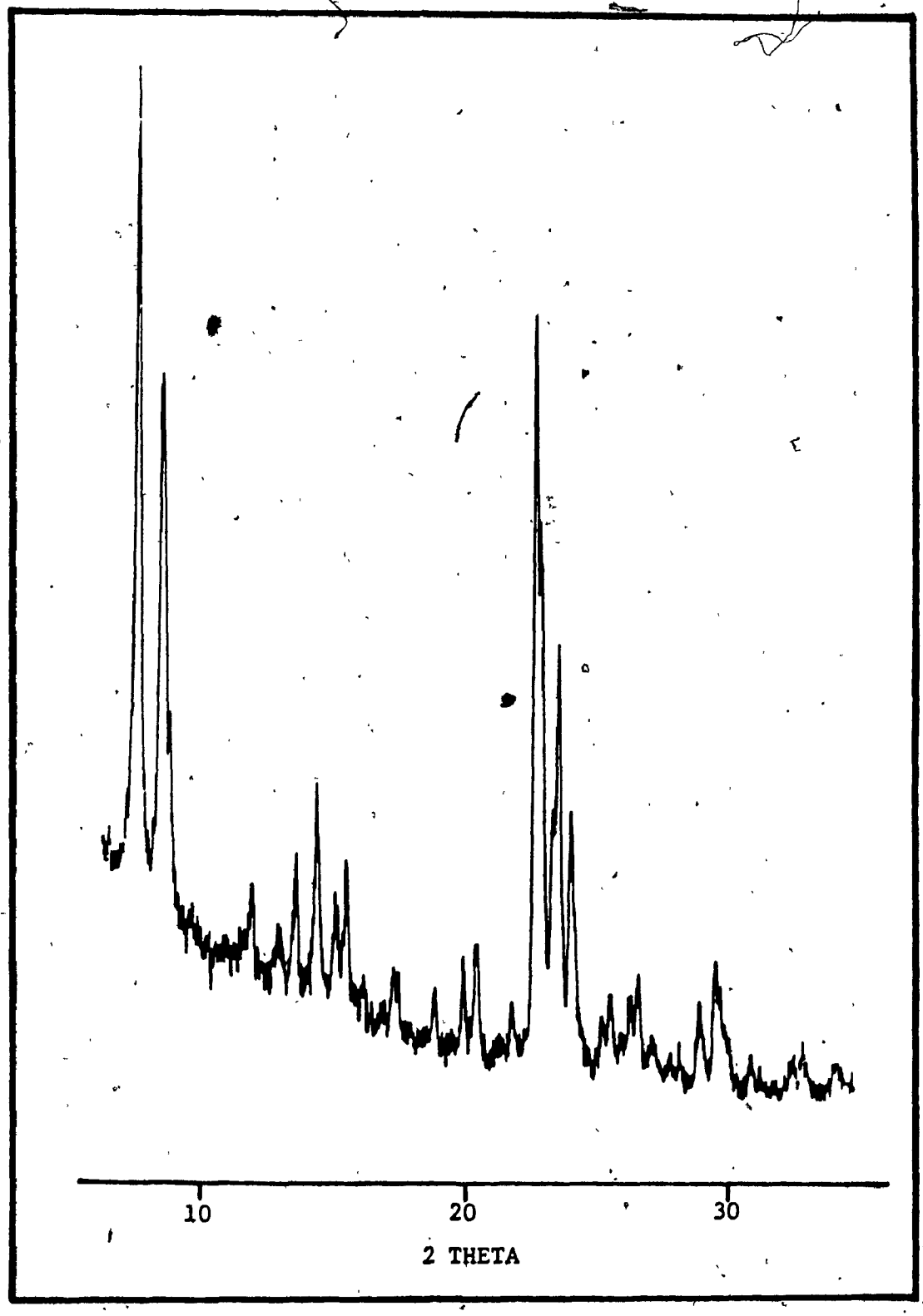

Figure 4.2. X-ray powder pattern of chryso-zeolite ZSM-5, HA-(26/99).

4.1.3 Magic Angle Spinning NMR

The ^{29}Si-MAS-NMR of zeolite ZSM-5 and chryso-zeolite ZSM-5 having different MLD are shown in figures 4.3, 4.4 and 4.5.

As shown by the ^{29}Si-MAS-NMR spectra, two common peaks (resonance lines) were observed on both zeolites at -112ppm and -106ppm. The former peak corresponds to the tetrahedrally coordinated Si-atoms joined to other Si-atoms via oxygen bridges (Si-O-Si). While the latter is assigned to the Si-atoms present in the Si-O-Al bond (32). The chryso-zeolite ZSM-5 had an additional peak at -98ppm which corresponds to the Si-O-Mg bond and a shoulder between -90 and -100ppm, which was probably due to the asbestos remnants, where Si is surrounded by two entities of Mg atoms. These peaks and shoulder were found to increase with the chryso-zeolite ZSM-5 having lower MLD values. Thus, from the ^{29}Si-MAS-NMR results it was possible to postulate the existence of close interaction between the zeolite containing the acid sites and magnesium basic sites as shown in figure 4.6 (31).

In order to investigate the de-alumination, which normally occurs on zeolite ZSM-5 upon steaming at high temperatures, the ^{27}Al-MAS-NMR technique was employed and the spectra of the fresh zeolite ZSM-5 and steam treated zeolite ZSM-5 are shown in figure 4.7.

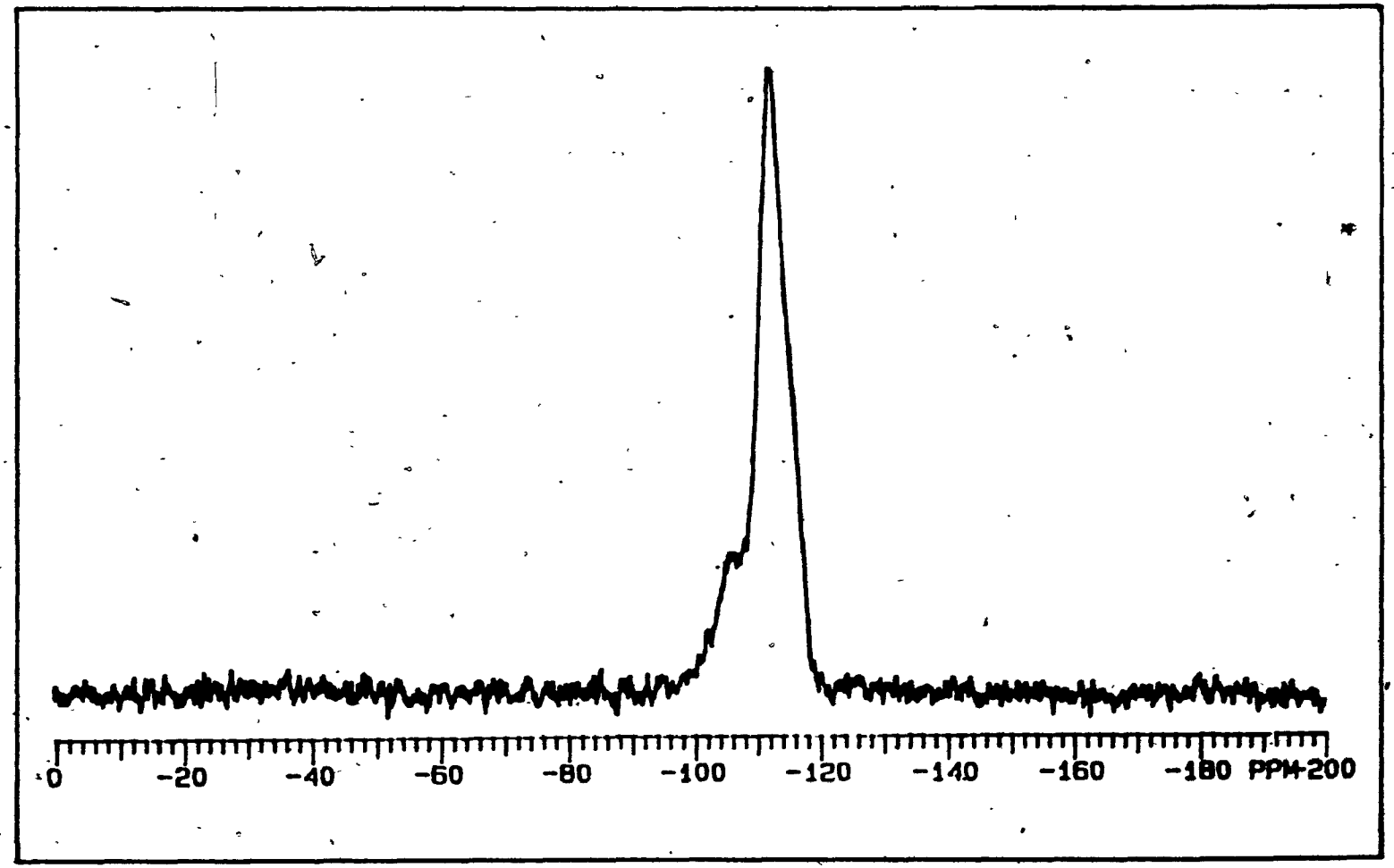

Figure 4.3. ^{29}Si-MAS-NMR spectrum of zeolite ZSM-5, HP-(21).

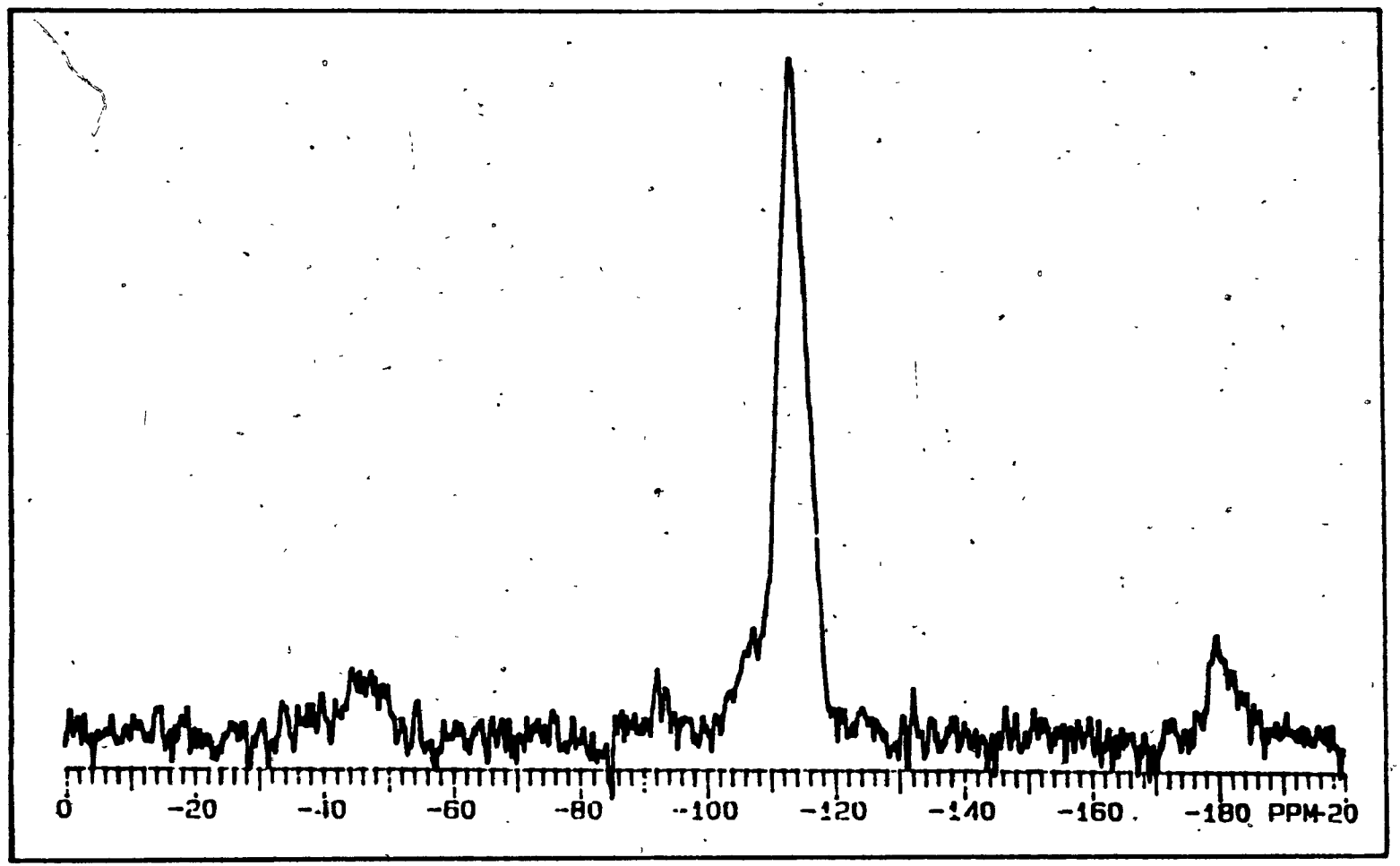

Figure 4.4. ^{29}Si-MAS-NMR spectrum of chryso-zeolite ZSM-5, HA-(26/99).

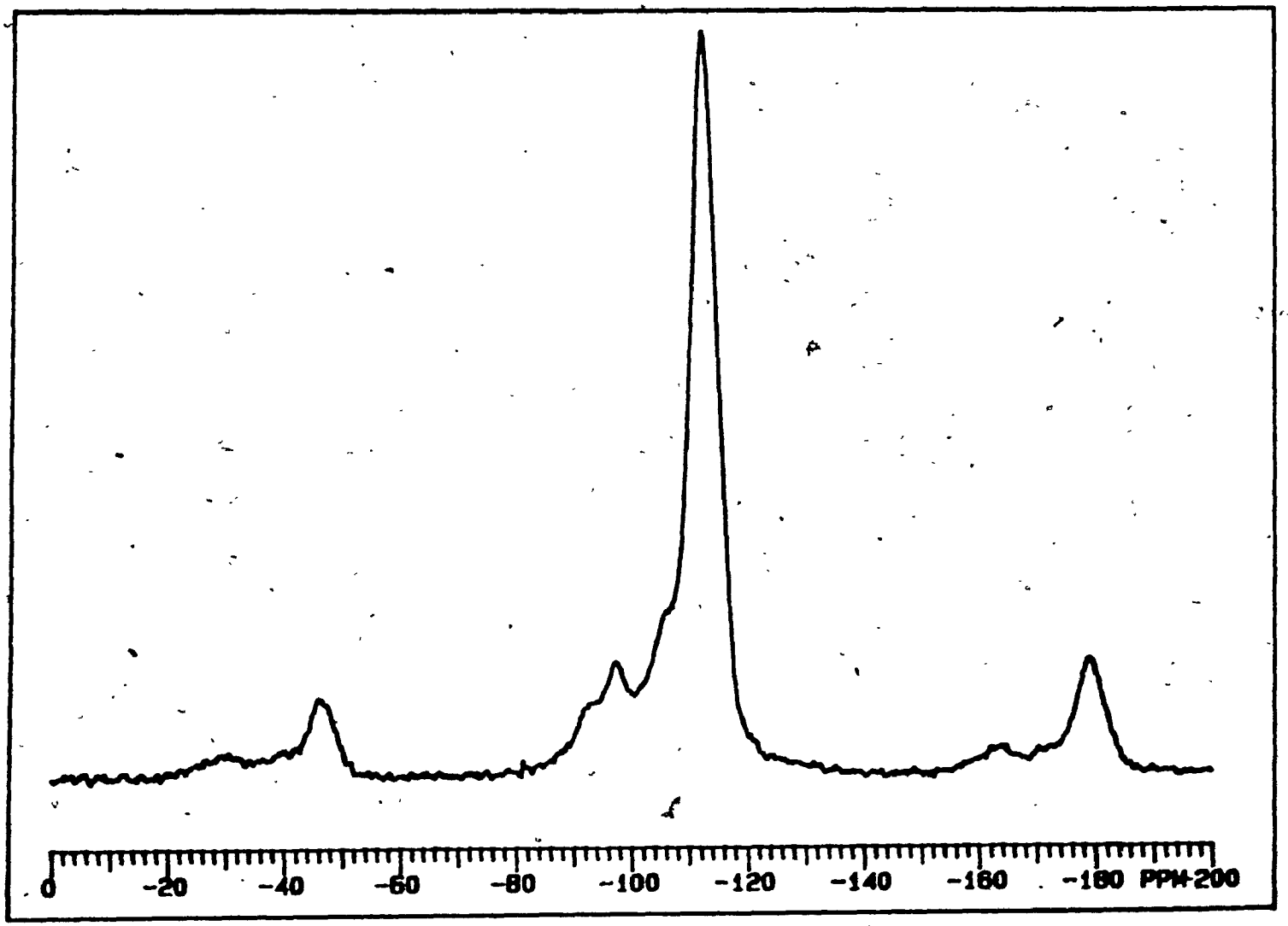

Figure 4.5. ^{29}Si-MAS-NMR spectrum of chryso-zeolite ZSM-5, HA-(21/83).

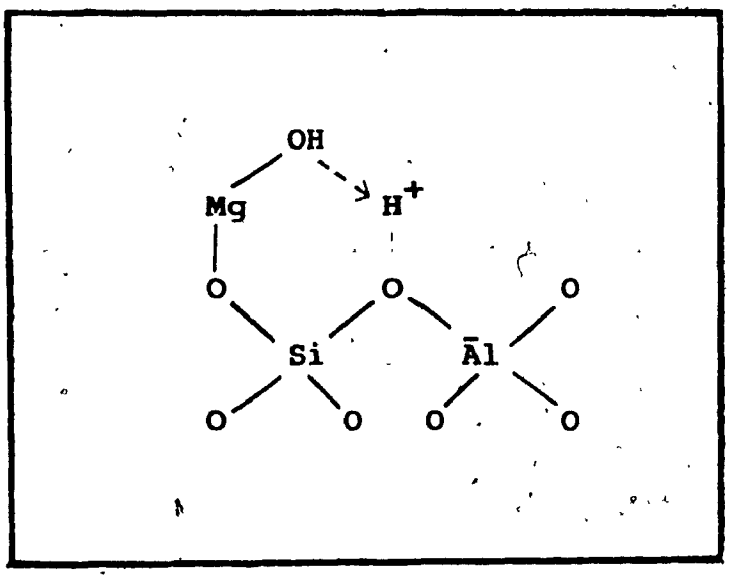

Figure 4.6. Possible interaction between adjacent acidic and basic sites in chryso-zeolite ZSM-5.

As observed by the ^{27}Al-MAS-NMR, the resonance line at 52ppm, which corresponds to the tetrahedral framework of aluminum, of the steam treated zeolite ZSM-5 was broadened and slightly decreased in intensity in comparison to the fresh zeolite ZSM-5 sample. The line broadening, according to Jacobs et al. (30), can be explained by the change in symmetry of some of the lattice unit cells from orthorhombic to monoclinic, while the slightly decreased line intensity is probably due to the de-alumination (32). It is well known that under the presence of steam at elevated temperatures that some of the Si-O-Al bonds of zeolite ZSM-5 are attacked resulting in the dislodgement of aluminum from their framework into interstitial positions, where their coordination is different than tetrahedral (33,34). Depending on the severity of steaming, the coordination of the dislodged aluminum species could be pentahedral (35,36) and/or octahedral (37,38). The former seems likely to occur under such steaming conditions as used in this work. The shoulder at 32ppm, which corresponds to the pentahedral dislodged aluminum (35), was observed on the ^{27}Al-MAS-NMR spectrum of steam treated zeolite ZSM-5 while the peak at 0ppm, which normally corresponds to the octahedral dislodged aluminum, was not.

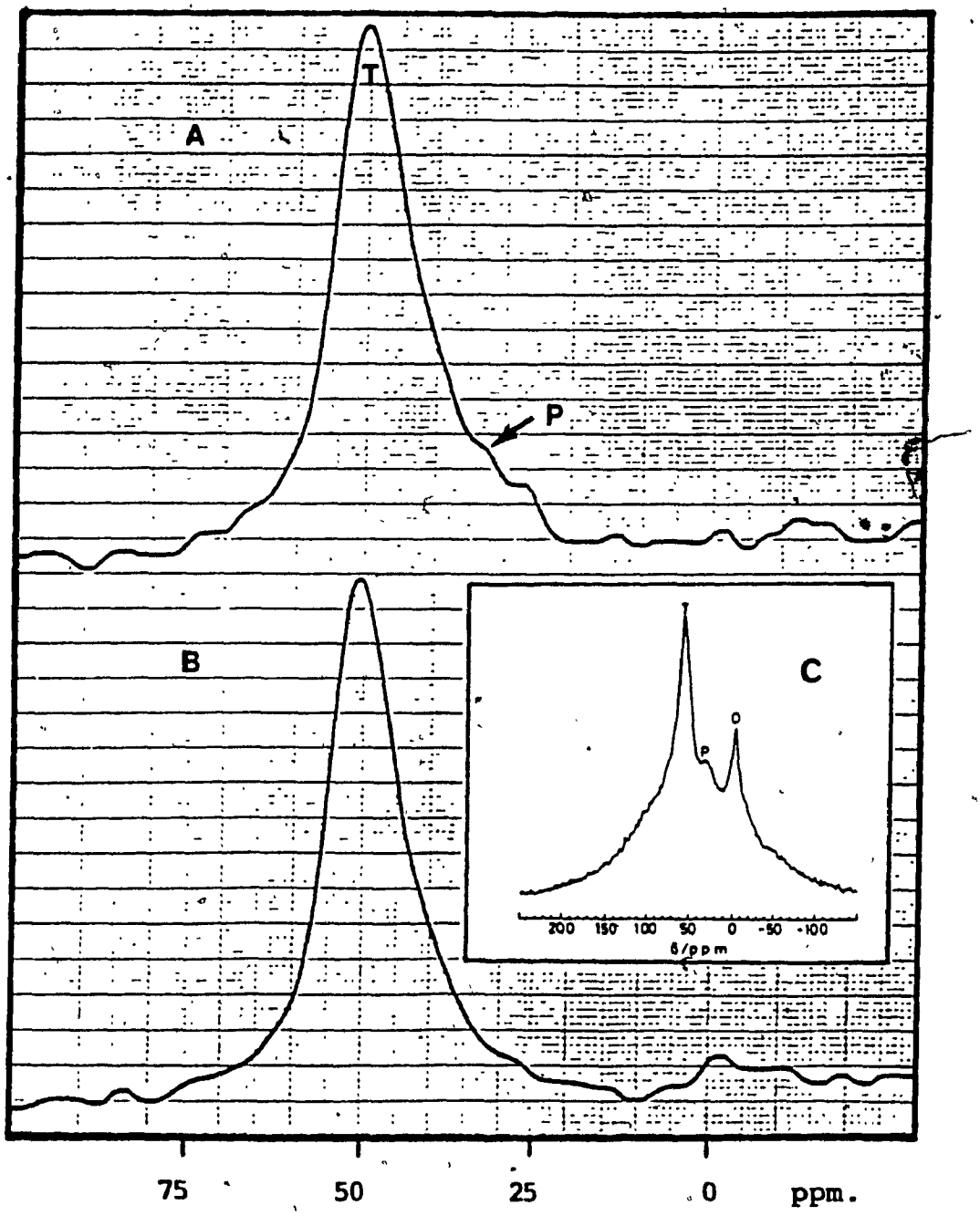

Figure 4.7. ^{27}Al-MAS-NMR spectra of (A) Steamed HP-(21) , (B) Fresh HP-(21), and (C) Steamed Faujasite (steam treated at 760^{o}C for 3 hours with 100% steam ; ref. 35).

T = Tetrahedral P = Pentahedral O = Octahedral.

Changes in symmetry and de-alumination of zeolite ZSM-5 upon steaming using the ^{27}Al-MAS-NMR technique as a probe has been the subject of many investigations and is presently under much debate (39).

4.1.4 TPD-NH_3

Figure 4.8 illustrates the TPD-NH_3 profiles of zeolite ZSM-5. Three desorption peaks were observed on both zeolite ZSM-5 and chryso-zeolite ZSM-5 catalysts. The peak at 220°C corresponds to the medium strength (M) Bronsted acid sites, which are responsible for dehydration of an alcohol to a primary olefin (38). Two peaks at 330°C and 500°C correspond to the strong (S) and very strong (VS) Bronsted acid sites, which are located at the channel intersection (27). These peaks are responsible for initialization of primary olefins to higher olefins and aromatic compounds (40,41). The difference in acid strength of the M, S and VS acid sites are related to the location (or environment) of such sites within the zeolite pore system, as a factor which could influence their delocalization character (27).

Table 4.3 is a summary of the acid density of the M, S and VS acid sites of zeolite ZSM-5 having different Si/Al ratios and chryso-zeolite having different MLD values. It was observed that the acid density of S and VS sites is

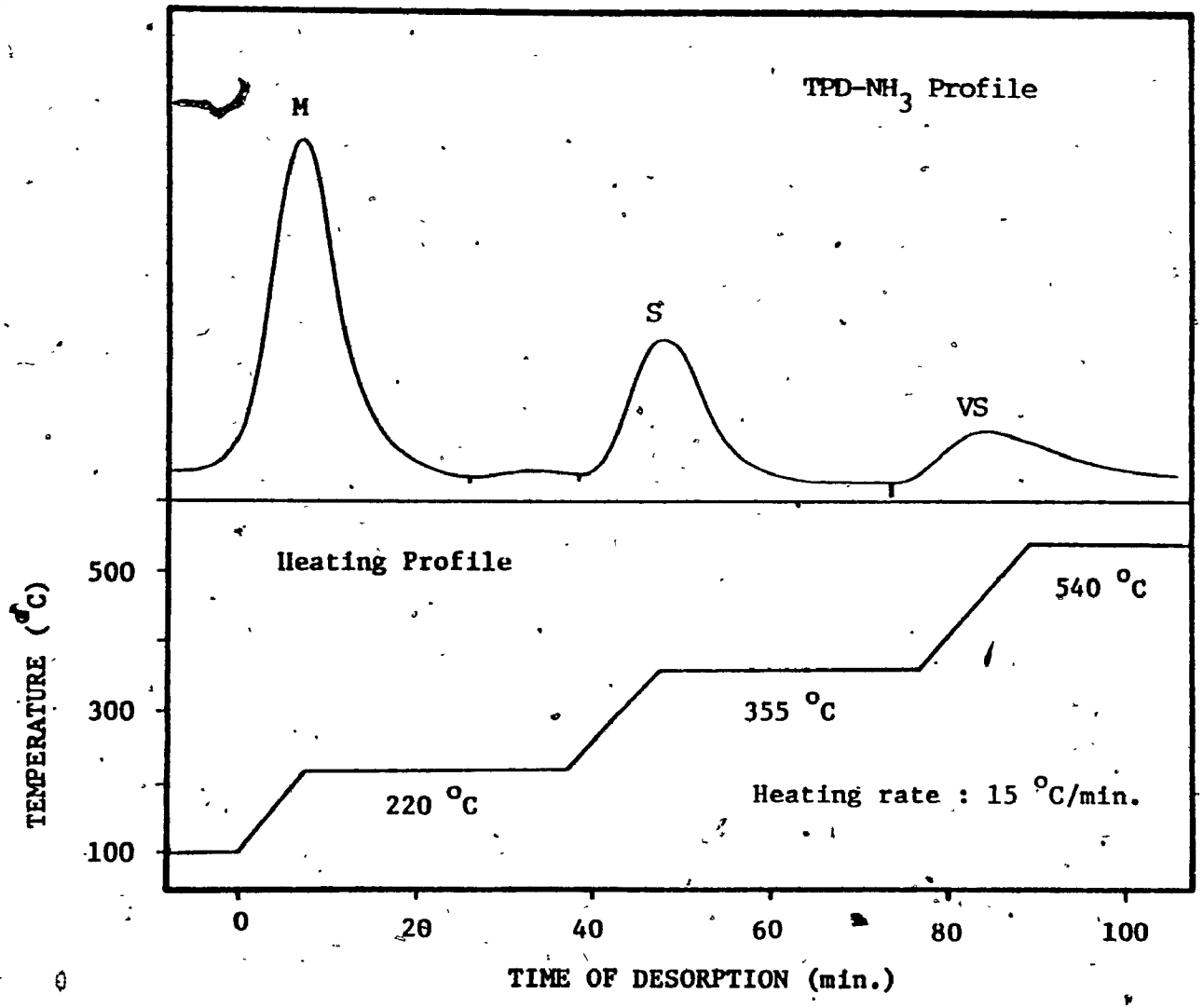

Figure 4.8. $TPD-NH_3$ and heating profiles of zeolite ZSM-5, HP-(21)

Catalysts	Si/Al	Al Content 10^2 atoms/g	Acid site distribution (%) M (%)	S (%)	VS (%)	Total acidity meqiv/g
HP-(21)	21	2.10	49.3	23.2	27.5	1.38
Std-HP-(21)	21	2.10	50.0	26.6	23.4	0.94
HP-(45)	45	1.02	60.5	16.1	23.4	1.24
HP-(75)	75	0.61	37.3	23.5	39.2	0.51
HP-(124)	124	0.31	25.6	25.6	48.8	0.39
HA-(26/99)	26	1.56	49.1	25.5	25.4	1.06
HA-(22/92)	22	1.79	53.0	26.5	20.5	1.17
HA-(21/83)	21	1.80	50.0	24.5	25.5	1.02

Table 4.3 Total acid density and acid site distribution of zeolite ZSM-5 and chryso-zeolite ZSM-5.

linearly increased with increase of tetrahedral framework content (or with decrease in the Si/Al ratio), while the acid density of M sites was also increased but not linearly (figure 4.9). The hydrothermally treated zeolite ZSM-5 shows significant decreases in the total acid density. However, the distribution of the M, S and VS sites was almost unchanged. The decrease in total acid density upon steaming of zeolite ZSM-5 was probably due in part to structural rearrangement and de-alumination as previously discussed.

The total acid density of chryso-zeolite ZSM-5 was lower in comparison with zeolite ZSM-5 having a similar Si/Al ratio. This is due to the presence of Mg which generates basic sites to neutralize some of the adjacent Bronsted sites as shown earlier in figure 4.6.

There has been the general observation in the conversion of alcohol to hydrocarbon, particularly in the conversion of methanol and ethanol to gasoline, that the catalytic activity and product selectivity of zeolite ZSM-5 depends strongly on its acid properties (5,51). Therefore, any intentional or accidental change in the total acid density or distribution on the M, S and VS acid sites of zeolite ZSM-5 and chryso-zeolite ZSM-5 is expected to influence the conversion of aqueous ethanol to ethylene.

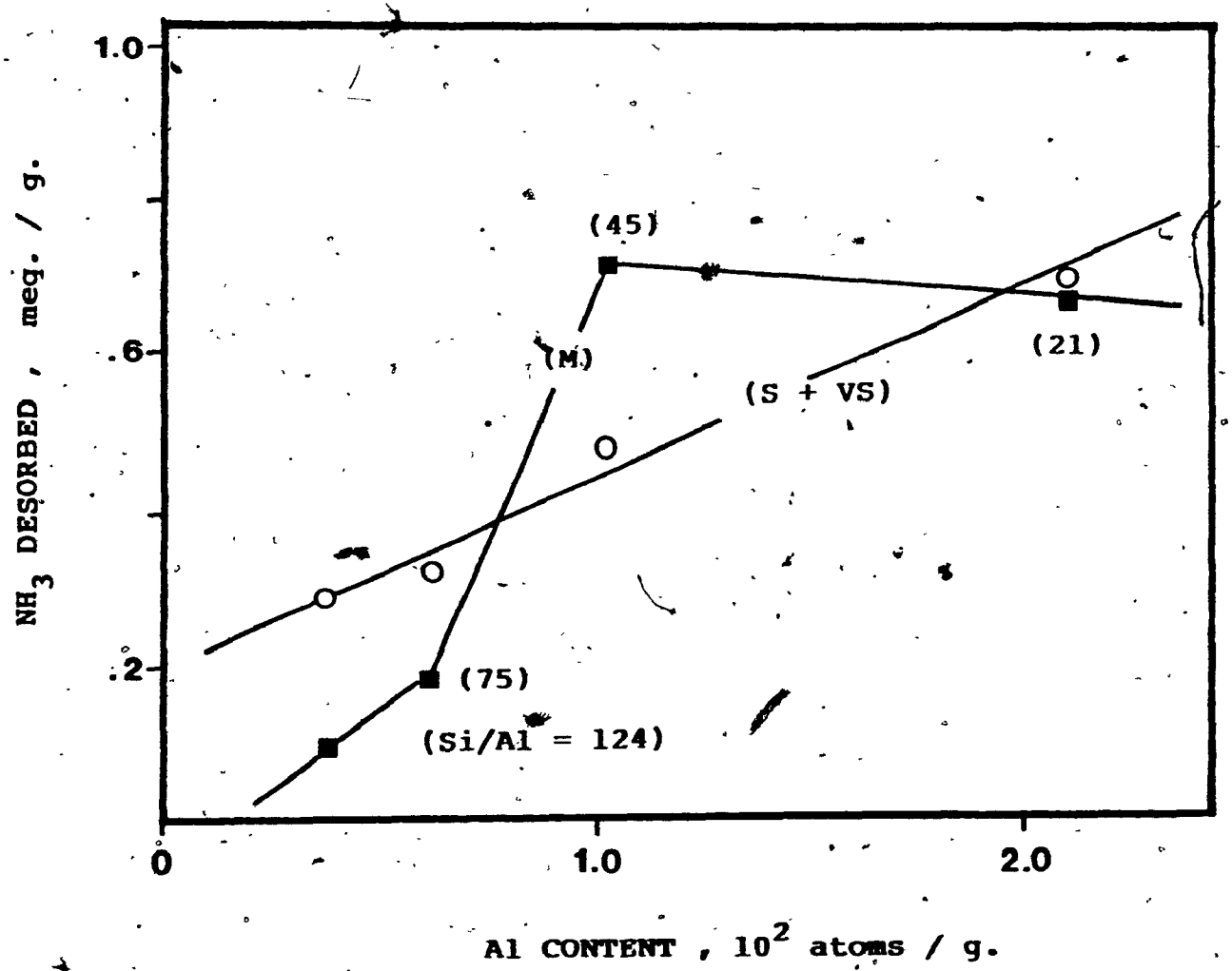

Figure 4.9. Distribution of medium, strong and very strong acid sites in zeolite ZSM-5 having different Si/Al ratios.

4.1.5 Hydrophobicity

Table 4.4 reports the hydrophobicity of zeolite ZSM-5 and chryso-zeolite ZM5.

It was observed that the hydrophobicity of chryso-zeolite ZSM-5 was smaller in comparison to zeolite ZSM-5 having the same Si/Al ratio. The RAI value decreased at lower MLD which suggested that the hydrophobicity of the chryso-zeolite ZSM-5 was closely dependant upon the magnesium content. Since increasing the magnesium content in chryso-zeolite ZSM-5 means increasing the number of terminal -Mg-OH which offer ample hydrogen bonding interaction for water sorption.

With steam treated zeolite ZSM-5, the hydrophobicity was dramatically enhanced due to a significant decrease in the amount of water being adsorbed while a slight increase in the adsorption of n-hexane was observed. The decrease in the absorption of water by the steam treated zeolite ZSM-5 can be explained on the basis of the tetrahedral framework aluminum being dislodged from their normal lattice positions into non-framework positions where they are inaccessible to water molecules (38). Moreover, steam is also known to remove some of the internal and external hydroxyl groups as noted by Desseau et al. (33), who proposed a mechanism which is outlined in figure 4.10. The removal of the hydroxyl groups resulted in reducing the number of terminal hydroxyl

Catalysts	n-Hexane (% ml/g)	Water (% ml/g)	R.A.I
HP-(21)	17.21	7.97	2.16
Steamed HP-(21)	21.48	4.36	4.92
HP-(45)	17.43	7.21	2.42
HA-(26/99)	13.27	7.14	1.86
HA-(22/92)	11.92	7.27	1.64
HA-(21/83)	12.49	8.27	1.51
Alumina	18.61	17.54	1.05

Table 4.4. Hydrophobicity of zeolite ZSM-5 and chryso-zeolite ZSM-5.

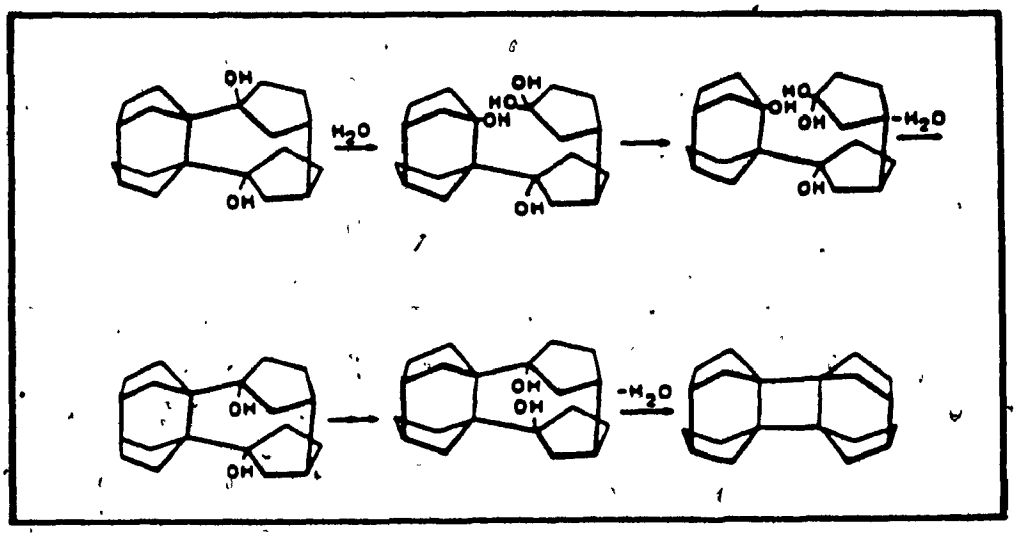

Figure 4.10. Plausible mechanism of the removal of the silanol groups in zeolite ZSM-5.

groups which leads to a limited amount of hydrogen bonding occuring between water molecules and the surface of the zeolite.

4.2 Catalysis - Conversion of Aqueous Ethanol to Ethylene

4.2.1 Comparison of Catalysis in the Literature

Table 4.5 reports the catalytic results obtained for the conversion of aqueous ethanol over various types of catalysts.

As mentioned earlier, alumina has been used as an industrial dehydration catalyst for the conversion of ethanol (95%) to ethylene which gave very high yields (94%) and selectivity to ethylene (>99%) at 300 - 400°C. However, under similar conditions, alumina gave very low yields in the conversion of aqueous ethanol (15 wt%) to ethylene although the selectivity to ethylene was very high. This was due to the fierce competition, in the adsorption onto the catalyst surface, between molecules of ethanol and water. The detrimental effect of water on the yield in ethylene was due to the stronger adsorption of water on the hydrophillic active sites of the alumina catalyst (3,4).

Catalysts	Temp. (°C)	Conv. HC (%)	Product selectivity (%)			
			Ethylene	Propylene	Butenes	Others
Silica	400	20.0	99.5	0.1	0.1	0.3
Alumina	400	35.7	99.7	0.1	0.1	0.1
HP-(21)	400	98.4	22.6	18.3	14.1	45.0
HP-(21)	300	98.2	80.6	6.2	8.2	5.0
HP-(21)	275	98.9	87.1	2.8	6.3	3.8
HP-(21)	240	87.7	94.5	1.9	2.3	1.3
HA-(26/99)	400	96.4	96.8	1.5	1.1	0.0
HA-(26/99)	300	99.8	99.2	0.5	0.2	0.1

Table 4.5. Conversion of aqueous ethanol (15 wt%) to ethylene over various type of catlysts at WHSV 3.2 h^{-1}.

On the other hand, silica rich ZSM-5 zeolites exhibited a large hydrophobic surface which prevented saturation of the catalyst surface by water molecules.. Furthermore, the strength of the acid site in zeolite ZSM-5 was much stronger than in alumina, as observed by the TPD-NH_3 measurement. Therefore, the conversion of aqueous ethanol over zeolite ZSM-5 at 400°C gave very high yields in hydrocarbons. However, the selectivity to ethylene, which is a desired product in this work, was relatively low. The low selectivity to ethylene was due to the occurrence of oligomerization of ethylene on strong and very strong acid sites of the zeolite catalyst which can lead to higher olefins and aromatic compounds, this can be visualized in figure 4.11 (42). The oligomerization reaction to ethylene could be suppressed under certain conditions, such as decreasing the reaction temperature, since this reaction was favored at relatively high temperatures (>300°C) or by decreasing the acid strength and the pore size of the zeolite catalysts by incorporating some metals such as Zn, Mn, P, B etc. into the zeolite structure (19.20).

Decreasing the reaction temperature enhanced the selectivity to ethylene, [HP(21) at 220 and 240°C], however the yield of the reaction was decreased.

Chryso-zeolite ZSM-5, HA-(26/99) at 400°C and 300°C gave very high yield and selectivity to ethylene. Chryso-zeolite ZSM-5 is a typical modified type of zeolite ZSM-5

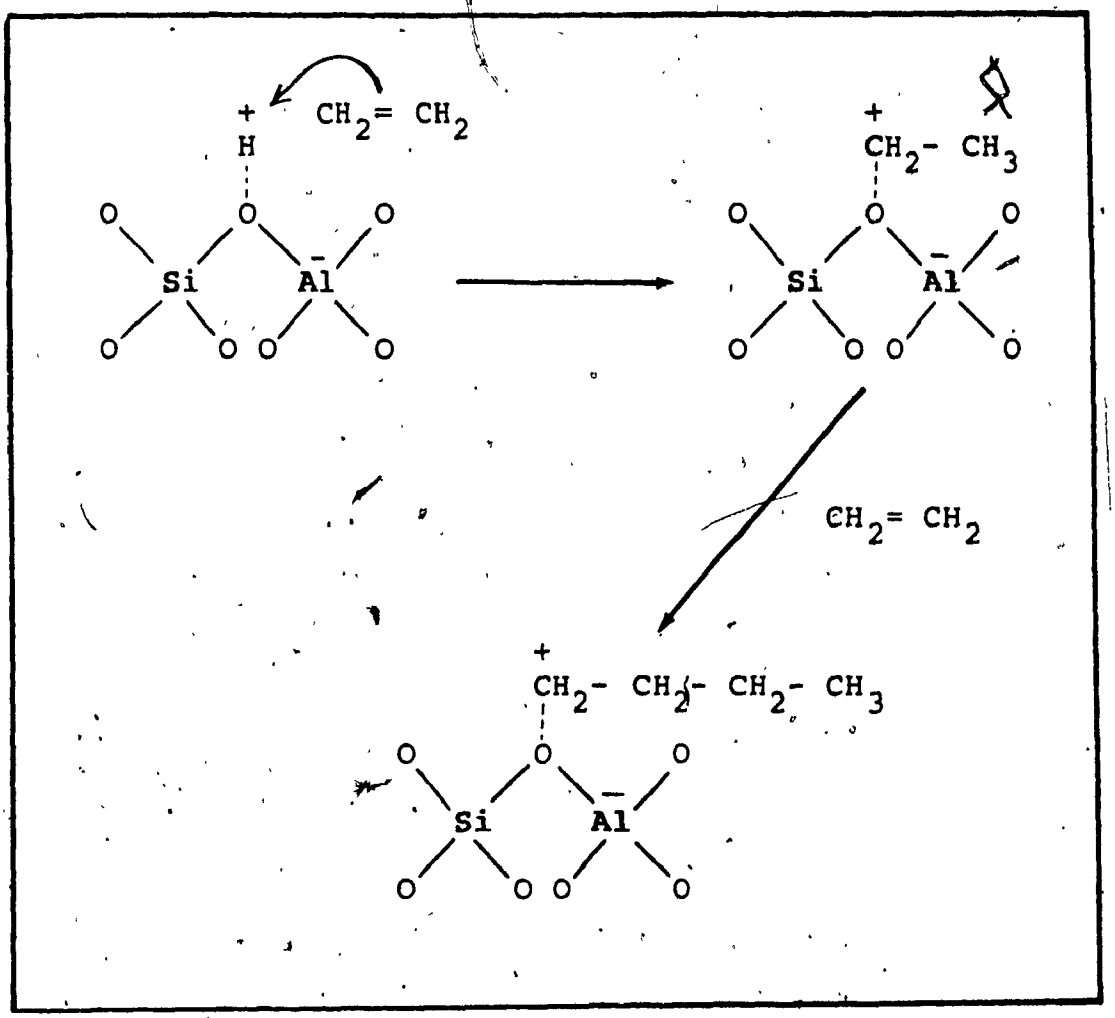

Figure 4.11. Oligomerization of ethylene to higher olefins on Zeolite ZSM-5.

containing some basic sites of the -Mg-OH groups which stabilized and prevented the ethyl carbonium ions from further reaction to higher olefins and aromatic compounds as shown in figure 4.12 (31).

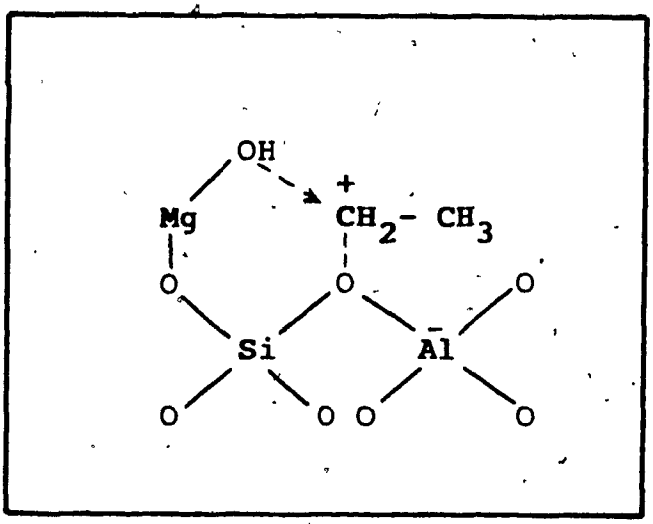

Figure 4.12. Interaction and stabilization of the carbonium intermediate in the presence of basic site

4.2.2 Effect of Chemical Composition

As observed by TPD-NH_3, the acidic properties of zeolite ZSM-5 and chryso-zeolite ZSM-5 are dependant on their chemical composition (i.e. Si/Al ratio, MLD) and the conversion of aqueous ethanol to ethylene is an acid catalyzed reaction. Therefore, in order to investigate the effects of the chemical composition on the catalytic activity, the conversion of aqueous ethanol over steamed zeolite ZSM-5 having different Si/Al ratios and chryso-zeolite ZSM-5 having different MLD were performed.

4.2.2.1 Si/Al Ratio in Zeolite ZSM-5

Figure 4.13 shows the relation between the Si/Al ratio and the conversion of aqueous ethanol to ethylene, together with the effect of the Si/Al on the density of M, S and VS acid site. The temperature chosen was 300°C in order to limit the oligomerization of ethylene to other hydrocarbons. As can be seen, the dehydration of aqueous ethanol to ethylene seems to be promoted by the medium strength acid sites since the selectivity to ethylene varied with the change in density of the medium strength acid sites in the zeolite. This is in perfect agreement with data from many other researchers (40,41).

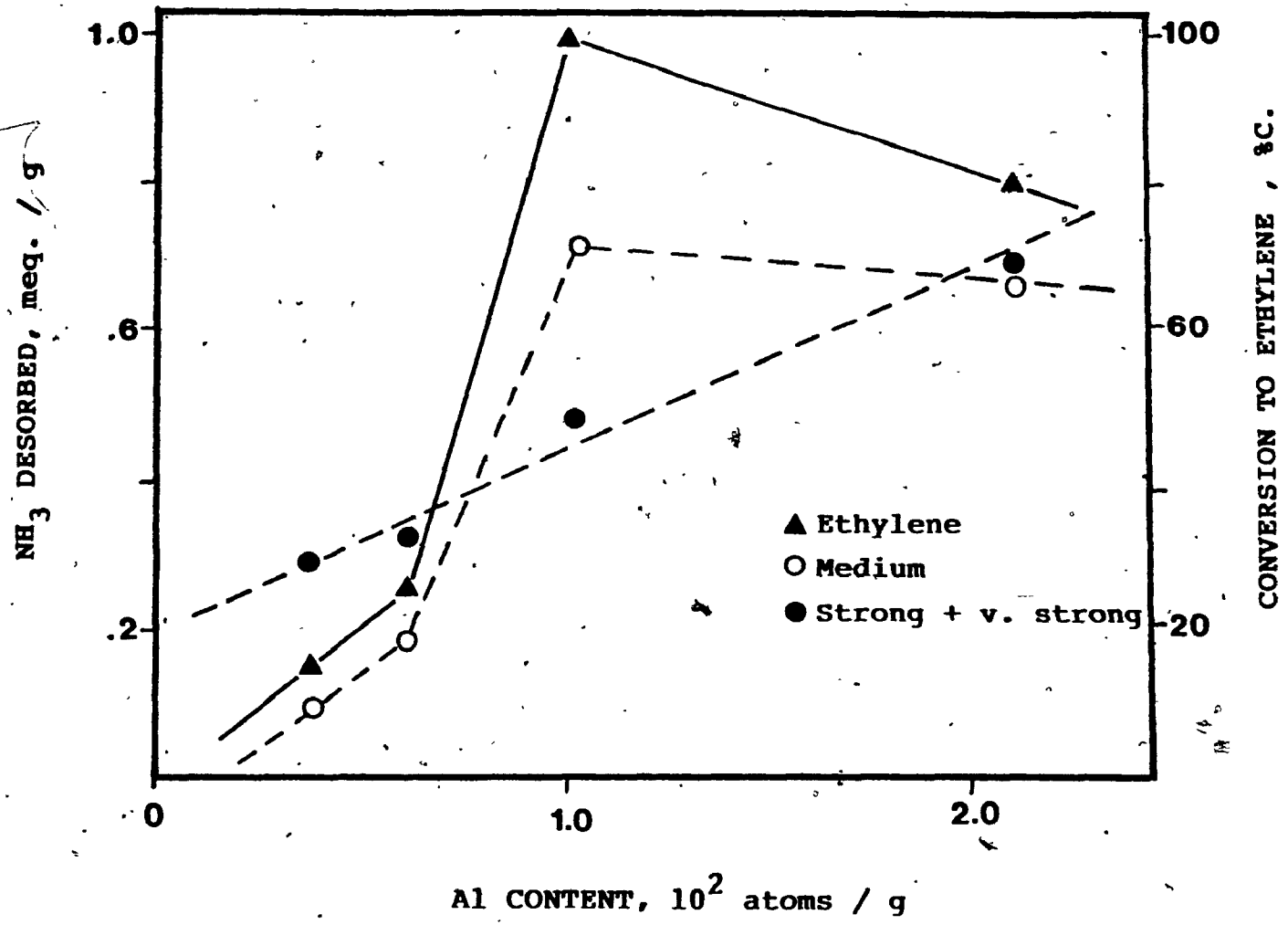

Figure 4.13. Effect of distribution of acid sites on the conversion of aqueous ethanol (10 wt%) to ethylene over zeolite ZSM-5.

The strong and very strong acid sites obviously contributed to the conversion of aqueous ethanol to ethylene at low temperatures, however, they would promote the oligomerization of ethylene to other hydrocarbons as the reaction temperature increased.

The optimum conversion of aqueous ethanol to ethylene was found with the zeolite ZSM-5 having the Si/Al ratio at about 45. The selectivity to ethylene was decreased with decreasing Si/Al ratio and it could be improved with increasing the Si/Al ratio, however, the conversion to hydrocarbon was dramatically dropped (Table 4.6).

4.2.2.2 MLD of Chryso-Zeolite ZSM-5

Table 4.7 reports the catalytic results obtained with chryso-zeolite ZSM-5 having two values of MLD.

Chryso-zeolite ZSM-5 exhibited extremely high selectivity to ethylene. However, higher temperatures were needed for chryso-zeolite ZSM-5 having low MLD to become active. With higher Mg content in the chryso-zeolite ZSM-5, the catalyst became more hydrophilic and the adsorption of water molecules on the surface of the catalyst was enhanced. Therefore, the accessibility to the active sites for the ethanol molecules was reduced and subsequent oligomerization was inhibited.

Catalysts	Si/Al	Temp °C	HC %	Selectivity (%)	
				Ethylene	C_3^+ Olefin
HP-(21)	21	300	98.2	80.6	19.4
HP-(45)	45	300	98.4	99.3	0.7
HP-(75)	75	300	22.4	99.9	0.1
HP-(124)	124	300	14.8	100.0	0.0
HP-(21)	21	275	98.9	87.1	12.9
HP-(45)	45	275	87.6	99.6	0.4

Table 4.6. Effect of Si/Al ratio of zeolite ZSM-5 on the conversion of aqueous ethanol (15 wt%) at various temperatures and WHSV 3.2 h^{-1}.

Catalysts	Temp °C	Conversion (%)		Selectivity (%)	
		Total	HC	Ethylene	C_3^+ Olefin
HA-(26/99)	175	14.38	0.01	100.00	0.00
	200	27.01	0.53	100.00	0.00
	225	35.04	10.27	100.00	0.00
	250	63.63	42.65	99.86	0.14
	275	97.88	96.57	99.63	0.37
	300	99.80	99.80	99.50	0.50
	325	99.88	99.88	99.42	0.58
HA-(21/83)	225	17.10	0.86	100.00	0.00
	250	30.48	11.75	100.00	0.00
	275	55.54	52.63	99.41	0.59
	300	86.03	85.47	99.37	0.63
	325	99.22	99.22	99.42	0.58

Table 4.7. Effect of MLD of chryso-zeolite ZSM-5 on the conversion of aqueous ethanol (10 wt%) at various temperatures and WHSV 3.2 h^{-1}.

Thus, chryso-zeolite ZSM-5 having high MLD values is preferred for the conversion of aqueous ethanol to ethylene in this work.

4.2.3 Effect of Steaming

4.2.3.1 Zeolite ZSM-5 Catalyst

Table 4.8 reports the effect of steaming on the conversion of aqueous ethanol.

In order to investigate rapidly the effect of steam on the catalytic behaviour of zeolite ZSM-5, particularly on the product selectivity, reactions were performed at relative high temperatures i.e. 400°C. The results show that the selectivity toward ethylene was gradually increased from 22% to 78% after four consecutive catalytic runs, while the conversion to hydrocarbons was almost unchanged. The increase in selectivity to ethylene might be due to the steam caused structural distortion and de-alumination. The latter resulted in the formation of dislodged aluminum which remains in the zeolite channel system as cationic species (39,43). This could be represented as follows:

$$[Si(OAl)_n]^{n-1} \longrightarrow [Si(OAl)_{n-1}]^{(n-1)} \quad Al^{3+}(n-1)/3 \qquad (4.1)$$

RUN	Conv. HC (%)	Product selectivity (%)			
		Ethylene	Propylene	Butenes	Others
1	98.4	22.6	18.3	14.1	50.0
2	98.6	41.8	16.5	12.8	28.9
3	99.8	60.7	12.4	10.3	16.6
4	99.8	78.2	8.3	6.2	7.3

Table 4.8 Effect of steaming on the conversion of aqueous ethanol (15 wt%) over zeolite ZSM-5 ,HP-(21) at 400°C and WHSV 3.2 h^{-1}.

It was observed earlier that the total acidity of zeolite ZSM-5 is dependant on the content of aluminum atoms in the zeolite framework,and the catalytic properties, especially the product selectivity, are strongly dependant on the distribution of the different strength acid sites in the zeolite. The decrease in total acidity upon steaming due to the formation of the above complex type species altered the catalytic properties of zeolite ZSM-5 somehow and this did not favour the formation of hydrocarbons other than ethylene. However, the exact role and nature of the dislodged aluminum species involved in the catalytic reaction remains to be elucidated to date (37).

The effect of steam in the conversion of aqueous ethanol on zeolite ZSM-5 is not avoidable, and it shows a markedly positive shift in terms of product selectivity (to ethylene). Therefore, it was decided to use the steam treated zeolite ZSM-5 having low Si/Al for the conversion of aqueous ethanol to ethylene rather than using the zeolite ZSM-5 having higher Si/Al. Although the zeolite ZSM-5 with high Si/Al gave very high selectivity to ethylene, its conversion to hydrocarbons was observed to be lower at 275°C as can be seen in Table 4.6. Thus, with the use of the low Si/Al ratio and steam treated zeolite ZSM-5 in the conversion of aqueous ethanol, very high conversion and selectivity to ethylene is expected.

4.2.3.2 Chryso-Zeolite ZSM-5

Table 4.9 reports the effect of steaming on the conversion of aqueous ethanol.

RUN	Conversion (%)		Selectivity (%)	
	Total	HC	Ethylene	C_3^+ Olef.
1	99.88	99.88	99.42	0.58
2	99.90	99.90	99.66	0.44
3	99.89	99.89	99.71	0.29
4	99.90	99.90	99.69	0.31

Table 4.9. Effect of steaming on the conversion of aqueous ethanol (10 wt%) over chryso-zeolite ZSM-5 HA-(26/99) at 325°C and WHSV 3.2 h^{-1}.

Chryso-zeolite ZSM-5 [HA(26/99)] was observed to be very stable under the presence of steam. Even after three runs, the catalytic activity and selectivity to ethylene was almost unchanged. The long lasting run at the same condition was also performed on this catalyst, and the results shows that there was no significant change after 200

hours on the stream. The same observations were obtained on the steamed treated zeolite ZSM-5.

4.2.4 Effect of Ethanol Concentration

Table 4.10 reports the catalytic results obtained with the feed having different concentration of ethanol.

Ethanol in feed (wt %)	Conv. HC (%)	Selectivity (%)	
		Ethylene	C_3^+ Olef.
15	99.55	99.14	0.86
10	99.89	99.83	0.17
5	99.82	99.88	0.12

Table 4.10. Effect of concentration of ethanol in the feed on the conversion over steamed HP-(21) at 325°C and WHSV 3.2 h^{-1}.

The aqueous ethanol solution obtained from the fermentation broth usually had a concentration of ethanol ranging from 8 to 15 wt%. However, under such variation in concentration, the catalytic activity and selectivity were

not significantly changed when the conversion were performed on the steamed zeolite ZSM-5 (HP) catalyst. This observation was also applied for chryso-zeolite ZSM-5 (HA) catalysts.

4.2.5 Effect of Reaction Parameters

The reaction temperature, weight hourly space velocity, WHSV, are important parameters in a heterogeneous catalytic reaction as in the conversion of aqueous ethanol to ethylene over zeolite ZSM-5 type catalysts.

In order to obtain optimum reaction conditions, the effect of temperature and 1/WHSV (contact time) on the conversion were studied

4.2.5.1 Temperature

Figure 4.14 shows the product distribution of the conversion at various temperature and WHSV = 3.2 hr^{-1}.

Both steamed zeolite ZSM-5 [steamed HP(21)] and chryso-zeolite ZSM-5 [HA (26/99)] revealed similar trends. At low temperatures, diethyl ether was a main product and the maximum ether formation was at the temperature about 215°C. By increasing the temperature, diethyl ether started to decrease and more ethylene was obtained in the product. The complete conversion (>99%) was achieved at temperatures

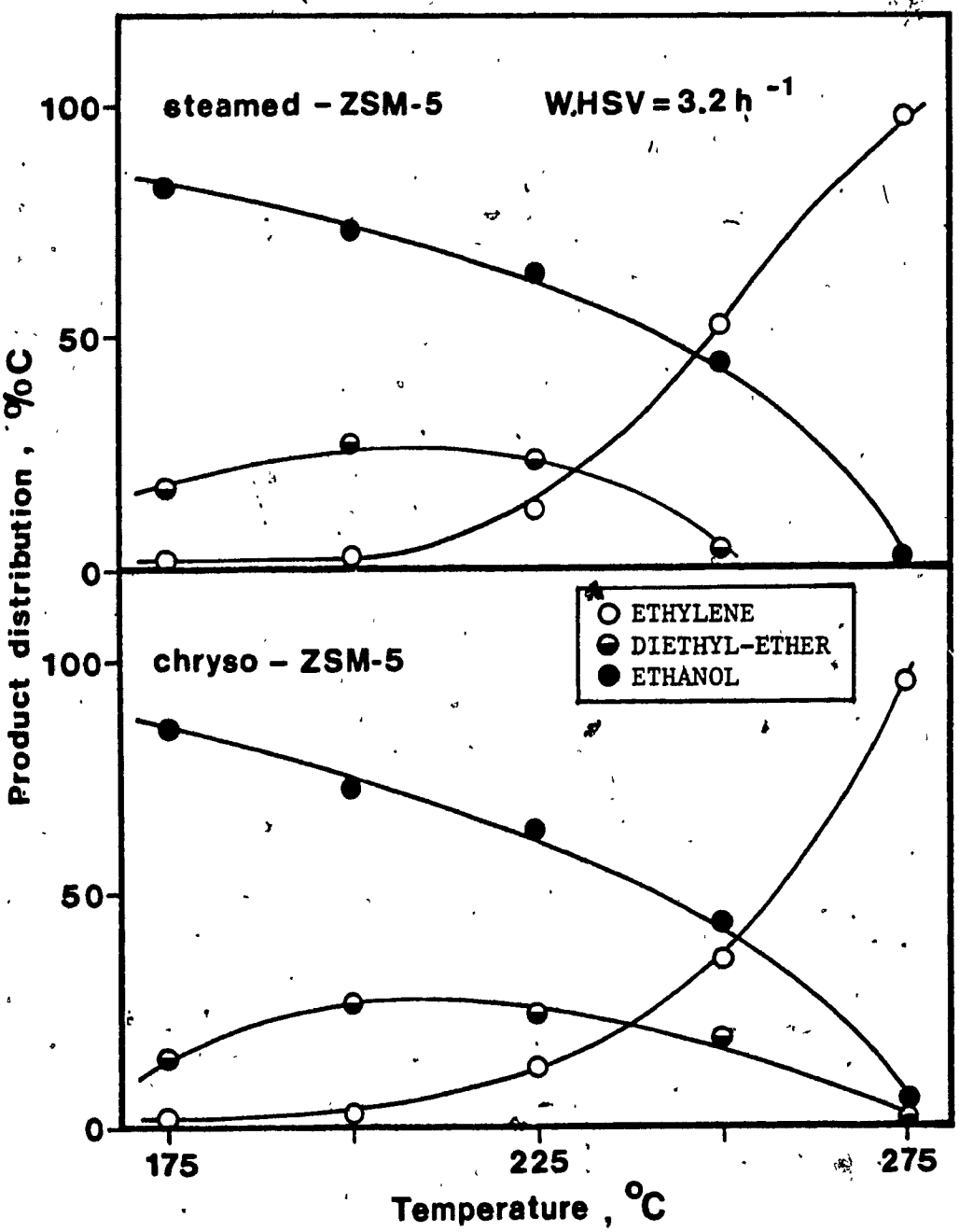

Figure 4.14. Effect of temperature on the conversion of aqueous ethanol (10 wt%) over steamed HP-(21) and HA-(26/99).

above 275°C and the selectivity to ethylene was also very high (>99%). The complete conversion of aqueous ethanol to ethylene could be achieved at lower temperatures if the reaction was performed at longer contact times or lower WHSV.

4.2.5.2 Contact Time

Figures 4.15 and 4.16 show the product distributions of the conversion at 250°C and 300°C with various contact times.

The results show that steam treated zeolite ZSM-5 and chryso-zeolite ZSM-5 gave similar selectivity. At 250°C diethyl ether was a main product at very short contact times The conversion and selectivity to ethylene increased with increasing contact time. Chryso-zeolite ZSM-5 was shown to be less active than steam treated zeolite ZSM-5 at this temperature. At 300°C, the complete conversion was observed at the contact times of 0.9 hours. Ethylene was a main product even at very short contact times. It should be noted that chryso-zeolite ZSM-5 was observed to be more active than steam treated zeolite ZSM-5 at 300°C and above.

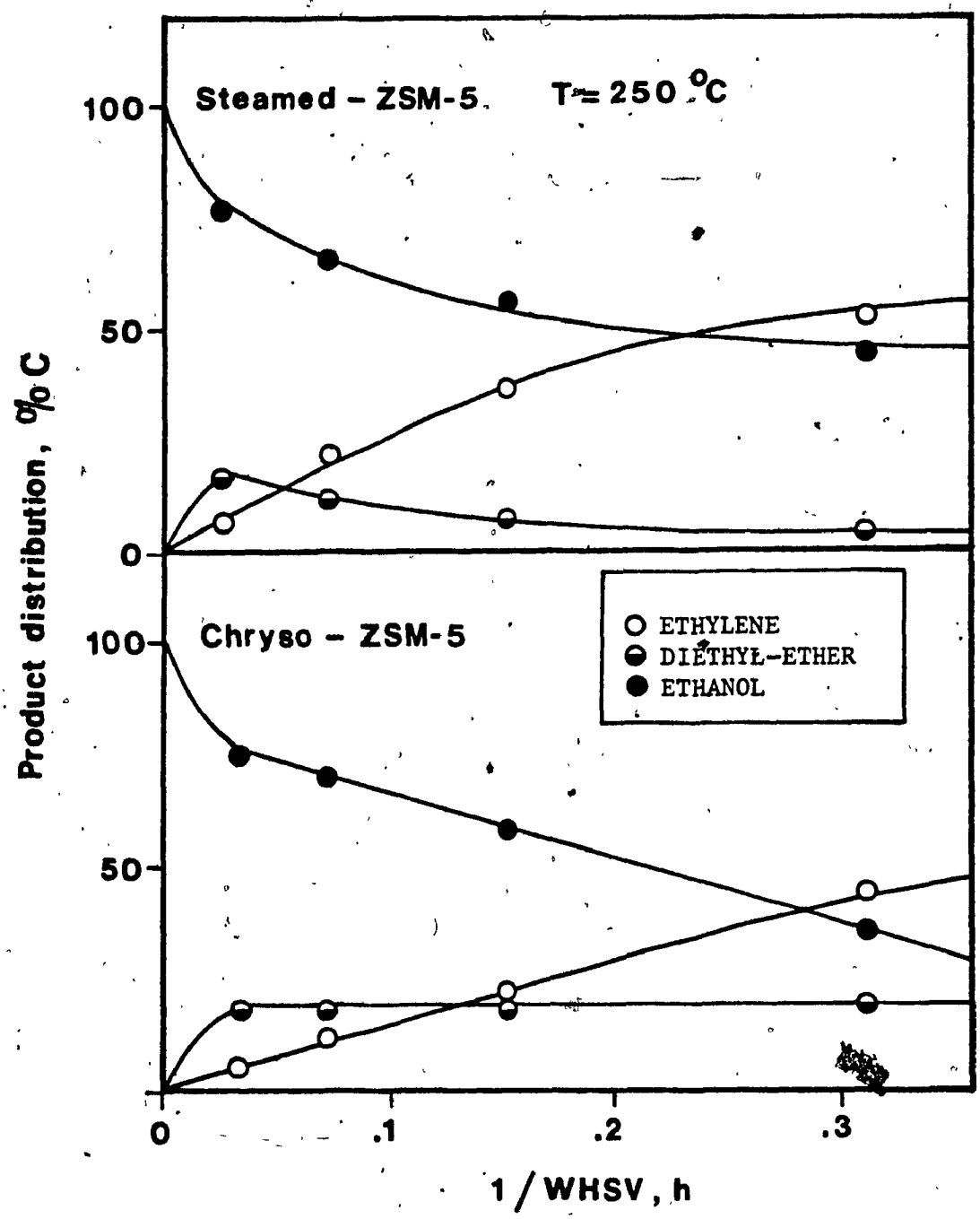

Figure 4.15.- Effect of contact time on the conversion of aqueous ethanol (10 wt%) over steamed HP-(21) and HA-(26/99).

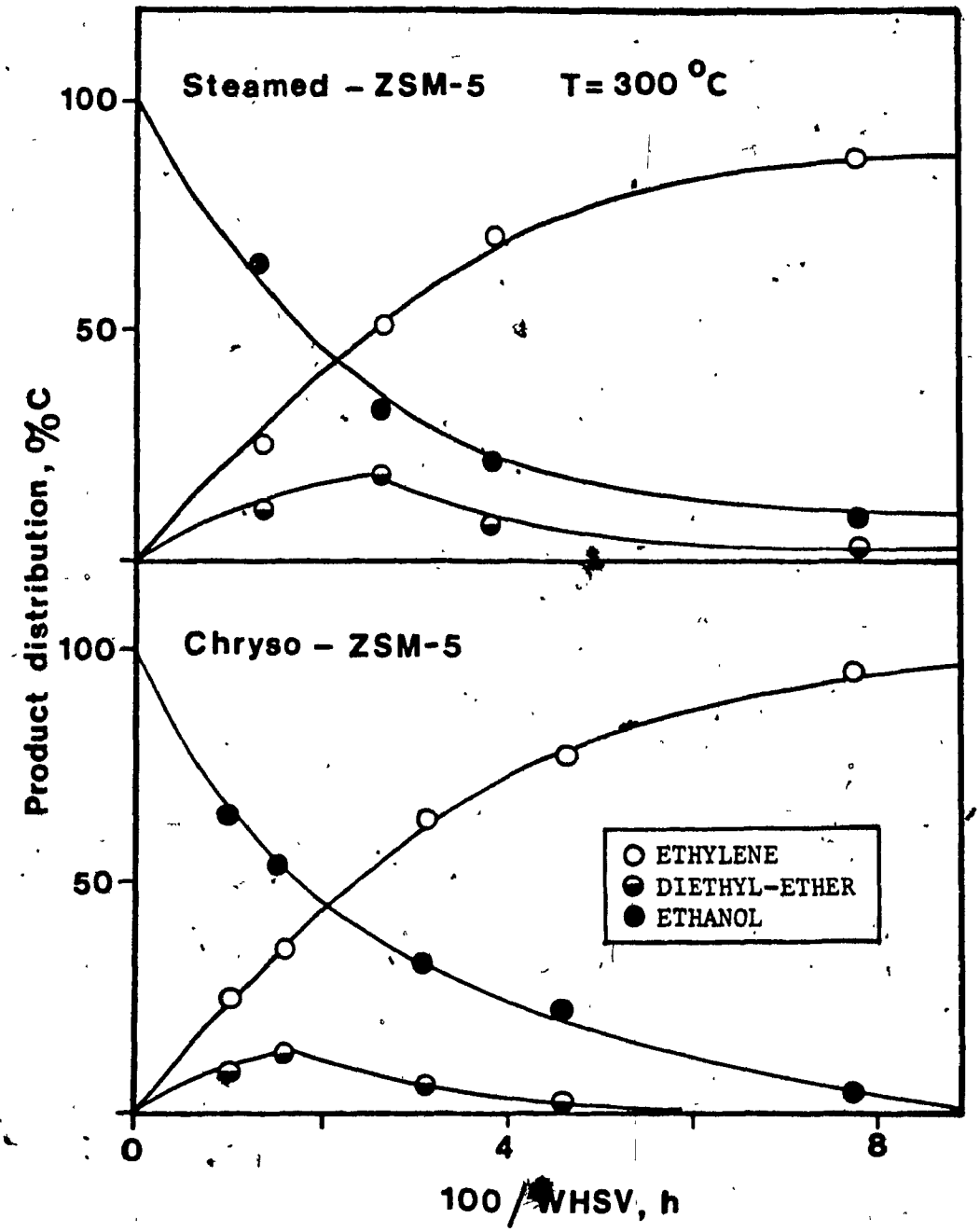

Figure 4.16. Effect of contact time on the conversion of aqueous ethanol (10 wt%) over steamed HP-(21) and HA-(26/99).

4.3 Reaction Mechanism

4.3.1 Reaction Scheme

The results in the previous section show that diethyl ether was a main product in the conversion of aqueous ethanol to ethylene over zeolite ZSM-5 type catalysts at low temperatures and very short contact times while ethylene was the main product at higher temperatures and longer contact times. In order to gain more information about the reaction scheme and also the reaction mechanism, the conversion of aqueous diethyl ether on zeolite ZSM-5 type catalysts was also investigated.

Figure 4.17 shows the product distribution of the conversion of aqueous diethyl ether at various temperatures. At temperatures below 200°C, the conversion of aqueous diethyl ether on steam treated zeolite ZSM-5 catalyst was low. The product was mainly ethanol, which was produced by the hydration of diethyl ether (reverse reaction). At higher temperatures, more ethanol and ethylene were found in the product. This indicated that both hydration and decomposition of diethyl ether to ethanol and ethylene reactions were simultaneously taking place. At even higher temperatures, ethanol reached a maximum and then gradually decreased while ethylene was sharply increased. This indicates that the dehydration of diethyl ether was favored

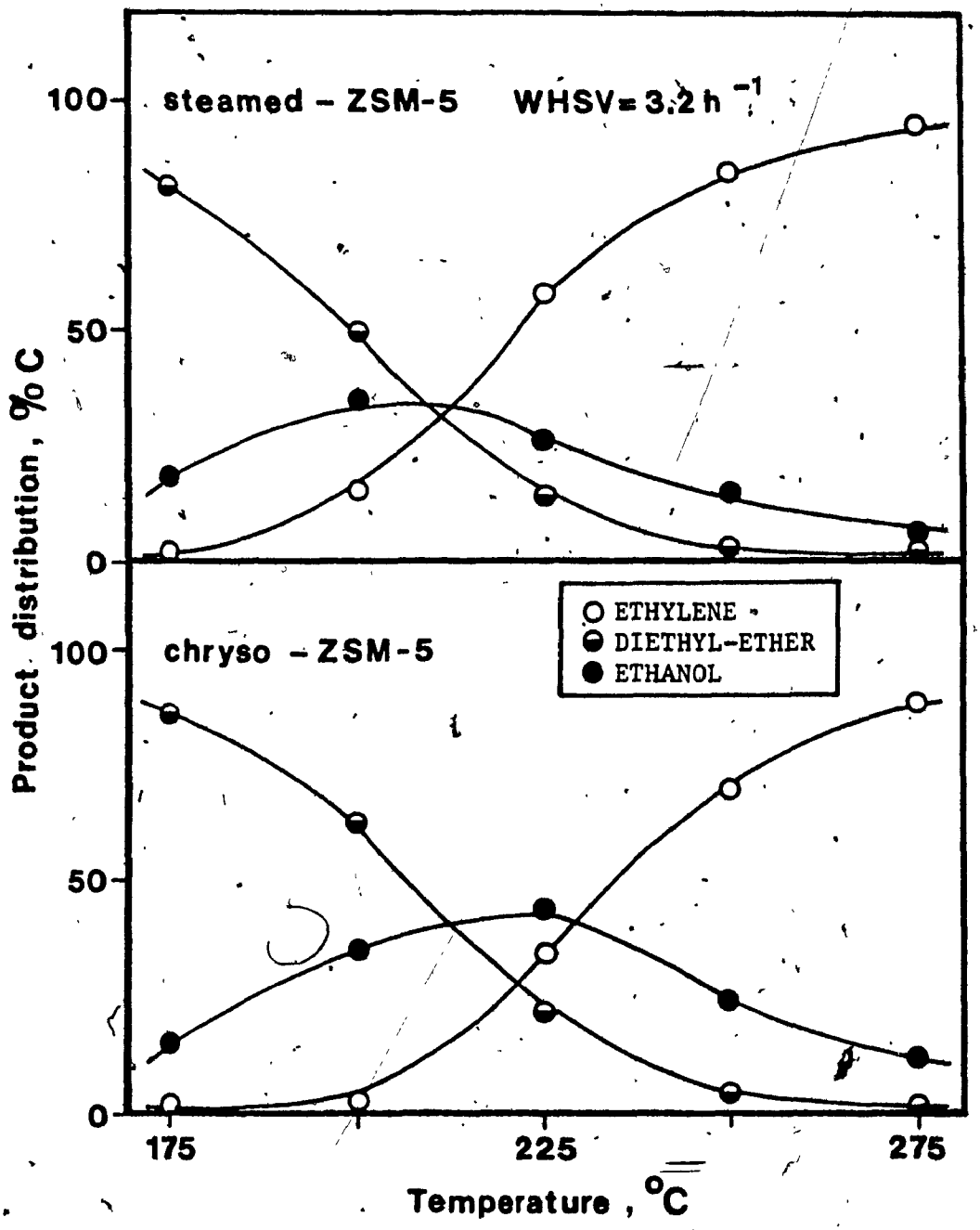

Figure 4.17. Conversion of aqueous diethyl ether (6.5 wt%) to ethylene over steamed HP-(21) and HA-(26/99) at various temperatures.

at higher temperatures, while the hydration of diethyl ether was preferred at lower temperatures.

The product distribution of the conversion of aqueous diethyl ether over steamed HP and chryso-zeolite ZSM-5 (HA) catalysts at various contact times are shown in fig. 4.18. The experiments were performed at 300°C in order to prevent the occurrence of the reverse reaction. At short contact times, ethanol and ethylene were almost produced in one to one molar ratio on both steam treated zeolite ZSM-5 and chryso-zeolite ZSM-5. This indicated that one mole of diethyl ether formed to one mole of ethylene and one mole of ethanol rather than two moles of ethylene. Increasing the contact time, ethanol passed through a maximum and then gradually decreased, which was probably due to the re-adsorption and de-hydration as was observed in the case when ethanol was used in the feed.

Thus, from the obtained results, it is suggested that the reaction of aqueous ethanol to ethylene over zeolite ZSM-5 type catalysts occurred according to the following scheme;

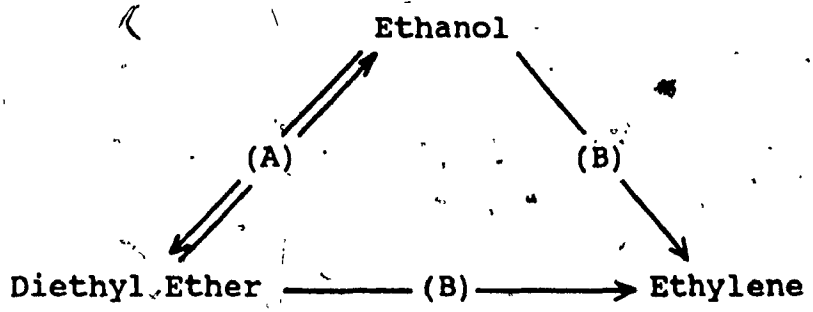

(A) Low temperature and short contact times.

(B) High temperature and long contact times.

This reaction scheme could be explained by the following reaction mechanism.

4.3.2 Reaction Mechanism

The mechanism of ethylene and diethyl ether formation from ethanol on the surface of zeolite ZSM-5 catalysts, according to Aronson et al. (44,45), can be represented in figure 4.19.

The ethanol molecules were first adsorbed on the Bronsted acid site which is in the vicinity of the Al atoms. Then proton transfer from the zeolite framework to ethanol takes place forming a dihydroethyl oxonium ion. The less stable dihydroethyl oxonium ion is then rapidly attacked by another ethanol molecule to form the more stable hydrodiethyl oxonium ion.

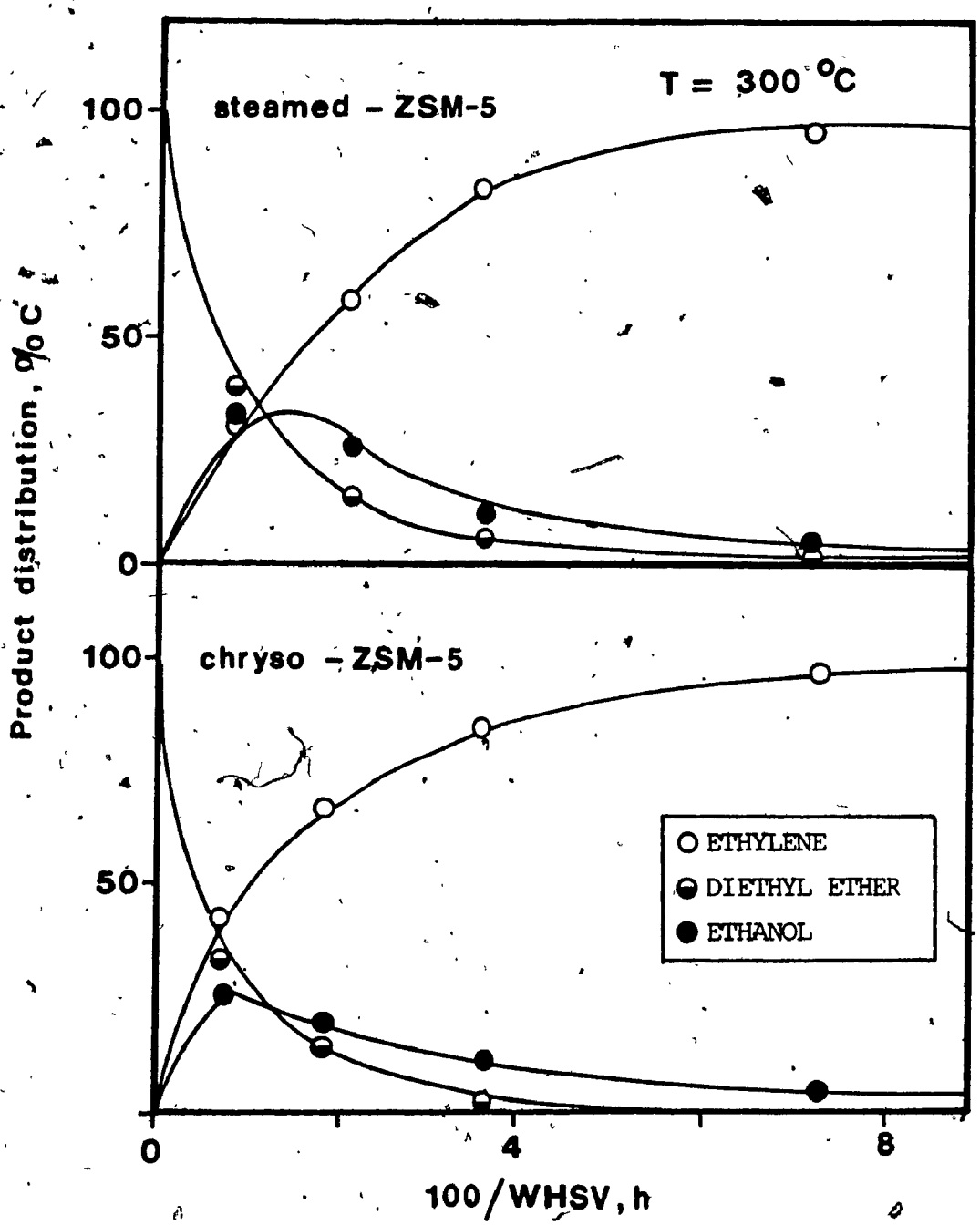

Figure 4.18. Conversion of aqueous diethyl ether (6.5 wt%) to ethylene over steamed HP-(21) and HA-(26/99) at various contact times.

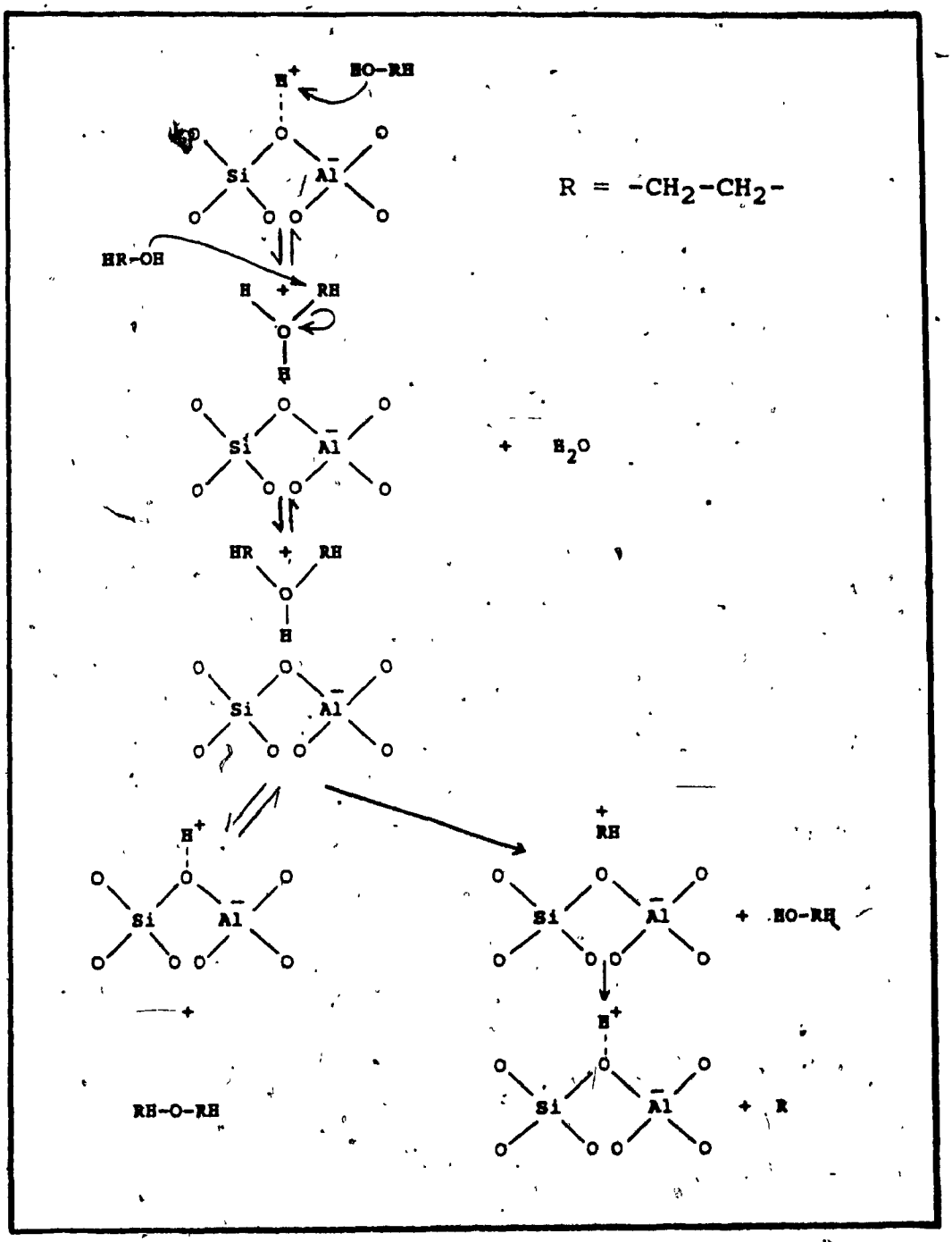

Figure 4.19. reaction mechanism of the conversion of aqueous ethanol to ethylene and diethyl ether on zeolite ZSM-5 catalysts.

Depending on the reaction conditions, the adsorbed oxonium ion will either decompose by reverse proton transfer to give diethyl ether as it is observed at low temperatures, or react via a carbonium ion at high temperatures. The ethylene is then produced by the loss of a proton from the carbonium intermediate to the zeolite framework, which is known as an E1 mechanism.

The direct conversion of ethanol to ethylene by E_2 mechanism could occur on the chryso-zeolite ZSM-5 catalyst. According to Chang (16) and Figuras et al. (46), the coexistence of the basic and acidic sites, which are presented in chryso-zeolite ZSM-5, could facilitate the bond dissociation of ethanol to ethylene as shown in figure 4.20.

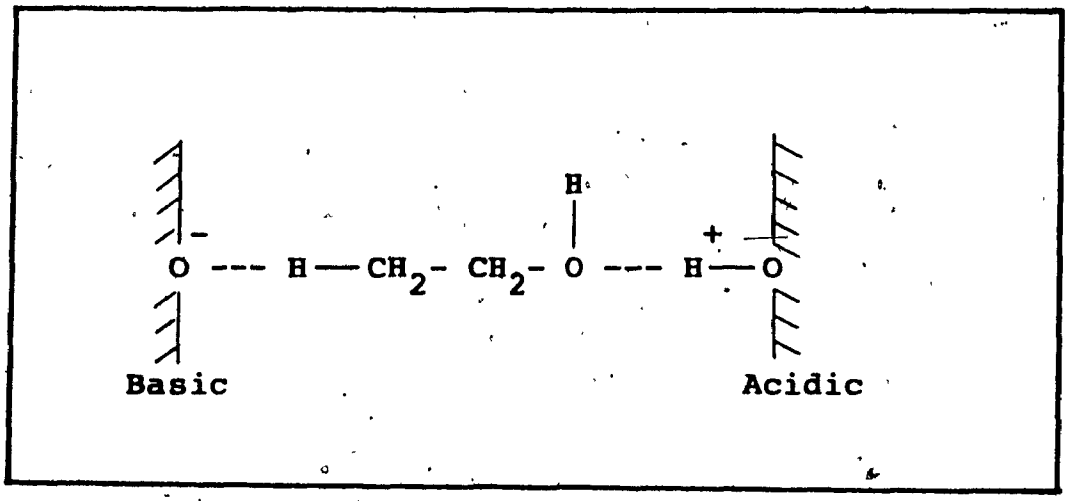

Figure 4.20. Effect of simultaneous presence of acidic (zeolite) and basic sites (MgO) on the conversion of aqueous ethanol to ethylene (E2 mechanism).

The dehydration of an alcohol to olefin by E_2 mechanism, according to Poustma et al. (47), was favored at high temperatures. Therefore, it can be used to explain why chryso-zeolite ZSM-5 was less active at low temperatures and was more active at high temperatures compared to steam treated zeolite ZSM-5.

4.4 Apparent Activation Energy

When a heterogeneous catalytic reaction occurs, several physical and chemical processes take place in proper sequence (figure 4.21). Hill (48) presented those steps in the following manner:

- Mass transfer of the reactants from the main body of the fluid to the gross exterior surface of the catalyst particles.
- Molecular diffusion of reactants from the exterior surface of the particle into the interior pore structure.
- Chemisorption of the reactants on the catalyst surface.
- Reaction on the surface possibly involving many steps.
- Desorption of chemically adsorbed species from the surface of the catalyst.

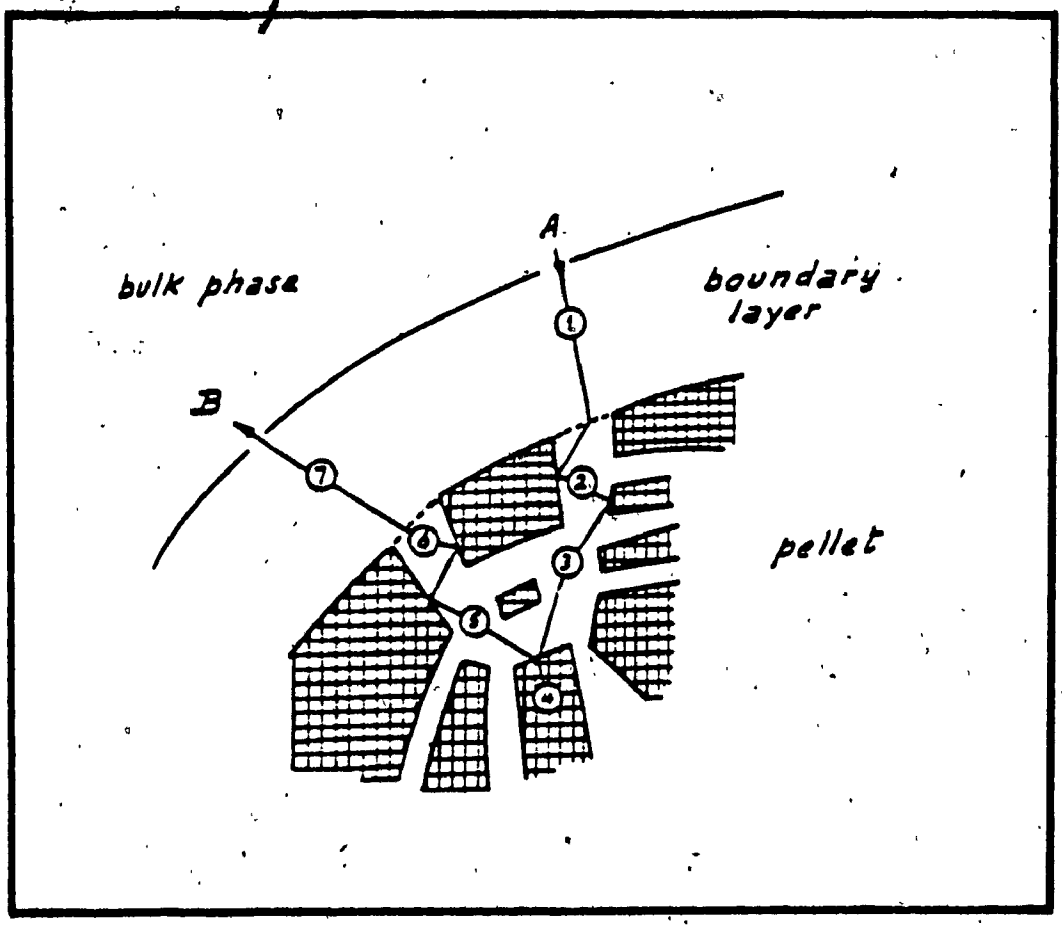

Figure 4.21. Physical and chemical steps in heterogeneous catalysis

1- external diffusion
2- internal diffusion
3- adsorption of reactant A
4- chemical reaction
5- desorption of product B
6- internal counter-diffusion
7- external counter-diffusion.

- Transfer of the products from the interior catalyst to the gross external surface of the catalyst by molecular diffusion.

- Mass transfer of the products from the exterior surface of the particles into the bulk of the fluid.

In order to evaluate the apparent activation energy, some assumptions were made: First, the mass transfer of the species between the catalyst particles and the bulk fluid was not a limiting step in the process and could be neglected. By changing the weight of the catalyst and the molal feed flow rate so as to maintain the weight hourly space velocity constant, the conversion of the product distribution did not significantly change (Table 4.11).

Feed (g/h)	Weight (g)	Conv.HC (%)	Selectivity (%)	
			Ethylene	C_3^+ Olef.
19.20	6.00	99.64	99.38	0.62
12.80	4.00	99.55	99.36	0.64
8.10	2.53	99.57	99.42	0.58
4.90	1.53	99.63	99.41	0.59

Table 4.11. Conversion of aqueous ethanol (10 wt%) over steamed HP-(21) at 300°C and WHSV 3.2 h^{-1}.

Feed : ethanol solution
Weight : weight of catalyst.

Second, the molecular diffusion of the reactants and the products, which is not negligible, was assumed to be small and was not taken into account. Thus, the process depended on the adsorption, the reaction, and the desorption steps. The dehydration reaction and desorption process were endothermic while the adsorption process is exothermic, therefore the apparent activation energy could be written as follows:

$$E_{app} = H_{ads} - E_{rxn} - H_{des} \qquad (4.2)$$

In general, the activation energy of a reaction could be obtained according to the Arrhenius equation, if the reaction rate at various temperatures were known, that is:

$$k = A \cdot \exp(-E/RT) \qquad (4.3)$$

where k is the rate constant.

A is the pre-exponential factor.

E is the apparent activation energy.

R is the gas constant.

For the dehydration reaction of an alcohol, the reaction rate could be expressed as follows:

$$r = k P^{n}_{A} \qquad (4.4)$$

where r is the reaction rate.

k is the rate constant.

P_A is the partial pressure of the reactants.

By substituting the equation (4.3) to (4.4), the reaction rate becomes:

$$r = A \exp(-E/RT) \; P_A^n \qquad (4.5)$$

When an experiment was performed on a fixed bed reactor, at low conversion and particularly with a dilute aqueous solution as a feed, the partial pressure of the reactant changed only by small amounts and the reaction system approached to that of a differential reactor. The reaction rate per gram of the catalyst, therefore, was given by (49):

$$r = \frac{F \cdot C}{w} \qquad (4.6)$$

where C is the conversion expressed in %C-atoms.

w is the weight of the catalyst in grams.

F is the molar feed in mole/hr.

Rearrangement of equation (4.6) yields:

$$r = \frac{C}{w/F} = \frac{C}{t} \qquad (4.7)$$

where t (=w/F) is the space time or contact time in g.hr/mole.

Thus, the reaction rate is a function of contact time and could be determined from a plot of conversion versus contact times.

In this work, the initial rate of reaction, (r_o), which is the rate of the reaction at contact time zero, was used for evaluation of the apparent activation energy, because the partial pressure of the reactants was unchanged. Equation (4.5) then becomes

$$r_o = k' \cdot \exp(-E/RT) \qquad (4.8)$$

where $k' = A \cdot P^n_A$ is a constant.

The initial rate of the reaction could be obtained graphically in which the initial rate is equal to the slope of the conversion versus contact time curve at contact time equal to zero. However, this method gives a large error for determination of Eapp. A more accurate method to obtain the initial rate is to fit the experimental data into a function (f(t)), obtained by trial and error. Then, the initial rate

of the reaction can be determined by taking the derivative of the function and extrapolating to zero contact times.

$$r_o = \lim_{dt_t \to o} \frac{d[C]}{} = \lim_{dt_t \to o} \frac{d[f(t)]}{} \qquad (4.9)$$

After obtaining initial reaction rates at various temperatures, the apparent activation energy is evaluated using the Arrhenius plot.

In this work, not only the apparent activation energy of the aqueous ethanol to ethylene reaction, but also the apparent activation energies of the aqueous ethanol to diethyl ether reaction and diethyl ether to ethylene reaction were investigated and the results are reported in the following section.

4.4.1 Aqueous Ethanol to Ethylene Reaction

Tables 4.12 and 4.13 report the catalytic conversion of aqueous ethanol to ethylene over steamed zeolite ZSM-5 and chryso-zeolite ZSM-5 at various space times and temperatures.

The dehydration of ethanol to ethylene on zeolite ZSM-5 and chryso-zeolite ZSM-5 was observed to be a first order reaction. Therefore, the conversion to ethylene versus the contact times can be represented by the following equation:

Temp	t	Conversion (%)			Selectivity (%)	
k	g.h/mol	Total	Ether	HC	Ethylene	C_3^+ Olef
598	0.00	0.00	0.00	0.00	0.00	0.00
	3.59	49.47	0.78	48.69	99.99	0.01
	6.17	75.56	0.34	75.22	99.95	0.05
	8.00	80.05	0.18	79.87	99.93	0.07
	17.97	93.68	0.00	93.68	99.90	0.10
	46.00	97.67	0.00	97.67	97.77	0.23
	71.88	99.75	0.00	99.75	99.70	0.30
573	0.00	0.00	0.00	0.00	0.00	0.00
	6.20	34.69	10.05	24.64	99.93	0.07
	11.95	69.32	19.21	50.11	99.82	0.18
	17.97	79.36	8.98	70.38	99.81	0.19
	35.94	90.32	3.74	86.58	99.78	0.22
	71.88	99.36	3.79	95.57	99.75	0.26
	143.75	99.55	0.00	99.55	99.26	0.64
548	0.00	0.00	0.00	0.00	0.00	0.00
	11.95	35.44	13.53	20.14	99.99	0.01
	17.97	57.42	25.30	32.12	99.99	0.01
	35.94	70.42	8.58	61.84	99.78	0.22
	71.88	92.05	3.50	88.55	99.66	0.34
	143.75	99.69	0.00	99.69	99.71	0.29
523	0.00	0.00	0.00	0.00	0.00	0.00
	11.95	23.96	18.13	5.83	99.87	0.13
	17.97	23.54	12.05	11.49	99.94	0.06
	35.94	33.56	11.37	22.19	99.97	0.03
	71.88	45.19	6.63	38.53	99.92	0.08
	143.75	55.21	3.65	51.56	99.84	0.16

Table 4.12. Conversion of aqueous ethanol (10 wt%) to ethylene at vatious temperatures and contact times over steamed zeolite ZSM-5, steamed HP-(21).

Temp. K	t g.h/mol	Conversion (%)			Selectivity (%)	
		Total	Ether	HC	Ethylene	C_3^+ Olef
623	0.00	0.00	0.00	0.00	0.00	0.00
	1.61	52.47	1.14	51.33	99.97	0.03
	2.42	59.42	0.49	58.93	99.97	0.03
	3.52	74.51	0.27	74.24	99.86	0.14
	6.17	88.75	0.06	88.15	99.85	0.15
	11.95	94.70	0.00	94.70	99.85	0.15
	17.97	97.40	0.00	97.40	99.78	0.22
	35.94	99.80	0.00	99.80	99.71	0.29
598	0.00	0.00	0.00	0.00	0.00	0.00
	2.82	39.19	8.39	30.80	99.85	0.15
	4.95	58.87	13.91	44.96	99.83	0.17
	8.73	72.08	8.47	63.61	99.83	0.17
	17.97	90.30	0.04	90.26	99.83	0.17
	35.94	97.52	0.02	97.50	99.80	0.20
	46.00	99.05	0.00	99.05	99.78	0.22
	71.88	99.45	0.00	99.45	99.74	0.26
	143.75	99.99	0.00	99.99	99.42	0.58
573	0.00	0.00	0.00	0.00	0.00	0.00
	4.82	34.38	9.94	24.44	99.99	0.01
	7.28	48.10	12.56	35.54	99.92	0.08
	14.20	69.75	7.61	62.14	99.83	0.17
	21.70	79.06	1.36	77.70	99.69	0.31
	35.94	96.17	0.00	96.17	99.68	0.32
	71.88	99.05	0.00	99.05	99.60	0.40
	143.75	99.80	0.00	99.80	99.50	0.50
548	0.00	0.00	0.00	0.00	0.00	0.00
	8.04	20.55	10.90	9.65	99.95	0.05
	17.97	39.46	16.72	22.74	99.98	0.02
	35.94	52.27	9.43	43.84	99.84	0.16
	71.88	78.18	3.04	75.14	99.73	0.27
	143.75	97.88	1.31	96.57	99.63	0.37
523	0.00	0.00	0.00	0.00	0.00	0.00
	17.97	26.67	19.99	6.68	99.87	0.13
	35.94	29.12	18.74	10.38	99.93	0.07
	71.88	40.13	20.49	19.64	99.98	0.02
	143.75	62.63	19.98	42.65	99.86	0.14

Table 4.13 Conversion of aqueous ethanol (10 wt%) to ethylene at various temperatures and contact times over chryso zeolite ZSM-5 HA-(26/99).

$$f(t) = 100 - 100\exp(-at) \qquad (4.9)$$

The initial rate of reaction was then derived as:

$$r_o = \frac{d[f(t)]}{dt_{t->0}} = 100a \qquad (4.10)$$

The parameter, a, of the equation was obtained by using a non-linear curve fitting program which was ran on an Olivetti PC (see Appendix III). The results are reported in Table 4.14 and the Arrhenius plot as shown in figure 4.22.

4.4.2 Aqueous Ethanol to Diethyl Ether Reaction

To evaluate the apparent activation energy of the aqueous ethanol to diethyl ether reaction, experiments were performed at relatively low temperatures, i.e. 175, 200 and 225°C, in order to get very high selectivity to diethyl ether. The catalytic conversion versus the space times are reported in Table 4.15 and 4.16.

The following type of function:

$$f(t) = \frac{at}{b + t} \qquad (4.11)$$

was found to well fitted for the experimental data, and the initial rate was obtained as:

$$r_o = \frac{d[f(t)]}{dt_{t->0}} = \frac{a}{b} \qquad (4.12)$$

The results are reported in Table 4.17.

4.4.3 Diethyl Ether to Ethylene Reaction

Tables 4.18 and 4.19 report the catalytic conversion of aqueous diethyl ether (6.5 wt%) to ethylene versus the space time on steamed zeolite ZSM-5 and chryso-zeolite ZSM-5 catalysts.

The conversion of diethyl ether to ethylene was also observed to obey the first order reaction. Therefore both equations (4.9) and (4.10) were employed for obtaining the initial rate and apparent activation of reaction. The results are reported in Table 4.20.

The apparent activation energy of the aqueous ethanol to ethylene and diethyl ether reactions on both steam treated zeolite ZSM-5 and chryso-zeolite ZSM-5 were comparable to the results reported by Van Hooft et al. (50) which are 29.2kcal/mol and 7.2kcal/mol respectively

Catalysts	Temp. K	f(t)=100-100EXP(-at) a	Deviation	r_o mole/g.h	E_{app} Kcal/mole
Steamed HP-(21)	598	0.20184	2.48	20.184	28.55
	573	0.05837	3.26	5.837	
	548	0.02518	3.82	2.518	
	523	0.00582	3.14	0.582	
HA-(26/99)	623	0.38819	2.17	38.819	29.45
	598	0.12151	2.92	12.151	
	573	0.06714	3.12	6.714	
	548	0.01744	3.45	1.744	
	523	0.00357	2.84	0.357	

Table 4.14. Initial rate and apparent activation energy of the aqueous ethanol (10 wt%) to ethylene reactions.

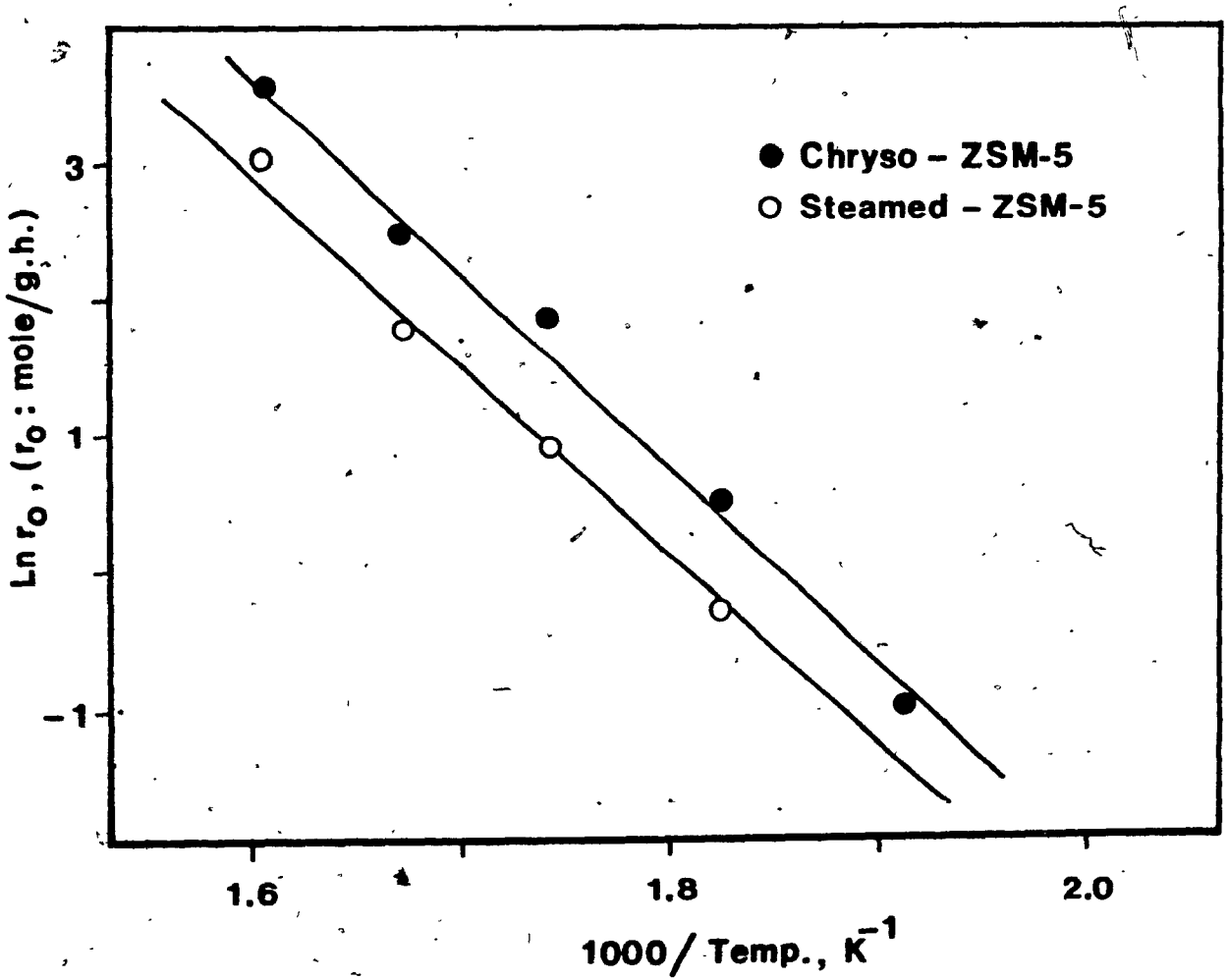

Figure 4.22. Arrhenius plot of the initial rate for the conversion of aqueous ethanol (10 wt%) on steamed HP-(21) and HA-(26/99).

Temp. K	t g.h/mole	Conv. HC (%)	Selectivity (%)	
			Ether	Ethylene
498	0.00	0.00	0.00	0.00
	17.97	14.90	13.83	1.07
	35.94	20.04	18.53	1.51
	71.88	29.52	26.92	2.60
473	0.00	0.00	0.00	0.00
	17.97	8.04	7.92	0.12
	35.94	12.90	12.74	0.16
	71.88	24.78	24.59	0.19
	143.75	28.75	28.02	0.73
448	0.00	0.00	0.00	0.00
	35.94	7.70	7.68	0.02
	71.88	10.96	10.92	0.04
	143.75	18.56	18.53	0.01
	184.00	20.85	20.83	0.02

Table 4.15. Conversion of aqueous ethanol (10 wt%) to diethyl ether at various temperatures and contact times over steamed zeolite ZSM-5, steamed HP-(21).

Temp. K	t g.h/mole	Conv. HC (%)	Selectivity (%)	
			Ether	Ethylene
498	0.00	0.00	0.00	0.00
	11.95	10.14	9.94	0.20
	21.49	14.91	13.75	1.16
	35.94	28.94	27.04	1.90
	71.88	33.27	30.46	2.81
473	0.00	0.00	0.00	0.00
	21.48	8.08	7.97	0.11
	35.94	12.11	11.89	0.22
	71.88	19.42	18.93	0.49
	143.75	27.01	26.48	0.53
	184.00	30.93	30.15	0.78
448	0.00	0.00	0.00	0.00
	35.94	6.94	6.92	0.02
	71.88	10.35	10.32	0.03
	143.75	14.38	14.37	0.01
	184.00	16.86	16.81	0.05

Table 4.16. Conversion of aqueous ethanol (10 wt%) to diethyl ether at various temperatures and contact times over chryso-zeolite ZSM-5 , HA-(26/99).

Catalysts	Temp. K	f(t) = at / (b + t) a	b	Deviation	r_o mole/g.h.	E_{app} Kcal/mole
Steamed HP-(21)	498	40.667	38.404	0.74	1.059	13.39
	473	44.359	74.944	1.59	0.592	
	448	40.075	170.700	0.61	0.235	
HA-(26/99)	498	52.497	46.755	2.37	1.123	13.36
	473	47.119	107.278	0.26	0.439	
	448	25.619	103.819	0.34	0.247	

Table 4.17. Initial rate and apparent activation energy of the aqueous ethanol (10 wt%) to diethyl ether reactions.

Temp. K	t g.h/mole	Conversion (%)			Selectivity (%)	
		Total	Ethanol	HC	Ethylene	C_3^+ Olef.
573	0.00	0.00	0.00	0.00	0.00	0.00
	8.17	60.09	28.29	31.80	99.77	0.23
	24.22	80.68	21.24	59.04	99.79	0.21
	41.25	93.94	10.06	83.28	99.86	0.14
	82.45	99.86	5.43	94.43	99.82	0.18
548	0.00	0.00	0.00	0.00	0.00	0.00
	20.51	66.59	32.74	33.85	99.88	0.12
	41.25	80.67	22.77	57.97	99.89	0.11
	82.45	94.24	18.59	75.65	99.86	0.14
	164.99	98.30	7.80	90.50	99.86	0.14
523	0.00	0.00	0.00	0.00	0.00	0.00
	41.25	61.88	33.76	28.12	99.63	0.37
	82.45	79.23	29.67	49.56	99.78	0.22
	123.73	88.82	23.57	65.25	99.83	0.17
	164.99	93.54	20.34	73.20	99.82	0.18

Table 4.18. Conversion of aqueous diethyl ether (6.5 wt%) at various temperature and contact times over steamed zeolite ZSM-5 , steamed HP-(21).

Temp. K	t g.h/mole	Conversion (%0			Selectivity (%)	
		Total	Ethanol	HC	Ethylene	C_3^+Olef
573	0.00	0.00	0.00	0.00	0.00	0.00
	8.24	68.84	26.86	41.98	99.84	0.16
	20.47	86.84	19.58	67.26	99.79	0.21
	41.47	97.99	12.86	85.13	99.77	0.23
	82.63	99.95	4.26	95.69	99.64	0.36
	165.75	99.98	0.93	99.05	99.63	0.37
548	0.00	0.00	0.00	0.00	0.00	0.00
	11.38	37.04	14.50	22.54	99.66	0.34
	20.47	79.24	30.66	48.58	99.83	0.17
	41.47	95.29	26.26	69.03	99.71	0.29
	82.93	99.65	9.13	90.52	99.82	0.18
	124.35	99.95	6.93	93.02	99.76	0.24
	165.74	99.99	3.96	96.03	99.49	0.51
423	0.00	0.00	0.00	0.00	0.00	0.00
	41.47	74.99	39.89	35.10	99.77	0.23
	82.93	92.03	26.56	65.47	99.89	0.11
	124.35	98.99	23.40	75.59	99.90	0.10
	165.74	98.99	18.86	80.13	99.88	0.12

Table 4.19. Conversion of aqueous diethyl ether (10 wt%) at various temperatures and contact times over chryso-zeolite ZSM-5, HA-(26/99).

Catalysts	Temp. K	f(t)=100-100EXP(-at) a	Deviation	r_o mole/g.h	$E_{app.}$ Kcal/mole
Steamed HP-(21)	573	0.04051	2.59	4.501	I8.96
	548	0.01890	3.28	1.890	
	523	0.00824	0.84	0.824	
HA-(26/99)	573	0.05555	3.25	5.555	19.06
	548	0.02811	3.12	2.801	
	523	0.01124	3.07	1.124	

Table 4.20. Initial rate and apparent activation energy of the aqueous diethyl ether (6.5 wt%) to ethylene reactions.

CHAPTER 5 - CONCLUSION

The results obtained in this work clearly demonstrated that both steam treated zeolite ZSM-5 and chryso-zeolite ZSM-5 could be used for dehydration of very dilute aqueous ethanol obtained from fermentation broth into very pure ethylene. The complete conversion of aqueous ethanol to ethylene could be achieved under the following conditions:

1) The reaction temperature range employed should fall between 250°C and 400°C.

2) A weight hourly space velocity range between 0.5 h^{-1} to 100h^{-1} should be used as determined by the reaction temperature, with a lower reaction temperature requiring a lower W.H.S.V.

3) The silicon to aluminum of both catalysts should be less than 45. For the chryso-zeolite ZSM-5, the magnesium leaching degree should be higher than 95% in order to obtain a very active and stable catalyst.

Although, in this work, the reaction mechanism of the dehydration of aqueous ethanol over steam treated zeolite ZSM-5 and chryso-zeolite ZSM-5 was not investigated in detail, however, the change in product selectivity (between diethyl ether and ethylene) at various temperatures and contact times was very well explained with the 'alkyl

oxonium intermediates' mechanism as proposed by Aronson et al. In addition, the obtained kinetic results, which were comparable to those reported by Van Hooft et al., also supported this mechanism.

The obstacle in attempting to utilize biomass as an ethylene source according to the scheme 'biomass - glucose- ethanol - ethylene' due to a huge energy consumption for distillation and further dehydration of ethanol could be overcome by replacement with an economical catalytic process as demonstrated in this work. However, further studies are needed in order to develop a new type of catalyst which can be used at lower temperatures so less energy will be consumed and the production cost will be less expensive. Also, more information on the reaction mechanism, using such techniques as FTIR, TPD-alcohol and TGA, needs to be obtained. Research is presently underway on the development of new types of catalysts, such as triflic acid doped onto the surface of zeolite ZSM-5. The acidity of the catalyst is dramatically enhanced and the complete conversion of aqueous ethanol to ethylene could be achieved at temperatures as low as 170°C (51). Undoubtedly, with more research effort, the biomass to ethylene route will become as economically feasible route in the years to come (52).

CHAPTER 6 - REFERENCES

1. R. Le Van Mao, Paper presented at Transtech Conference, Montreal, Canada.
2. D.R. Whitcraft, X.E. Veryklos and R. Mutharasan, Ind. Eng. Chem. Process Des. Dev., 22, 452-457, (1983).
3. R. Le Van Mao and L.H. Dao, U.S. Patent applic., Sept. 29, (1987).
4. O.M. Kut, R.D. Tanner, J.E. Prenosil and K. Kamholz, Catalysis Conversion of Synthesis Gas and Alcohol to Chemical, R.G. Hermas Ed., Plenum Press, 361-393, (1984).
5. E. Costa, A. Uguina, J. Aguado and P.J. Hernandez, Ind. Eng. Chem. Process. Des Dev., 24, 239-244, (1985).
6. G.A. Aldridge, X.E. Veryklos, J. Mutharasan, Ind. Emg. Chem. Process Des. Dev., 23, 733-737, (1984).
7. O.A. Anunziata, O.A. Orio, E.R. Herrero, A.F. Lopez, C.F. Parez and A.R. Suarez, App. Cat., 15, 235-245, (1985).
8. R. Le Van Mao, P. Levesque, G.P. McLaughin and L.H. Dao, App. Cat., 34, 163-179, (1987).
9. H.F. Wenzel, The Chemical Technology of Wood, Academic Press, 34-38, (1970).
10. L. Pazner, H.J. Cho, Biomass (In press).
11. I.S. Goldstein, Organic Chemical from Biomass, CRC Press Inc, 1981.

12. B. Atkinson and F. Mavitra, Biochemical Engineering & Biotechnology Handbook, Macmillan Publ. Ltd, 1983, 403.

13. L. Kniel, O. Winter and K. Stork, Ethylene: Keystone to the Petrochemical Industry, Marcel Dekker Inc., (1980)

14. H. Knozinger and R. Kohne, J. Cat., 5, 264-270, (1966).

15. N.Y. Chen and T.F. Degnan, Chem. Eng. Prog., Feb. iss., 32-41, (1988).

16. C.D. Chang, Hydrocarbon from Methanol, Marcel Dekker Inc., 1983.

17. E.G. Derouane, Catalysis on the Energy Scene, Elsevier Amsterdam, 1986.

18. R. Le Van Mao and P.H. Bird, Can. Patent, 1-195-311, 1985 and U.S. Patent 4-511-667, 1985.

19. R. Le Van Mao, P. Levesque and B. Sjiariel, Can. J. Chem. Eng., 64, 514-516, (1986).

20. R. Le Van Mao, P. Levesque, B. Sjiariel and N.T. Do, Can. J. Chem. Eng., 64, 462-467 (1986).

21. R.J. Argauer and G.R. Landolt, U.S. Patent, 3-702-886, 1972.

22. K. Fujisawa, T. Sano, K. Suzuki, H. Okada, K. Kawamura, Y. Kohoku, S. Shin, H. Hagiwara and H. Takaya, Bull. Chem. Soc. Jpn., 60, 791-793, (1987).

23. S.B. Kulkarmi, V.P. Shiralkar, A.N. Kotasthane, R.B. Borade and P. Ratnasamy, Zeolites, 2, (1982).

24. R. Le Van Mao, P. Levesque, B. Sjiariel and P.H. Bird,

Can. J. Chem, 63, (1985),

25. S. Brunauer, P.H. Emmett and E. Teller, J. Am. Chem. Soc., 60, 309, (1938).

26. B.M. Lok, B.K. Marcus and C.L. Angell, Zeolite, 6, 185 -194, (1986).

27. R. Le Van Mao and J. Yao, J. Cat. (submitted).

28. R. Le Van Mao, React. Kinect. Cat. Lett., 12, 69, (1979).

29. R. Le Van Mao, O. Pilati, A. Marzi, G. Leofanti, A. Villa and V. Ragaini, React. Kinect. Cat. Lett, 15, 293, (1980).

30. M. Inomata, M. Yamada, S. Okada, M. Niwa, Y. Murakin, J. Cat., 100, 264, (1986).

31. P. Levesque, Ph.D. Thesis, Concordia University, June 1987.

32. P.A. Jacobs, M. Tielen, J.B. Nagy, G. Debras, E.G. Deronane and Z. Gabelica, Proceedings of the 7th International Zeolite Conference, Kodansha Tokyo, Elsevier Amsterdam, 783-792, 1987.

33. R.M. Dessau, K.D. Schmidt, G.T. Kerr, G.L. Woolery and L.B. Alemay, J. Cat., 104, 484-489, (1987).

34. A.G. Ashton, S. Batmanian, D.M. Clark, J. Dwyer, F.R. Machado, Catalysis by Acids and Bases, Elsevier Amsterdam, 101-109, 1985.

35. J.P. Gilson, G.C. Edwards, A.W. Peters, K. Rajagopalan, R.F. Wormshecher, T.G. Roberie and M.P. Shatlock, J.

Chem. Soc., Chem. Commun., 91, (1987).

36. M.C. Cruickshank, L.S. Dent Glasser, S.A. Barri and J.F. Poplett, J. Chem. Soc., Chem. Commun., 23, (1986).

37. N.Y. Topsoe, F. Joensen and E.G. Derouane, J. Cat., 110, 404-406, (1986).

38. P.S. Yarlagadda, H. Yaollang and N.N. Bakhshi, Ind. Eng. Chem. Prod. Res. Dev, 25, 251-257, (1986).

39. Y. Sendoda and Y. Ono, Zeolites, 8, (1988).

40. H. Itoh, C.V. Hidalgo, T. Hattori, M. Niwa and Y. Murakami, J. Cat., 85, 527-529, (1984).

41. T. Inui, T. Suzuki, M. Inoue, Y. Murakami and Y. Takegami, Catalysis by Acids and Bases, Elsevier, Amsterdam, 1985.

42. L.M. Kustov, V.Y. Borovkov and V.B. Kazansky, Structure and Reactivity of Modified Zeolites, Elsevier, Amsterdam, 241-247, 1984.

43. K.G. Ione, G.V. Echevskii and G.N. Nosyreva, J. Cat., 85, 287-294, (1984).

44. M.T. Aronson, R.J. Gorte and W.E. Farneth, J. Cat., 98, 434-443, (1986).

45. M.T. Aronson, R.J. Gorte and W.E. Farneth, J. Cat, 105, 455-468, (1987).

46. F. Figneras, A. Nohl, L. de Mourgnes, Y. Trambouze, J. Chem. Soc. Faraday Trans. I, 67, 1155, (1971).

47. M.L. Poustuma, Zeolite Chemistry and Catalysis, J.A. Rabo Ed., A.C.S. Monograph, Chapter 9, 171, 1976.

48. C.G. Hill, Introduction to Chemical Engineering Kinetics and Reactor Design, J. Wiley and Sons Ed., Chapter 6, 1977.

49. S.J. Thomson and G. Webb, Heterogeneous Catalysis, Oliver and Boyd Ltd., 95-98, 1968.

50. J.H.C. Van Hooff, J.P. Van den Berg, J.P. Wothuizen and A. Volmer, Proc. 6th Int. Zeolite Conf., Olson and Bisio Ed., Butterworth Pub., 489-496, 1984.

51. R. Le Van Mao and T.M. Nguyen, U.S. Patent, applied (April 5, 1988).

52. R. Le Van Mao, T.M. Nguyen and G.P. McLaughlin, paper presented at the 3rd Chemical Congress of North America, American Chemical Society, Toronto, (Canada), June 5-11, 1988.

APPENDIX I

B.E.T. Basic Program

```
10 REM -- Surface Measurement Calculation (B.E.T.)----------
20 REM                          by
30 REM                    Nguyen, Thanh My
40 REM ------------------------------------------------------
50 CLS
60 DIM V(6),LVL1(10),LVL2(10),LVL3(10),LVL4(10)
70 DIM P1(10),P2(10),P3(10),P4(10),X(10),Y(10),FD(40)
80 CLEAR
90 DATA 0,13.32,32.2,59.61,93.23,136.43
100 REM -----read in the standard volumes-------------------
110 FOR I=1 TO 6
120 READ V(I)
130 NEXT I
140 INPUT " Sample name : ";SAMPLE$
150 PRINT "-----------------------------------------------"
160 LPRINT "  Sample name : ";SAMPLE$
170 LPRINT "-----------------------------------------------"
180 REM ----input the experimental data--------------------
190 INPUT " No. of equilibrium in step 1 : ";NEP1
200 INPUT " The equilibrium temperature in step 1 : ";TC1
210 PRINT " Enter the levels and equilibrium pressures in
    step 1"
220 PRINT
230 FOR I = 1 TO NEP1
240    INPUT LVL1(I),P1(I)
250 NEXT I
260 PRINT " -----------------------------------------------"
270 INPUT " No. of equilibrium in step 2  ";NEP2
280 INPUT " The equilibrium temperature in step 2 : ";TC2
290 PRINT " Enter the levels and equilibrium pressures in
    step 2"
300 PRINT
310 FOR I = 1 TO NEP2
320    INPUT LVL2(I),P2(I)
330 NEXT I
340 PRINT " -----------------------------------------------"
350 INPUT " No. equilibrium in step 3 : ";NEP3
360 INPUT " The equilibrium temperature in step 3 : ";TC3
370 PRINT " Enter the levels and equilibrium pressures in
    step 3"
380 PRINT
390 FOR I = 1 TO NEP3
400    INPUT LVL3(I),P3(I)
410 NEXT I
420 PRINT " -----------------------------------------------"
430 INPUT " No. of equilibrium in step 4 : ";NEP4
```

```
440 INPUT " The equilibrium temperature in step 4 : ";TC4
450 PRINT " Enter the levels and equilibrium pressures in
    step 4"
460 PRINT
470 FOR I = 1 TO NEP4
480    INPUT LVL4(I),P4(I)
490 NEXT I
500 PRINT "-------\----------------------------------------"
510 PRINT : INPUT " The weight of sample : ";W
520 REM calculate the dead volume
530 SUM = 0
540 FOR I = 1 TO (NEP1-1)
550    V1 = V(LVL1(I))
560    V2 = V(LVL1(I+1))
570    V3 =  ((V2 * P1(I+1)) - (V1 * P1(I)))/(P1(I) -
    P1(I+1))
580    SUM = SUM + V3
590    NEXT I
600 DEAD = SUM / (NEP1-1)
610 LPRINT : LPRINT " Dead volume : ";DEAD;"cc."
620 REM calculate the total volume of Helium
630 SUM = 0
640 FOR I = 1 TO NEP1
650    V1 = V(LVL1(I)) + DEAD
660    SUM = SUM + (V1*P1(I)*273.15/((TC1+273.15)*760))
670    NEXT I
680 HE = SUM / NEP1
690 LPRINT : LPRINT " Total volume of He : ";HE;"cc."
700 REM calculate the free space
710 SUM = 0
720 FOR I = 1 TO NEP2
730    V1 = V(LVL2(I)) + DEAD
740    V2 = HE - (V1*P2(I)*273.15/((TC2+273.15)*760))
750    FREE = V2 / P2(I)
760    LPRINT : LPRINT " Free space ";I;"  :   ";FREE
770    SUM = SUM + FREE
780    NEXT I
790 AVE = SUM / NEP2
800 LPRINT : LPRINT " Average free volumes : ";AVE
810 REM calculate volume absorbing gas introduced
820 SUM = 0
830 FOR I = 1 TO NEP3
840    V1 = V(LVL3(I)) + DEAD
850    SUM = SUM + (V1*P3(I)*273.15/((TC3+273.15)*760))
860    NEXT I
870 N2 = SUM / NEP3
880 LPRINT : LPRINT " Volume of N2 introduced  : ";N2;"cc."
890 REM calculate the added volumes of N2 at various
    pressures
900 LPRINT : LPRINT " Vol. ads.","P. relative","P.
    equil.","T. equil."
910 LPRINT " ----------","----------","----------","----------"
```

```
920 PO = 10^2.8806618#
930 FOR I = 1 TO NEP4
940    V1 = V(LVL4(I)) + DEAD
950    V2 = V1 * P4(I)*273.15/((TC4+273.15)*760)
960    V3 = P4(I) * AVE
970    VADD = N2 - V2 - V3
980    X(I) = P4(I) / PO
990    Y(I) = P4(I) / (VADD * (PO-P4(I)))
1000    LPRINT : LPRINT VADD,X(I),P4(I),TC4
1010    NEXT I
1020 REM Calculate the slope and intercept by least square
1030 SX = 0
1040 SY = 0
1050 SXX = 0
1060 SXY = 0
1070 SYY = 0
1080 FOR I = 1 TO NEP4
1090    SX = SX + X(I)
1100    SY = SY + Y(I)
1110    SXX = SXX + X(I)*X(I)
1120    SXY = SXY + X(I)*Y(I)
1130    SYY = SYY + Y(I)*Y(I)
1140    NEXT I
1150 ITC = ((SXX * SY)-(SXY * SX))/((NEP4 * SXX)-(SX * SX))
1160 LPRINT : LPRINT : LPRINT " Intercept  : ";ITC
1170 SLP = ((NEP4 * SXY)-(SX * SY))/((NEP4 * SXX)-(SX * SX))
1180 LPRINT : LPRINT " Slope      : ";SLP
1190 VM = 1 / (SLP + ITC)
1200 C = (SLP / ITC) + 1
1210 REM Calculate the surface area
1220 SA = VM * (6.023E+23) * 16.2 * (9.999999E-21)/(22414 *
     W)
1230 REM Calculate the correlation coefficient (r)
1240 CXY = 0
1250 XVARI = 0
1260 YVARI = 0
1270 FX = 0
1280 XAVE = SX / NEP4
1290 YAVE = SY / NEP4
1300 FOR I = 1 TO NEP4
1310    CXY = CXY + (X(I) - XAVE) * (Y(I) - YAVE)
1320    XVARI = XVARI + (X(I) - XAVE)^2
1330    YVARI = YVARI + (Y(I) - YAVE)^2
1340    FX = FX + X(I)*Y(I)
1350    NEXT I
1360 R = ABS(CXY) / SQR(YVARI * XVARI)
1370 LPRINT : LPRINT " Correlation coefficient  r : ";R
1380 REM Calculate standard deviation
1390 MEAN = FX / SY
1400 DEVI = ABS((SYY - SY^2 /NEP4)/(NEP4 -1))
1410 STDEV = SQR(DEVI)
1420 LPRINT : LPRINT " Standard deviation  : ";STDEV
```

```
1430 REM Calculate the surface area error
1440 FOR J = 1 TO 10
1450    READ FD(J)
1460    NEXT J
1470 DATA 12.706,4.303,3.182,2.776,2.571,2.447,2.365,2.306,
     2.262,2.228
1480 DATA 2.201,2.179,2.16,2.145,2.131,2.12,2.11,2.101,
     2.093,2.086,2.08
1490 DATA 2.074,2.069,2.064,2.06,2.056,2.052,2.048,
     2.045,2.042
1500 CORR = ABS(1 - R*R)
1510 ERROR1 = FD(NEP4-2) * SQR(CORR) * STDEV
1520 LPRINT : LPRINT " Error on the intercept  : ";ERROR1
1530 XM1 = 1 / (SLP + ITC + ERROR1)
1540 XM2 = 1 / (SLP + ITC - ERROR1)
1550 XM12 = ABS(XM1 - XM2)/VM
1560 ERROR2 = SA * XM12
1570 LPRINT : LPRINT " Monolayer volume  : ";VM;"cc."
1580 LPRINT : LPRINT " Parameters C per BET  : ";C
1590 LPRINT
1600 LPRINT : LPRINT : LPRINT " SPEC. AREA (m^2/g. ads.)   :
     ";SA
1610 LPRINT : LPRINT " ERROR (+/-)  : ";ERROR2
1620 END
```

APPENDIX II

Basic Program to Calculate Yield and Selectivity

```
10 CLEAR
20 REM -- Ethanol Calculation ---------------------------
30 REM                  by
40 REM            Nguyen , Thanh My
50 REM ------------------------------------------------
60 DIM NO$(18),CO(18),ORG(18)
70 DIM NA$(7),CA(7),AQU(7)
80 DIM NG$(15),CG(15),GAS(15),GASW(15)
90 DIM NOUT$(11),PCCAR(11),ATCAR(11)
100 REM ------- Correction factors of organic phase -----
110 DATA "DME          :",.793,"MeOH         :",1,"DEE
    :",.753
120 DATA "EtOH         :",.983,"C5           :",.806
130 DATA "C6           :",.776,"Benzene      :",.748,"C6+C7
    :",.781
140 DATA "Toluene      :",.765,"C8alip       :",.882,"Ethylben
    :",.820
150 DATA "p+m-Xylene   :",.744,"o-Xylene     :",.736,"C9alip
    :",.787
160 DATA "C9arom       :",.783,"4MeBen       :",.821,"Durene
    :",.806
170 DATA "C10+         :",.807
180 REM ------- Correction factors of aqueous phase ------
190 DATA "DME          :",.793,"MeOH         :",1.017,"DEE
    :",1.054
200 DATA "EtOH         :",1.00,"C5-C9alip    :",.793,"BTX
    :",.749
210 DATA "C9+arom      :",.795
220 REM -------- Corection factors of gas phase-----------
230 DATA "Methane        :",1.55,"Ethylene
    :",1.45,"Ethane        :",1.69
240 DATA "Propylene      :",1.40,"Propane
    :",1.70,"iso-butane    :",1.30
250 DATA "1+I-Butenes    :",1.63,"1,3-Butadiene
    :",1.41,"n-Butane      :",1.30
260 DATA "t-2 Butene     :",1.38,"c-2 Butene     :",1.40,"C5+
    :",1.01
270 DATA "Benzene        :",1.28,"DEE
    :",1.00,"2,2-DMB       :",1.00
280 REM -------- Names of the output compounds -----------
290 DATAethylene,propylene,butenes,C1-C4(other),C5-C9
    (alip),Ethylben,BTX
300 DATA C9+arom,4Ben,Durene,C10+
310 REM -------- Read in the correction factors ----------
320 FOR I = 1 TO 18
330     READ NO$(I),CO(I)
```

```
340     ORG(I) = 0
350      NEXT I
360 FOR I = 1 TO 7
370      READ NA$(I),CA(I)
380     AQU(I) = 0
390      NEXT I
400 FOR I = 1 TO 15
410      READ NG$(I),CG(I)
420     GAS(I) = 0
430      NEXT I
440 FOR I = 1 TO 11
450     READ NOUT$(I)
460     NEXT I
470 REM -------- Input the reaction parameters ----------
480 CLS
490 INPUT "Catalyst                    : ";CAT$
500 INPUT "Run#                        : ";RN$
510 INPUT "Date of performent          : ";DT$
520 INPUT "Temperature (C)             : ";TEMP$
530 INPUT "N2 flow (ml/min)            : ";N2$
540 INPUT "WHSV (h-1)                  : ";WHSV$
550 INPUT "EtOH injected (g)           : ";WETOH
560 INPUT "Concentration of EtOH (%) : ";CONC
570 REM -------- Print the parameters on the printer -----
580 LPRINT " Catalyst : ";CAT$,"Run# : ";RN$,"Date : ";DT$
590 LPRINT " ------------------------------------------"
600 LPRINT "      Temp (C)   : ";TEMP$,"N2 flow   : ";N2$
610 LPRINT "      WHSV (h-1): ";WHSV$,"EtOH ";CONC;"%
    injected (g) : ";WETOH
620 LPRINT " ------------------------------------------"
630 LPRINT
640 WETOH = WETOH * CONC / 100
650 RE -- Input experimental data for organic phase ------
660 PRINT : PRINT "ORGANIC PHASE "
670 PRINT : INPUT "Enter the weight of organic phase (g) :
    ";WORG
680 SUM = 0
690 SUM1 = 0
700 IF WORG = 0 THEN 710 ELSE 750
710      FOR I = 1 TO 18
720         ORG(I) = 0
730         NEXT I
740      GOTO 910
750 PRINT "Enter Area% of organic phase (g) : "
760 FOR I = 1 TO 18
770     PRINT NO$(I);
780     INPUT ORG(I)
790     ORG(I) = ORG(I) * CO(I)
800     SUM1 = SUM1 + ORG(I)
810     NEXT I
820 INPUT "Area%  OK (Y/N) : ";CHECK$
830 FOR I = 1 TO 18
```

```
840     ORG(I) = ORG(I) / SUM1
850     ORG(I) = ORG(I) * (WORG/14.02)
860     IF I >= 5 THEN 870 ELSE 880
870         SUM = SUM + ORG(I)
880     NEXT I
890 ETOH1 = ORG(4) / 2 * 46.07
900 REM -- Input experimental data for aqueous phase -----
910 PRINT : PRINT "Aqueous phase "
920 INPUT "Weight of aqueous phase (g) : ";WAQU
930 INPUT "Volume of aqueous phase (ml): ";VOL
940 INPUT "Concentration of STD (c/ml) : ";STD
950 INPUT "Area (not Area%) of STD     : ";AREA
960 PRINT "Enter Area (not Area%) of aqueous phase"
970 NONEHC = 0
980 FOR I = 1 TO 7
990     PRINT NA$(I);
1000    INPUT AQU(I)
1010    AQU(I) = AQU(I) * CA(I)
1020    IF I <= 4 THEN 1030 ELSE 1040
1030        NONEHC = NONEHC + AQU(I)
1040    NEXT I
1050 RETOH = AQU(4)
1060 INPUT "Area  OK (Y/N) : ";CHECK$
1070 FOR I = 1 TO 7
1080    AQU(I) = ((AQU(I)*STD)/AREA)*VOL
1090    IF I >= 5 THEN 1100 ELSE 1110
1100        SUM = SUM + AQU(I)
1110    NEXT I
1120 REM -- Input experimental data for gas phase --------
1130 PRINT : PRINT " GAS PHASE "
1140 INPUT "Volume of sample flask (ml) : ";FLASK
1150 INPUT "Number of carbon injected   : ";CARB
1160 INPUT "Total count on totalizer    : ";TOTAL
1170 INPUT "Average MFM                 : ";MFM
1180 INPUT "Average flow                : ";FLOW
1190 PRINT : PRINT "Enter average Area% of gas phase "
1200 SUM2 = 0
1210 FOR I = 1 TO 15
1220    PRINT NG$(I);
1230    INPUT GAS(I)
1240    GAS(I) = GAS(I) * CG(I)
1250    SUM2 = SUM2 + GAS(I)
1260    NEXT I
1270 INPUT "Area%  OK (Y/N) : ";CHECK$
1280 IF CHECK$ = "N" OR CHECK$ = "n" THEN GOTO 1190
1290 FOR I = 1 TO 15
1300    GAS(I) = GAS(I) * 100 / SUM2
1310    NEXT I
1320 SUM3 = 0
1330 FOR I = 1 TO 14
1340    SUM3 = SUM3 + GAS(I)
1350    NEXT I
```

```
1360 REM ------------------------------------------------
1370 CARB = CARB / FLASK
1380 TOTAL1 = (TOTAL * FLOW / MFM) * (CARB * (100 - GAS(15))
     / GAS(15))
1390 FOR I = 1 TO 14
1400    GAS(I) = (GAS(I) / SUM3) * TOTAL1
1410    SUM = SUM + GAS(I)
1420    NEXT I
1430 SUM = SUM - GAS(14)
1440 DEE2 = GAS(14)
1450 REM -------- Calculation based on 2,2 DMB -----------
1460 LPRINT "   Weight of organic phase (g)       : ";WORG
1470 LPRINT "   Weight of aqueous phase (g)       : ";WAQU
1480 LPRINT "   Volume of aqueous phase (ml)      : ";VOL
1490 LPRINT "   Total count on totalizer          : ";TOTAL
1500 LPRINT "   Average MFM                       : ";MFM
1510 LPRINT "   Average flow                      : ";FLOW
1520 LPRINT "   Concentration of standard (C/ml)  : ";STD
1530 LPRINT "   Area of standard                  : ";AREA
1540 LPRINT : LPRINT "*** Calculation based on 2,2-DMB ***"
     : LPRINT
1550 REM -------- Summary for output --------------------
1560 ATCAR(1) = GAS(2)
1570 ATCAR(2) = GAS(4)
1580 ATCAR(3) = GAS(7) + GAS(8) + GAS(10) + GAS(11)
1590 ATCAR(4) = GAS(1) + GAS(3) + GAS(5) + GAS(6) + GAS(9)
1600 ATCAR(5) = GAS(12) + AQU(5) + ORG(5) + ORG(6) + ORG(8)
     + ORG(10) + ORG(14)
1610 ATCAR(6) = ORG(6)
1620 ATCAR(7) = AQU(6) + ORG(7) + ORG(9) + ORG(12) + ORG(13)
     + GAS(13)
1630 ATCAR(8) = AQU(7) + ORG(15)
1640 ATCAR(9) = ORG(16)
1650 ATCAR(10) = ORG(17)
1660 ATCAR(11) = ORG(18)
1670 LPRINT "Compounds","% C. atom","C. atom"
1680 LPRINT "---------","---------","-------"
1690 FOR J = 1 TO 11
1700    PCCAR(J) = ATCAR(J) * 100 /SUM
1710    LPRINT NOUT$(J),PCCAR(J),ATCAR(J)
1720    NEXT J
1730 CVTT = ((AREA - RETOH) / AREA) * 100
1740 CARBON = (WETOH * 2 / 46.07)
1750 CVHC1 = ((AREA - NONEHC) / AREA)
1760 CVHC  = ((CVHC1 * CARBON) - DEE2) / CARBON * 100
1765 CVHCS = SUM / CARBON * 100
1770 LPRINT "-----------------------------------------"
1780 LPRINT "Conversion total                    (%) :
     ";CVTT
1790 LPRINT "Conversion to HC (based on aqueous phase (%) :
     ";CVHC
1795 LPRINT "Conversion to HC (based on 2,2 DMB      (%) :
```

```
      ";CVHCS
1800 LPRINT "-----------------------------------------"
1810 END
```

APPENDIX III

Non-linear Curve Fitting Program

```
10 REM      Simplex Curve fitting for nonlinear function
20 REM                        by
30 REM                  Nguyen Thanh my
40 CLS
50 CLEAR
60 INPUT " Enter the title of calculation : ";HEAD$
70 INPUT " Function to be fitted : ";FUNC$
80 LPRINT : LPRINT "  ";HEAD$ : LPRINT
90 LPRINT " ------------------------------------------------"
100 LPRINT "           ";FUNC$
110 REM ------------------------------------------------
120 INPUT " Enter the maximium number of iteration :
    ";MAXITER
130 INPUT " Enter total number of variable per data point :
    ";NVPP
140 INPUT " Enter number of data points : ";MNP
150 INPUT " Enter number of parameter to be fitted : ";M
160 N = M + 1
170 ALFA = 1
180 BETA = .5
190 GAMA = 2
200 ROOT2 = 1.414214
210 DIM SIMP(N,N),STP(N),DAT(MNP,NVPP),MAXER(N)
220 DIM P(N),Q(N),L(N),H(N),CENTER(N),NEXV(N)
230 DIM ERRS(N),MEAN(N)
240 PRINT " Enter the initial value for parameters : "
250 FOR J = 1 TO M
260    INPUT SIMP(1,J)
270    NEXT J
280 REM ------------------------------------------------
290 PRINT " Enter the starting step : "
300 FOR J = 1 TO M
310    INPUT STP(J)
320    NEXT J
330 REM ------------------------------------------------
340 PRINT " Enter the maximium desired errors : "
350 FOR J = 1 TO N
360    INPUT MAXER(J)
370    NEXT J
380 REM ------------------------------------------------
390 PRINT " Enter the data    x,y : "
400 FOR J = 1 TO MNP
410    READ DAT (J,1),DAT(J,2)
420    NEXT J
430 FOR J = 1 TO MNP - 1
```

```
440     DAT(J,1) = 46/(DAT(J,1)*.1)
450     NEXT J
460 REM ----------- Starting Simplex --------------------
470 FOR J = 1 TO M
480     NEXV(J) = SIMP(1,J)
490     NEXT J
500 GOSUB 2160
510 SIMP(1,N) = NEXV(N)
520 REM -----------------------------------------------
530 FOR J = 1 TO M
540     P(J) = STP(J) * ((N^.5) + M-1)/(M * ROOT2)
550     Q(J) = STP(J) * ((N^.5) - 1) /(M * ROOT2)
560     NEXT J
570 REM -----------------------------------------------
580 FOR J = 2 TO N
590     FOR JJ = 1 TO M
600         SIMP(J,JJ) = SIMP(1,JJ) + Q(JJ)
610         NEXT JJ
620     SIMP(J,J-1) = SIMP(1,J-1) + P(J-1)
630     FOR JJ = 1 TO M
640         NEXV(JJ) = SIMP(J,JJ)
650         NEXT JJ
660     GOSUB 2160
670     SIMP(J,N) = NEXV(N)
680     NEXT J
690 PRINT : PRINT " The starting Simplex : "
700 GOSUB 2230
710 REM -----------------------------------------------
720 FOR J = 1 TO N
730     L(J) = 1
740     H(J) = 1
750     NEXT J
760 REM -----------------------------------------------
770 GOSUB 2310
780 REM -----------------------------------------------
790 NITER = 0
800 DONE$ = "true"
810 NITER = NITER + 1
820 FOR J = 1 TO N
830     CENTER(J) = 0
840     NEXT J
850 REM -----------------------------------------------
860 FOR J = 1 TO N
870     IF J = H(N) THEN 910
880     FOR JJ = 1 TO M
890         CENTER(JJ) = CENTER(JJ) + SIMP(J,JJ)
900         NEXT JJ
910     NEXT J
920 REM -----------------------------------------------
930 FOR J = 1 TO N
940     CENTER(J) = CENTER(J) / M
950     NEXV(J) = (1 + ALFA) * CENTER(J) - ALFA *
```

```
    SIMP(H(N),J)
960     NEXT J
970 REM ------------------------------------------------
980 GOSUB 2160
990 REM ------------------------------------------------
1000 IF NEXV(N) > SIMP(L(N),N) THEN 1070
1010    GOSUB 2390
1020    FOR J = 1 TO M
1030       NEXV(J) = GAMA * SIMP(H(N),J) + (1 - GAMA) *
    CENTER(J)
1040       NEXT J
1050 REM ------------------------------------------------
1060 GOSUB 2160
1070 IF NEXV(N) > SIMP(H(N),N) THEN 1100
1080    GOSUB 2390
1090    GOTO 1260
1100 FOR J = 1 TO M
1110    NEXV(J) = BETA * SIMP(H(N),J) + (1 - BETA) *
    CENTER(J)
1120    NEXT J
1130 GOSUB 2160
1140 IF NEXV(N) > SIMP(H(N),N) THEN 1170
1150 GOSUB 2390
1160 GOTO 1260
1170 FOR J = 1 TO N
1180    FOR JJ = 1 TO M
1190       SIMP(J,JJ) = (SIMP(J,JJ) + SIMP(L(N),JJ)) * BETA
1200       NEXV(JJ) = SIMP(J,JJ)
1210       NEXT JJ
1220     GOSUB 2160
1230     SIMP(J,N) = NEXV(N)
1240    NEXT J
1250 REM ------------------------------------------------
1260 GOSUB 2310
1270 REM ------------------------------------------------
1280 FOR J = 1 TO N
1290    ERRS(J) = (SIMP(H(J),J) - SIMP(L(J),J)) /
    SIMP(H(J),J)
1300    IF ERRS(J) > MAXER(J) THEN DONE$ = "false"
1310    NEXT J
1320 REM ------------------------------------------------
1330 IF (DONE$ = "true") OR (NITER > MAXITER) THEN 1350
1340    GOTO 800
1350 REM ------------------------------------------------
1360 FOR J = 1 TO N
1370    MEAN(J) = 0
1380    FOR JJ = 1 TO N
1390       MEAN(J) = MEAN(J) + SIMP(JJ,J)
1400       NEXT JJ
1410     MEAN(J) = MEAN(J) / N
1420     NEXT J
1430 PRINT : PRINT " The final simplex after ";NITER;"
```

```
    iteration :"
1440 GOSUB 2230
1450 PRINT : PRINT " The mean is :"
1460 FOR J = 1 TO N
1470     PRINT MEAN(J);
1480     NEXT J
1490 REM ------------------------------------------------
1500 PRINT : PRINT " The estimated fractional error is : "
1510 FOR J = 1 TO N
1520     PRINT ERRS(J);
1530     NEXT J
1540 REM ------------------------------------------------
1550 LPRINT : LPRINT " Parameter ..... a = ";MEAN(1)
1560 LPRINT " Parameter ..... b = ";MEAN(2)
1570 LPRINT " ----------------------------------------"
1580 PRINT : LPRINT " Space time "," Conv HC % "," Y (func.)
     "," Differences"
1590 LPRINT " -------- "," ------ "," ------- "," ---------"
1600 SIGMA = 0
1610 FOR J = 1 TO MNP
1620    Y = (MEAN(1)*DAT(J,1)) / (MEAN(2) + DAT(J,1))
1630    DY = DAT(J,2) - Y
1640    SIGMA = SIGMA + DY*DY
1650 PRINT : LPRINT DAT(J,1),DAT(J,2),Y,DY
1660    NEXT J
1670 LPRINT " ----------------------------------------"
1680 SIGMA = SQR(SIGMA /MNP)
1690 PRINT : LPRINT " The standard deviation of the function
     is : ";SIGMA
1700 SIGMA = SIGMA /SQR(MNP - M)
1710 PRINT : LPRINT " The estimated error of the function is
     : ";SIGMA
1720 LPRINT " ----------------------------------------"
1730 INPUT " Would you like to see the plot ? (Y/N) : ";AA$
1740 IF (AA$ = "n") OR (AA$ = "N") THEN 2080
1750 PRINT " Enter the minimium and maximium on X-axis "
1760 INPUT " X(min) = ";XL
1770 INPUT " X(max) = ";XR
1780 PRINT " Enter the minimium and maximium on Y-axis "
1790 INPUT " Y(min) = ";YB
1800 INPUT " Y(max) = ";YT
1810 REM ------------------------------------------------
1820      GOSUB 2440
1830 REM ------------------------------------------------
1840 XA = (564 - 84) / XD
1850 YA = (360 - 40) / YD
1860 REM - Print all the data points on the grid ---------
1870 FOR I = 1 TO MNP
1880    XP = 84 + (480 / XD) * (DAT(I,1) - XL)
1890    IF XP < 84 OR XP > 564 THEN 1930
1900    YP = 360 - (320 / YD) * (DAT(I,2) - YB)
1910    IF YP < 40 OR YP > 360 THEN 1930
```

```
1920    CIRCLE (XP,YP),2
1930    NEXT I
1940 REM --- Draw the equation -------------------------
1950 FOR XG = 84 TO 564
1960    XT = XL + (XG - 84) / 484 * XD
1970    YT = (MEAN(1) * XT) / (MEAN(2) + XT)
1980    YG = 360 - (YT - YB) * YA
1990    IF YG < 40 OR YG > 360 THEN 2010
2000       PSET (XG,YG)
2010    NEXT XG
2020 LOCATE 1,1
2030 INPUT " Would you like to rescale your plot ? (Y/N) :
     ";BB$
2040 IF (BB$ = "n" OR BB$ = "N") THEN 2070
2050 CLS
2060     GOTO 1750
2070 CLS
2080 END
2090 REM --- Sum of residuals 1 ----------------------
2100 SIMP(J,N) = 0
2110 FOR I = 1 TO MNP
2120    FX = (SIMP(J,1)*DAT(I,1))/(SIMP(J,2)+DAT(I,1))
2130    SIMP(J,N) = SIMP(J,N) + (FX - DAT(I,2))^2
2140    NEXT I
2150 RETURN
2160 REM --- Sum of residuals 2 ----------------------
2170 NEXV(N) = 0
2180 FOR I = 1 TO MNP
2190    FX = (NEXV(1)*DAT(I,1))/(NEXV(2)+DAT(I,1))
2200    NEXV(N) = NEXV(N) + (FX - DAT(I,2))^2
2210    NEXT I
2220 RETURN
2230 REM --- Print -----------------------------------
2240 FOR K = 1 TO N
2250    FOR KK = 1 TO N
2260       PRINT SIMP(K,KK);
2270       NEXT KK
2280    PRINT
2290    NEXT K
2300 RETURN
2310 REM --- Order -----------------------------------
2320 FOR K = 1 TO N
2330    FOR KK = 1 TO N
2340       IF SIMP(KK,K) < SIMP(L(K),K) THEN L(K) = KK
2350       IF SIMP(KK,K) > SIMP(H(K),K) THEN H(K) = KK
2360       NEXT KK
2370    NEXT K
2380 RETURN
2390 REM -------- New vertex ----------------------------
2400 FOR K = 1 TO N
2410    SIMP(H(N),K) = NEXV(K)
2420    NEXT K
```

```
2430 RETURN
2440 REM ------- Subroutine draw the grid ----------------
2450 CLS
2460 SCREEN 3
2470 LINE (74,40)-(564,40)
2480 LINE (74,360)-(564,360)
2490 LINE (84,40)-(84,376)
2500 LINE (564,40)-(564,376)
2510 FOR Y1 = 104 TO 296 STEP 64
2520   LINE (74,Y1)-(84,Y1)
2530  NEXT Y1
2540 FOR X1 = 180 TO 468 STEP 96
2550    LINE (X1,362)-(X1,376)
2560    NEXT X1
2570 XD = XR - XL
2580 YD = YT - YB
2590 R = 23
2600 FOR K = 0 TO 5
2610    LOCATE R,1
2620    S = YB + YD * K/5
2630    PRINT USING "####.##";S
2640    R = R-4
2650    NEXT K
2660 CC = 7
2670 FOR K = 0 TO 5
2680    LOCATE 24,CC
2690    S = XL + XD * K/5
2700    PRINT USING "####.##";S;
2710    CC = CC + 12
2720    NEXT K
2730 RETURN
2740 DATA 6.4,33.27,12.8,27.06,25.6,12.0,38.5,10.14,0,0
```